

**DEVELOPMENT OF NANOPATTERNS ON SELF  
ASSEMBLED MONOLAYER (SAM) ORGANIC  
FILMS USING SCANNING PROBE MICROSCOPE  
(SPM) NANOLITHOGRAPHY TECHNIQUE**

**A Thesis Submitted to  
the Graduate School of Engineering and Science of  
İzmir Institute of Technology  
in Partial Fulfillment of the Requirements for the Degree of**

**MASTER OF SCIENCE**

**in Material Science**

**by  
Semra GÜL**

**August 2006  
İZMİR**

We approve the thesis of **Semra GÜL**

**Date of Signature**

.....  
**Assoc. Professor Salih OKUR**  
Supervisor  
Department of Physics  
İzmir Institute of Technology

**10 August 2006**

.....  
**Assoc. Professor Metin TANOĞLU**  
Co-Supervisor  
Department of Mechanical Engineering  
İzmir Institute of Technology

**10 August 2006**

.....  
**Professor Devrim BALKÖSE**  
Department of Chemical Engineering  
İzmir Institute of Technology

**10 August 2006**

.....  
**Assoc. Professor Serdar ÖZÇELİK**  
Department of Chemistry  
İzmir Institute of Technology

**10 August 2006**

.....  
**Assist. Professor Yusuf SELAMET**  
Department of Physics  
İzmir Institute of Technology

**10 August 2006**

.....  
**Prof. Muhsin ÇİFTÇİOĞLU**  
Head of Department  
İzmir Institute of Technology

**10 August 2006**

.....  
**Assoc. Prof. Semahat ÖZDEMİR**  
Head of the Graduate School

## ACKNOWLEDGEMENT

Firstly, I would like to express my deep appreciation to my supervisor Assoc. Professor Salih Okur. I would like to thank him for giving me confidence to pursue my M.S, his encouragement, support and understanding. I also would like to thank to my co-supervisor Assoc. Professor Metin Tanođlu for his supervision and guidance at the all stages of my study.

I am also indebted to Assoc. Professor Serdar Özçelik and Assist. Professor Yusuf Selamet for their supports. I am also grateful Assoc. Professor Sedat Akkurt, Dr. Hüseyin Özgener and Ayaz Allahverdiev for their contributions. Furthermore, I appreciate the thesis committee members.

My other big “Thank you!” is for the staff of Center for Material Research of İzmir Institute of Technology for their contribution. This research was financially supported by DPT. This support is gratefully acknowledged.

I am also grateful to my colleagues; Mehtap Özdemir, Elçin Dilek Kaya and Serpil Kaya who have contributed to my experience and knowledge in science and my friends for their encouragement and sympathy.

Last but not least, thanks to my family, for their support, understanding and love.

# ABSTRACT

## DEVELOPMENT OF NANOPATTERNS ON SELF ASSEMBLED MONOLAYER (SAM) ORGANIC FILMS USING SPM NANOLITHOGRAPHY TECHNIQUE

Patterning and fabrication of nanostructures on surfaces is a great demand for nanoscale electronic and mechanical devices. Current techniques such as electron beam lithography and photolithography provides limited resolution and they are not capable of reproducible in nanoscale. Among those, Scanning Probe Microscopy (SPM) lithography that uses a nanometer sharpened tip has demonstrated outstanding capabilities for nanometer level patterning on various surfaces. Moreover, SPM techniques offer creating nanopatterns of Self Assembled Monolayers (SAMs) with molecular precision and visualizing surfaces with the highest spatial resolution. In this work, nanoscratches on gold surfaces and oxidation patterns on titanium surface were successfully performed as example of SPM lithography. In the second stage, Octadecylamine-HCl, Octadecanetriol (ODT) and Decylmercaptan (DM) SAM organic films were fabricated on various substrates; i.e., mica, silica, titanium surface deposited on silicon, n and p type silicon, using self assembly film preparation techniques. The film thicknesses were measured with Atomic Force Microscope (AFM). Nanopatterns were fabricated on SAM films using AFM tip by exerting a local high pressure at the contact that causes the displacement of SAM molecules by a high shear force. It was observed that there was no formation of SAMs on n type Si and silica substrates whereas there were organic assemblies on the other substrates. Fabricated nanopatterns were examined and thickness measurement was done. Molecular lengths of the organics were evaluated by using of SPARTAM 02 LINUX-UNIX with the method of PM3 and the measured values were compared with the calculated ones and it was concluded that monolayers were formed on the surfaces.

# ÖZET

## KENDİNDEN BAĞLANAN TEK KATMANLI ORGANİK FİMLER ÜZERİNDE (SAM) NANOLİTHOGRAFİ TEKNİĞİ KULLANILARAK NANODESENLERİN GELİŞTİRİLMESİ

Nanodesenlerin yüzeyler üzerine üretilmesi ve fabrikasyonu nanometre ölçeğinde elektronik ve mekanik cihazların üretilmesinde oldukça önemlidir. Fotolitografi, elektron lithografi gibi kullanılan geçerli tekniklerin çözünürlük ve kapasite özellikleri nanodesen üretimin sınırlandırmaktadır. Bu tekniklerden atomik boyutta sivri uç kullanılan taramalı uçlu mikroskop (SPM) lithografi tekniği, çeşitli yüzeyler üzerine moleküler boyutta desen üretme kapasitesinden dolayı dikkat çekicidir. Dahası, SPM tekniği ile Kendinden Bağlanan Tek Katmanlı Organik (SAM) filmler üzerine moleküler hassasiyette nanodesenler yapmak ve görüntülemek mümkündür. Bu çalışmada; altın yüzeyleri üzerine nanoçizgiler ve titanyum yüzeyi üzerine oksitleme yöntemi ile desenler SPM lithografi yöntemlerine örnek olarak yapıldı. İkinci aşamada, Octadecylamine-HCl, Octadecanetiol (ODT) ve Decylmercaptan (DM) organikleriyle mika, cam, titanyum ve çeşitli silikon yüzeyleri üzerine SAM filmleri hazırlandı. Hazırlanan filmlerin kalınlıkları Atomik Kuvvet Mikroskobu (AFM) ile ölçüldü. AFM tipi ile uygulanan lokal kontak kuvvetinin SAM moleküllerinin yer değiştirmesine neden olması ile SAM film yüzeyleri üzerinde nanodesenler geliştirildi. Cam ve n tip silikon yüzeyleri üzerine organik kaplama yapılmadığı ancak diğer örneklerde kaplamalar yapıldığı gözlemlendi. Üretilen nanodesenler incelenerek derinlik ölçümleri yapıldı. Organiklerin boyları SPARTAM 02 LINUX-UNIX programı yardımıyla ve PM3 methodu denen bir methodla ölçüldü ve ölçülen derinlikler ile organiklerin hesaplanan boyları karşılaştırılarak yüzeyler üzerinde tek katman oluşturulduğu gözlemlendi.

# TABLE OF CONTENTS

LIST OF FIGURE .....	ix
LIST OF TABLE .....	xiv
CHAPTER 1. INTRODUCTION .....	1
1.1. Self Assembled Monolayer (SAM) .....	2
1.1.1. Formation of SAMs .....	6
1.1.2. Parameters Affecting on SAM Formation .....	8
1.2. Nanolithography .....	12
1.3. Scanning Probe Microscope Lithography.....	14
1.3.1. Electrical Surface Modification .....	16
1.3.2. Mechanical Surface Modification .....	18
1.4. AFM Surface Characterization Techniques.....	21
1.4.1. AFM Surface Characterization with Contact Mode.....	22
1.4.2. AFM Surface Characterization with Semicontact Mode .....	24
1.4.3. AFM Spectroscopy.....	25
1.5. Substrates and Organics.....	27
1.5.1. Substrates .....	27
1.5.1.1. Mica.....	27
1.5.1.2. Silica.....	28
1.5.1.3. Silicon .....	28
1.5.2. Organics .....	29
1.5.2.1. Octadecylamine (ODA) .....	30
1.5.2.2. Decylmercaptan (DM) and Octadecanethiol (ODT).....	31
CHAPTER 2. EXPERIMENTAL PROCEDURE .....	34
2.1. Sample Preparations .....	34
2.1.1. Cleaning Procedure I.....	35
2.1.1.1. Cleaning Procedure for Silicon Substrates.....	35
2.1.1.2. Cleaning Procedure for Silica .....	36
2.1.1.3. Cleaning Procedure for Titanium.....	36



3.2.1.2. SAM of ODA-HCl with 0,1mM in Water on p type Silicon .....	86
3.2.2. SAM of ODA-HCl with 1mM in Water on Titanium.....	87
3.2.3. SAM of ODA-HCl with 0,1mM in Ethanol.....	88
3.2.3.1. SAM of ODA-HCl with 0,1mM in Ethanol on Mica.....	88
3.2.3.2. SAM of ODA-HCl with 0,1mM in Ethanol on p type Silicon .....	89
3.2.3.3. SAM of ODA-HCl with 0,1mM in Ethanol on Titanium.....	90
3.2.4. SAM of DM with 0,1mM in Ethanol on Mica.....	91
3.2.5. SAM of ODT with 0,1mM in Ethanol.....	92
3.2.5.1. SAM of ODT with 0,1mM in Ethanol on Mica .....	92
3.2.5.2. SAM of ODT with 0,1mM in Ethanol on Titanium.....	93
3.3. FTIR Results .....	94
3.3.1. ODA-HCl with 0,1mM in Water.....	95
3.3.1.1. SAM of ODA-HCl with 0,1mM in Water on Mica .....	95
3.3.1.2. SAM of ODA-HCl with 0,1mM in Water on p type Silicon.....	97
3.3.2. SAM of ODA-HCl with 1mM in Water on Titanium.....	98
3.3.3. SAM of ODA-HCl with 0,1mM in Ethanol.....	99
3.3.3.1. SAM of ODA-HCl with 0,1mM in Ethanol on Mica.....	99
3.3.3.2. SAM of ODA-HCl with 0,1mM in Ethanol on p type Silicon...	100
3.3.3.3. SAM of ODA-HCl with 0,1mM in Ethanol on Titanium .....	101
3.3.4. SAM of DM with 0,1mM in Ethanol on Mica.....	101
3.3.5. SAM of ODT with 0,1mM in Ethanol .....	102
3.3.5.1. SAM of ODT with 0,1mM in Ethanol on Mica .....	102
3.3.5.2. SAM of ODT with 0,1mM in Ethanol on Titanium.....	103
3.4. XRD Results .....	104
 CHAPTER 4. SUMMARY AND CONCLUSION.....	 106
 REFERENCES .....	 109

## LIST OF FIGURES

<u>Figure</u>	<u>Page</u>
Figure 1.1. Formation of SAM by immersing a substrate in appropriate solution.....	6
Figure 1.2. Schematic illustration of the formation of SAMs of surfactant molecules on a solid surface. ....	7
Figure 1.3. Schematic illustration of an alkanethiol with its principal components of time, and the formation of the self assembled monolayer.....	10
Figure 1.4. Lithographic stones were introduced by Alois Senefelder .....	13
Figure 1.5. By placing a bias between an electrically conductive probe and a surface, the surface can be modified. ....	17
Figure 1.6. By means of applying a high contact force on a sample, patterns are created in mechanical surface modification.....	19
Figure 1.6. Demonstration of both deflection and detection of laser on tip and photodiode respectively .....	21
Figure 1.8. The typical force-distance curve with the tip position.....	26
Figure 1.9. Demonstration of ODA molecules with $(\text{CH}_3(\text{CH}_2)_{17}\text{NH}_2\text{-HCl})$ (a) and without $(\text{CH}_3(\text{CH}_2)_{17}\text{NH}_2)$ (b) excess of HCl. The black atoms represent carbons, whites hydrogen blues nitrogen and the yellow one represent chlorine atom.....	31
Figure 1.10. Demonstration of (a) DM $(\text{CH}_3(\text{CH}_2)_9\text{SH})$ and (b) ODT $(\text{CH}_3(\text{CH}_2)_{17}\text{SH})$ molecules. The black atoms represent carbons, white hydrogen and green is sulfur atom .....	32
Figure 2.1. The photograph of thermal evaporation system used for deposition gold surface. ....	38
Figure 2.2. The schematic representation of thermal evaporation system.....	38
Figure 2.3. (a) The photograph of Ar-ion beam system. (b) Schematic representation of the same system .....	39
Figure 2.4. (a) The photograph of magnetron sputtering system. (b) Schematic representation of the same system .....	41
Figure 2.4. (a) The photograph of SPM system. (b) Schematic representation of the same system .....	44

Figure 2.5. Tip-sample interaction under DFL approach or retracting motion .....	46
Figure 3.1. Topographic images of substrates taken from AFM with semicontact mode (a) and (b) n and p type bare silicon substrates images respectively at the scale of 10X10 $\mu\text{m}$ , (c) silica surfaces at 80X80 nm scales, (d) and (e) mica and titanium surface images at the 10X10 $\mu\text{m}$ .....	51
Figure 3.2. (a) Two and (b) three dimensional topographic image of mica taken with AFM under 55.000 nN applied force. ....	52
Figure 3.3. Gold substrate growth on mica by (a) evaporation (b) magnetron sputtering systems with 800X800 nm .....	54
Figure 3.4. Physical surface modification of gold thin film deposited on mica substrates (a) nanoscratches with line depth and (b) applied force versus depth graph in 5X5 $\mu\text{m}$ scale and (c) nanoindentation with indent depth graph of chosen line with 10X10 $\mu\text{m}$ scales.....	56
Figure 3.5. Raster lithography on gold film on mica made by using sputtering method with (a) topographic and phase image of the patterns in 5X5 $\mu\text{m}$ scales and (c) writing with raster lithography on gold films on mica in 10X10 $\mu\text{m}$ .....	57
Figure 3.6. AFM surface images of (a) gold on titanium deposited on silicon made by using sputtering method, (b) applying nanoscratching lithography technique, (c) and (d) lithographic patterns on gold.....	58
Figure 3.7. Oxidation lithography on titanium thin film deposited on silicon substrates (a) two and three dimensional AFM images of oxide layer with decreasing oxidation time (b) cross-section of pointed line which is represented thickness of oxide layer according to changing oxidation time in 8X8 $\mu\text{m}$ scales .....	61
Figure 3.8. Two and three dimensional topographic AFM images of SAM consist of ODA-HCl with 0,1 mM in water on mica with represented (a) and (b) from different regions with the scale of 5X5 $\mu\text{m}$ .....	64

Figure 3.9. AFM images of SAM consist of ODA-HCl with 0,1 mM in water on mica with (a) before and after nanolithography (b) and after second nanolithography (c) with thickness measurements .....	66
Figure 3.10. Topographic AFM images of SAM consist of ODA-HCl with 0,1 mM in water (a) on p type silicon and (b) thickness measurement of the surface with the scale of 10X10 $\mu\text{m}$ .....	68
Figure 3.11. Topographic AFM images of SAM (ODA-HCl with 1 mM in water) on titanium deposited on silicon (a) after and before lithography and (b) thickness measurement of the surface with the scale of 5X5 $\mu\text{m}$ .....	69
Figure 3.12. Topographic AFM images of SAM consist of ODA-HCl with 0,1 mM in ethanol on mica with (a) two and (b) three dimensional with the scale of 3,5X3,5 $\mu\text{m}$ .....	71
Figure 3.13. Topographic images of the surface consist of organics (ODA-HCl with 0,1 mM in ethanol) on mica with (a) two and (b) three dimensional and (c) thickness measurement with the scale of 5X5 $\mu\text{m}$ .....	72
Figure 3.14. (a) Two and (b) three dimensional nanolithography images of logo of IYTE on mica surface containing ODA-HCl (with 0,1 mM in ethanol) within 7X7 $\mu\text{m}$ .....	73
Figure 3.15. Two dimensional topographic AFM images of surface prepared by ODA-HCl with 0,1 mM in water on p type silicon with the thickness measurement in the scale of 5X5 $\mu\text{m}$ .....	74
Figure 3.16. Topographic AFM images of titanium deposited on silicon with SAM of the solutions of ODA-HCl with 0,1 mM in ethanol (a) before and after nanopatterning surface image with the scale of 3,5X3,5 $\mu\text{m}$ (b) and nanoscratching with thickness measurement at 5X5 $\mu\text{m}$ .....	75
Figure 3.17. AFM topography images of SAM of DM with 0,1 mM in ethanol on mica: (a) bare DM film, (b) topography (right side) and phase (left side) images of surface after nanolithography in 3,5X3,5 $\mu\text{m}$ and (c) thickness measurement.....	78

Figure 3.18. (a) Two and three dimensional topographic AFM images in 2X2 $\mu\text{m}$ and (b) thickness measurement on one of the defects on mica with the SAM of ODT having the concentration of 0,1 mM in ethanol.....	80
Figure 3.19. Nanolithography on mica prepared with the SAM of ODT with 0,1 mM in ethanol.....	81
Figure 3.20. Two dimensional topographic AFM images with nanolithography of mica with the SAM of ODT having the concentration of 0,1 mM in ethanol at the scale of 4X4 $\mu\text{m}$ .....	82
Figure 3.21. Topographic AFM images of titanium surface with the SAM of ODT having the concentration of 0,1 mM in ethanol at different scales .....	83
Figure 3.22. (a) Two and three dimensional topographic AFM images at 5X5 $\mu\text{m}$ in scales and (b) thickness measurement of represented area of titanium surface with the SAM of ODT with 0,1 mM in ethanol.....	84
Figure 3.23. SEM images of ODA-HCl with 0,1mM in water on mica with (a) 2X2 $\mu\text{m}$ and (b) 500X500 nm in scales.....	85
Figure 3.24. EDX results of SAM consist of ODA-HCl with 0,1 mM in water on mica.....	86
Figure 3.25. SEM with EDX results of SAM consist of ODA-HCl with 0,1 mM in water on p type silicon .....	87
Figure 3.26. SEM with EDX results of SAM consist of ODA-HCl with 1 mM in water on titanium .....	88
Figure 3.27. SEM with EDX results of SAM consist of ODA-HCl with 0,1 mM in ethanol on mica .....	89
Figure 3.28. SEM with EDX results of p type silicon prepared by the solutions of ODA-HCl with 0,1 mM in ethanol .....	90
Figure 3.29. SEM with EDX results of titanium on silicon prepared by the solutions of ODA-HCl with 0,1 mM in ethanol .....	91
Figure 3.30. SEM with EDX results of mica prepared in the solutions of DM with 0,1 mM in ethanol .....	92

Figure 3.31. SEM with EDX results of mica contains SAM of ODT with 0,1 mM concentration in ethanol .....	93
Figure 3.32. SEM with EDX results of titanium contains SAM of ODT with 0,1 mM concentration in ethanol .....	94
Figure 3.33. FTIR results of transmitted method of SAM consist of ODA-HCl with 0,1 mM in water on mica .....	96
Figure 3.34. FTIR results of 80 spectroscopy method of SAM consist of ODA-HCl with 0,1 mM in water on mica .....	97
Figure 3.35. FTIR results of 80 spectroscopy method of SAM consist of ODA-HCl with 0,1 mM in water on p type silicon .....	98
Figure 3.36. FTIR results of SAM consist of ODA-HCl with 1mM in water on titanium deposited on silicon .....	99
Figure 3.37. FTIR results of SAM consist of ODA-HCl with 0,1 mM in ethanol on mica.....	100
Figure 3.38. FTIR results of p type silicon prepared by the solutions of ODA-HCl with 0,1 mM in ethanol .....	100
Figure 3.39. FTIR results of titanium on silicon with the SAM solution of ODA-HCl with 0,1 mM in ethanol .....	101
Figure 3.40. FTIR results of mica with the SAM solution of DM with 0,1 mM in ethanol.....	102
Figure 3.41. FTIR results of mica with the SAM solution of ODT with 0,1 mM in ethanol.....	103
Figure 3.42. FTIR results of titanium with the SAM solution of ODT with 0,1 mM in ethanol.....	104
Figure 3.14. XRD results of SAM consist of ODA-HCl with 0,1 mM in water on mica.....	105

## LIST OF TABLES

<b><u>Table</u></b>	<b><u>Page</u></b>
Table.2.1. Deposition conditions of thin films with sputtering system .....	40
Table 2.2. Organics of SAM used in the experiments with the preparation conditions.....	42
Table 3.1. Calculated molecular length of the organics.....	53
Table 3.2. SAM of amines with the substrates on which monolayers were formed.....	62
Table 3.3. SAM of thiols with the substrates on which monolayers were formed.....	76

# CHAPTER I

## INTRODUCTION

Organic thin films which have a thickness of a few nanometers have attracted considerable attention for the possibility of transferring the optical, electronic, optoelectronic and chemical properties of the adsorbed molecules to a liquid or solid surface. They are used in many practical and commercial applications such as sensors, detectors, displays and electronic circuit components. A sophisticated thin film deposition technique can enable synthesis of organic molecules with desired structure and functionality almost without limitations. Hence, the production of electrically, optically and biologically active components on a nanometer scale can be achieved (Kondrashkina et al. 1996).

Various techniques such as thermal evaporation, sputtering, molecular beam epitaxy, adsorption from solution, self-assembly, Langmuir-Blodgett (LB) technique, etc. are used for deposition of an organic thin film on a solid substrate. The thickness of the film is order at nanometer scale. Langmuir-Blodgett (LB) films and self-assembled monolayers (SAMs) have been used as resists and patterned with nanometer precision. These films are well-organized molecular assemblies that are formed layer-by-layer by monolayer deposition via either van der Waals force or chemical bonding. The size of the molecule determines the layer thickness and can be carefully controlled to produce layers of uniform coverage. The strengths of the interactions between molecules and substrates are highly dependent on their chemical natures. Thin and homogeneous SAM films are of much interest because of their potential applications: surface coatings to control wetting and adhesion, chemical resistance, biocompatibility, molecular recognition and more (Ulman 1991).

The formation of monolayers by self-assembly of surfactant molecules at surfaces is one example of the general phenomena of self-assembly. The field of self-assembly has grown rapidly since the discovery of these structures and their ability to modify the physical and chemical properties of a surface. In nature, self-assembly results in supermolecular hierarchical organizations of interlocking components that provides very complex systems (Ulman 1996). To increase fundamental understanding of self-organization, structure-property relationships, and interfacial phenomena, SAMs

offer unique opportunities. SAMs which are the most remarkable molecule-substrate interactions can be prepared with different types of molecules and different substrates. The capability of adapt both head and tail groups of the constituent molecules makes SAMs excellent systems for a fundamental understanding of phenomena affected by competing intermolecular, molecular-substrates and molecule-solvent interactions such as ordering and growth, wetting, adhesion, lubrication and corrosion. Because of all these properties besides being well-defined and accessible, SAMs are preferred as a good model of systems in physical chemistry and statistical physics (Rachel et al. 2004, Lee et al. 2001).

### **1.1. Self Assembled Monolayer (SAM)**

The spontaneous self organization (self-assembly) of atoms and molecules to matter with geometric repeat of symmetry at the molecular level is called as self assembly. Self-assembled monolayers (SAMs) are ordered molecular structures formed by the adsorption of an active surfactant on a solid surface. They occur spontaneously by chemisorptions of functionalized molecules with a specific affinity of their head groups for the substrate. They are robust, relatively stable, and capable of providing versatility at both the molecular and the bulk levels. They offer a vehicle for investigating specific interactions at interfaces, and stability of two-dimensional structures. Interest in the properties of organized monolayers has grown enormously in recent years because these monolayers can provide a means to control the interface at a molecular level. They are also widely studied because of their importance in wetting phenomena, chemical sensing, and nanotechnology.

In contrast to ultra thin films made by, for example, MBE and CVD, SAMs are highly ordered and oriented and can incorporate a wide range of groups both in alkyl chain and at the chain termina. Therefore, a variety of surfaces with specific interactions can be produced with fine chemical control (Ulman 1991). Due to their dense and stable structure, SAMs have potential applications in corrosion prevention, wear protection, and more. SAM experiments including the inter correlation between friction and molecular structure, elastic and adhesive properties have been studied so far. In addition, their high molecular order parameter in SAMs makes them ideal as components in electronic optic devices.

The field of self-assembly was started with Zisman in 1946. He published the preparation of a monomolecular layer by adsorption (self-assembly) of a surfactant onto a clean metal surface (Bigelow et al. 1946). As the potential of self-assembly was not recognized at that time, this publication just initiated a limited level of interest.

First examples of patterning on organic self-assembled monolayers were reported by U. Heinzmann. Research in this area began in 1982 and has seen an increasing number of published papers every year since then. In this case hexadecanethiol and N-biphenylthiol on Au (111) and octadecyltrichlorosilane (OTS) on Si (100) were utilized (Hamelmann et al. 2003). Many self-assembly systems have been investigated since to date whereas monolayer of alkanethiolates on gold is the most studied SAMs of these systems.

The application of STM to determine the SAM structures deserves special comment since the insulating nature of the alkyl chains imposes operation at very high tunneling gaps, a condition that was not realized in many earlier studies. Operation at high gaps is necessary to ensure the presence of a true vacuum gap, to avoid contact, between the tip and the CH<sub>3</sub> terminated surface. While this is easily feasible for short length chains (<10 carbons), it becomes difficult for the longer chains due to the rapidly decreasing tunneling probability. Calculations of the tunneling probability as a function of chain length show that only for lengths <10 carbon atoms is the tunnel current in a range that is within typical values of the preamplifiers used in STM. The calculations also predict that nonlinear increases of the tunneling current will occur during compression of the molecular layer, leading to an increase of the tilt angle. It would be very interesting to further pursue this line of research by determining both theoretically and experimentally the tunneling current changes due to increased distortions of the molecular structure.

SAMs are of prime technological interest. Because of the large number of properties that can be designed into SAM films, they offer almost unlimited possibilities for studies to correlate many surface and film parameters with friction and adhesion. For example, the binding to the substrate can be changed by using molecules with different head groups: -SH (thiols), -SiR<sub>3</sub> (silanes), -COOH (acids), etc. The softness or elastic compliance can also be changed by modifying the chain length and/or the type of chemical bonds inside the chains (single, double, and triple C-C bonds), by fluorination, and by inclusion of several heteroatoms, like O (in ethers), etc. All of these modify the rigidity of the chains. The end groups that are exposed to the vacuum or liquid interface

can also be conveniently modified to affect the friction and adhesion forces (Ivanisevic et al. 2001, Carpick et al. 1997). The most promising SAMs are formed on transition metal surfaces (e.g., Au, Ag, Si, Al) and surfactants with electron-rich head groups (e.g., S, O, N) and n-alkyl tails (Ulman 1996).

The self-assembled monolayers of thiols have been studied widely in recent years because they offer a rational and easy approach for fabricating interfaces with a well-designed composition, structure and thickness (Samuel et al. 2003). Alkyl thiols compounds and their derivatives are an exceedingly important and widely explored class of compounds for a host of different applications, particularly those in electro optical, biomedical and sensor related areas. In the field of electrochemistry, the strong interest in self-assembled monolayers based on thiols and related molecules are due to the following aspects:

- (1) They can be employed as insulating barriers between an electrode and a redox couple to study long range electron transfer.

- (2) They can be used to prepare microarray electrodes which have potential applications for creating selective voltammetric detectors or for measuring very fast electron transfer kinetics. Since pinhole and other defects may exist in the monolayer.

The most commonly studied and well-characterized self-assembling systems are alkanethiolate self-assembled monolayers (SAMs) on Au (111). Alkanethiolate SAMs form spontaneously on Au through chemisorptions of the S head group to the Au surface. The monolayers interact on the surface through van der Waals forces that occur amongst adjacent alkyl chains. The origin of the stability of SAMs is thus two-fold, due to the covalent S-Au bond and the attractive van der Waals forces between the methylene groups. As a result of the intrinsic stability of these systems, SAMs are known to have a low defect density and resist degradation in air. The process of self-assembly lends itself naturally to controlling the local placement of molecules. In particular, SAMs have been used as model systems for fabricating structures with controlled geometries, as well as essential components in the actual device (Hagenström et al. 1999, Samuel et al. 2003, Lemeshko et al. 2001).

Ordered monolayers of thiols on Au (111) have been widely used since they were discovered by Nuzzo and Allara. They have been studied by a variety of techniques that suggest dense packing of the chains and an absence of gauche defects. These studies have revealed the formation of S-S bonds at the metal interface, which indicates that not all the S atoms occupy the 3-fold hollow sites of the Au substrate as

assumed initially. A tilt of the molecular axis to about  $30^\circ$  from the normal is also observed and has been explained as a result of a space-filling configuration to maximize the van der Waals energy. This explanation is based on the molecular diameter of  $4.5 \text{ \AA}$ , which is smaller distance of the Au substrate. Other contributions to the tilt can be important, for example, the matching or in-phase locking, of C-C-C angles in adjacent chains. Fluorinated alkanethiols have also been studied. The diameter of the  $-\text{CF}_2-$  chains ( $5.76 \text{ \AA}$ ) is larger than the Au ( $5 \text{ \AA}$ ) distance and closer to  $2a_{\text{Au}}$  ( $5.8 \text{ \AA}$ ). Indeed, a hexagonal structure with  $5.8 \text{ \AA}$  periodicity is formed. However, the structure is incommensurate with the substrate by a  $30^\circ$  rotation. So it appears the S ends prefer again to bind to sites other than the 3-fold hollow sites which are usually the lower energy sites for S atoms adsorbing in hexagonal close packed surfaces (Ivanisevic et al. 2001, Carpick et al. 1997).

Alkylsiloxanes constitute (silanes group) another widely used class of self-assembling molecules. The active end group is  $\text{SiR}_3$ , where R usually stands for chlorine, ethoxy ( $\text{OCH}_2\text{CH}_3$ ) and other groups. These molecules also form compact and strongly bound monolayers on oxide substrates, notably  $\text{SiO}_2$ , in quartz and glass that contain surface hydroxyl groups. Besides many common characteristics with the alkanethiol, which derive from the similarity between the van der Waals chain interactions, the SAMs formed by the alkylsiloxanes exhibit some notable differences. The most important one is the covalent bonding between molecules by formation of siloxane bridges,  $\text{Si-O-Si}$ , linking adjacent molecules. This cross linking is absent in the case of thiols. Since the length of the siloxane bridge is  $2.6 \text{ \AA}$ , while the alkane chain diameter is  $4.5 \text{ \AA}$ , distortions at the head groups near the substrate are inevitable. Thus, while it has been established that the monolayer films are molecularly flat and have a thickness in agreement with their chain lengths, no long-range order has been detected by any of the aforementioned techniques. The importance of the intermolecular cross-linkage in stabilizing the film, particularly on mica, where no substrate OH groups are present, was demonstrated by a recent study by Xiao et al., using mono- and trisiloxane head groups. The former ones cannot form bonds to neighboring molecules and were found to form unstable films (Ivanisevic et al. 2001, Carpick et al. 1997).

### 1.1.1. Formation of SAMs

Self assembled monolayers are formed by the exposure of surfactant molecules on a solid surface. They have strong affinities for the substrate or a material patterned on it. Molecules binding to surfaces are described in terms of physisorption, in which the enthalpies of interactions are rather low (considered to be  $DH < 10$  kcal/mol, typically from van der Waals forces), or in terms of chemisorptions with  $DH > 10$  kcal/mol. Hydrogen bonding, donor–acceptor and/or ion pairing, and the formation of covalent bonds are strengthening between molecules and substrates (Rachel et al. 2004).

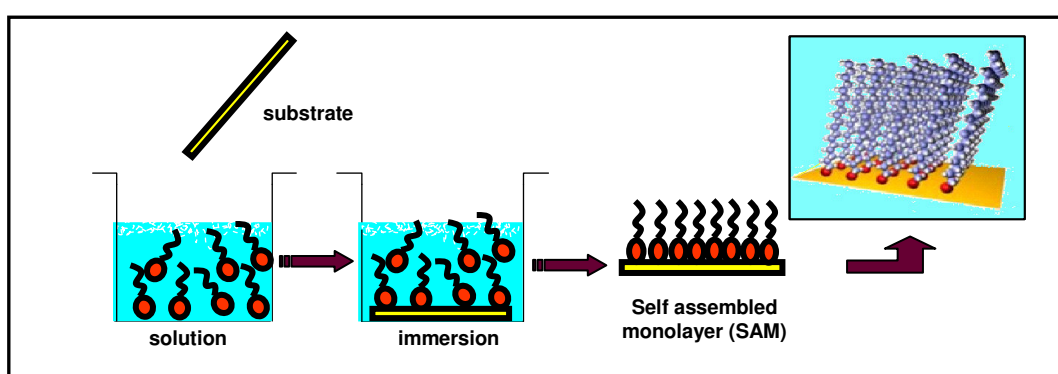


Figure 1.1. Formation of SAM by immersing a substrate in appropriate solution

Self-assembled monolayers (SAMs) are formed by immersing an appropriate substrate into a solution of an organic compound (surface-active material), possessing the ability to spontaneously form an ordered molecular layer on the substrate. The driving force for the spontaneous formation of the two-dimensional assembly includes chemical bond formation of molecules with the surface and intermolecular interactions. The order in these two-dimensional systems is produced by a spontaneous chemical synthesis at the interface, as the system approaches equilibrium (Figure 1.1). This simple process makes SAMs technologically attractive.

In detail, the constituting self-assembling surfactant molecules consist of three parts (Figure 1.2). The first part is the head group. It causes the exothermic process of chemisorptions on the surface of the substrate. It has specific affinity for the substrate. Organization of SAM starts with the interaction between the head and the substrate by means of chemisorptions and last to the thermodynamic equilibrium. The second part is the alkyl chain. It is responsible for the intermolecular distance, the molecular

orientation, and the degree of order in the film. The energies associated with the van der Waals interaction between alkyl chains are on the order of 10 kcal/mol (e.g. 14 kcal/mol for octanethiol (Nuzzo et al. 1990)). The third part is a functional group that constitutes the outer surface of the film. The principal driving force for the formation of these films is a specific interaction between the head group and the substrate surface. Provided these interactions are strong, SAMs form stable films. Also it is responsible for preventing formation of extra layer form. Alkyl chain and functional group are known as tail group together.

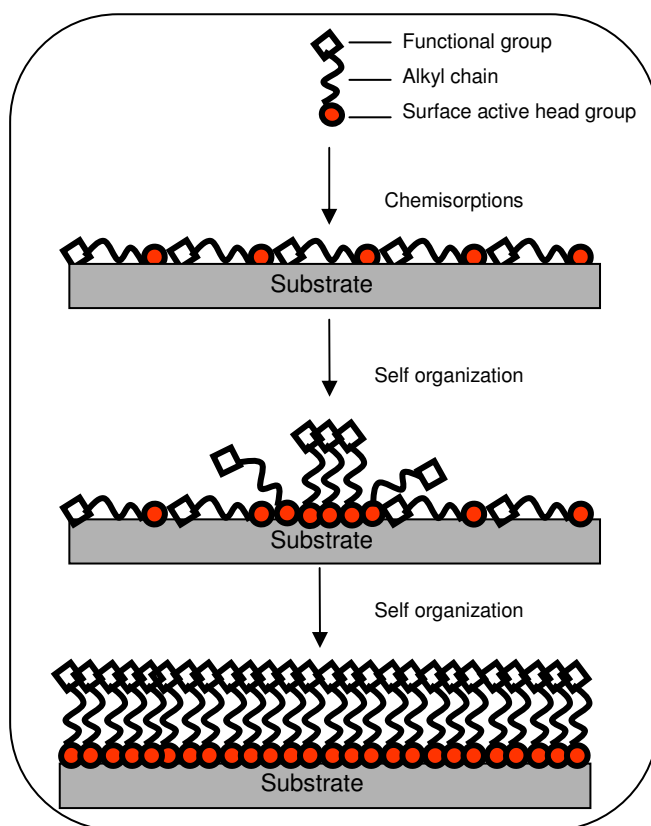


Figure 1.2. Schematic illustration of the formation of SAMs of surfactant molecules on a solid surface.

Depending on the structure of the molecules, these films can be disordered or well-packed (Figure 1.2). The degree of order in monolayers is a product of many factors, including geometric aspects, electrostatic, and dipole-dipole interactions within the monolayers. In 1983, *Nuzzo* and *Allara* showed that dialkyl disulfides (RS-SR) form

close packed and well-ordered monolayers due to strong Au-S bonds between sulfur atoms and gold (Nuzzo et al. 1983).

Under zero external loads, the film molecules exchange energy mostly by thermal processes. The short- and long-range structure of the monolayer is determined by intermolecular and substrate-film forces. The relative strength of these two interactions determines both the degree of order and the epitaxial relationship with the substrate. It is therefore useful to consider typical energy values for these interactions. In the common case of normal alkane chains, the van der Waals energy per CH<sub>2</sub> group in a close packed arrangement of straight, parallel chains at their crystalline separation of 4.5 Å, is 7 kJ/mol, provided that the chain length is above 6-8 carbon atoms long. This gives a total van der Waals energy of a C18 alkane of about 126 kJ/mol, which is comparable to the energy of a covalent bond, in the range of 100-300 kJ/mol. Thus we can predict that for short chains thiols (C<sub>n</sub>, n < 10), the molecule-substrate interaction is the dominating force, while for n > 12, chain-chain interactions play a determinant role. Studies that were made by using polycrystalline Au substrates show that closed packed hexagonal structures are formed by C18 thiols even in areas of the sample where the Au substrate is disordered, or at least not of (111) orientation. This indicates that for these chain lengths, the chain-chain interaction is the dominating force for the ordering of the long chain thiols. For alkylsilanes, covalent bonding between the chain heads, in addition to head-substrate bonding, will be a dominant interaction (Ivanisevic et al. 2001, Carpick et al. 1997).

### **1.1.2. Parameters Affecting on SAM Formation**

SAMs provide the needed design flexibility, both at the individual molecular and at the material levels. They also offer a vehicle for investigation of specific interactions at interfaces and of the effect of increasing molecular complexity on the structure and stability of two dimensional assemblies. So, to be able to prepare good prepared SAM films, some parameters must take into account. Low quality SAMs will lead to low quality results. The quality of the monolayer formed is very sensitive to reaction conditions.

The structural properties of the SAMs are strongly influenced by the interactions between the functional groups comprising the tails of the molecules. The molecule

ordering in SAMs is largely governed by molecular-substrate interactions, lateral chain-chain interactions are also quite important. In some cases, SAMs with short alkyl chains exhibit quite different film characteristics than with long alkyl chains. The length of the alkyl tail and the nature of the end group all impact on properties such as the angle of tilt with the surface and the extent of motion within the monolayer itself. The unique feature of a SAM is that the long chains work together to align neighboring molecules into a collective orientation. The advantage of using long chain is it increases value of van der Waals forces as additional molecules, and this cause increasing order of SAM. On the other hand, to use long chain causes rising in molecular weight and this is concluded with the deviation from the tilt angle. Beside this affect, because of molecules motion, increasing chain length causes rising formation time. The molecules move as; after binding a surface they are turning around theirself till equilibrium state. Formation time increases with increasing length. The tail groups are found to have a profound influence on the structure of the SAMs. This knowledge will undoubtedly prove useful in controlling the surface densities and lattice structures of SAMs in technological applications that employ these species.

It is no doubt that the lateral interactions play a key role in the molecular rearrangement at the 'physisorption' stage, and they may be responsible for the formation of metastable structures as well. These kinetically trapped structures can be relaxed or rearranged at the 'chemisorptions' stage. Due to formation of metastable structures, these SAMs are expected to comprise locally at samples surfaces. This also causes different molecular packing (Tamada et al. 1998).

In order to form structure of SAM, time has an effective role. Inefficient time causes incomplete composition. Since, to obtain well-ordered SAMs, convenient formation time which changes from molecule to molecule is required. Molecules in solutions find the surface for bonding by means of physisorption, and then they get a grip via to chemisorptions. This process changes from molecules to molecules. From chain to structure all individual properties affect this process. It can be said that, lack of time causes incomplete structures whereas enough time is needed for obtaining complete structure. Extra time may not produce serious problems but it can cause collapse of molecules. After forming SAMs if there are more free molecules in solution, since there is not any place for them on substrate surface, they mostly stay in solutions. In generally in literature, suitable time for SAM formation on substrate is more than 24

hours. The limited point here, SAMs formation lasts from the initial adsorption to the final thermodynamic equilibrium (Figure 1. 3).

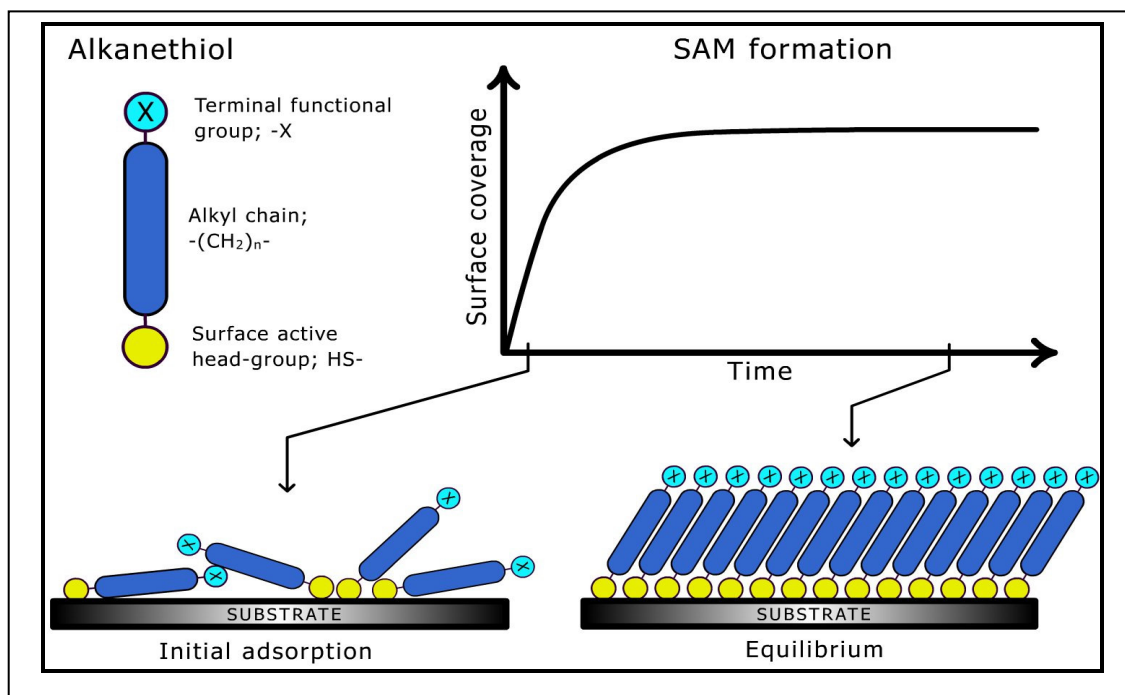


Figure 1.3. Schematic illustration of an alkanethiol with its principal components of time, and the formation of the self assembled monolayer.

Even though a self-assembled monolayer forms very rapidly on the substrate, it is necessary to use adsorption time of 24 hours or more to obtain well-ordered, defect-free SAMs. Multilayers do not form, and adsorption times of two to three days are optimal in forming highest-quality monolayers. It is also observed that it is possible to decrease defects by means of increasing time. Figure 1.3 simply demonstrates the time affect on SAM formation.

SAMs are differentiated from general amphiphilic surfactant monolayers by the molecular structures that have end functional groups that interact favorably and specifically with a solid substrate. Because of specific interactions between molecules and substrates, SAMs are formed with various solvents and diversely designed molecules resulting in controlled and modified surface properties. Several different solvents are usable at the low concentrations (typically 0,1-2 mM) that are used in preparation of SAMs. The most commonly used solvent is ethanol and water. It is advisable to minimize the water content in the solvent of ethanol. Since, it uses for

molecules which do not solve in water. Water content and more concentration cause defects on SAMs formation besides steric affects. Low concentration is preferred due to giving opportunity to the molecules to found a place on substrate and it reduces the steric affect. To make this process, solubility properties are gained fairly importance. To decrease molecular density SAMs need to be solved in their prefer solvents.

The other important parameter that plays significant role on SAM formation is water especially for water-soluble molecules. Concentration determines most of SAMs formation. Absence of water causes incomplete monolayers whereas excess water results in facile polymerization in solution and deposition on surface. Besides polymerization, solubility and density properties are also affected by water impact. Like water insoluble molecules, low concentration prefers for water soluble one. In this condition, to increase or decrease molecular densities water is used. Inconvenient concentration can also cause defects on SAMs formations.

Contact shape of molecules to surface can be counted as another factor that affect on SAMs formation. While the molecules are tied to substrates, they can also make angle with the surface which depends on individual properties of molecules. In the literature, the highest contact angle was recorded on monolayer where the diacetylene group is connected to carboxylic head group.

Defects are one of the parameter that affects SAMs formation. Both substrates and film defects that observed after formation can be effective parameter on SAMs. Naturally occurring defects within SAMs, such as domain boundaries, substrate vacancies, and lattice vacancies, can be utilized as "placeholders" for insertion of individual molecules. There are two kinds of defect in a thiols monolayer, pinhole and collapsed-site defects. A careful study of the literature on pinholes reveals that thiols monolayers usually contain electrochemically measurable pinholes when the adsorption time is short, but when the adsorption time extends to hours or a day, the monolayer is usually free of measurable pinholes. This means the condition of the defects keeps changing with increasing adsorption time (Diao et al. 2001).

In preparing SAMs contamination, smoothness, drying, temperature and size of the SAMs molecule are of course highly important. Except for temperature and size of molecules effects, the others cause defects on films. The effect of temperature and molecule size has not been clear yet. It is seen that they have ability to change reaction kinetics. Using bigger molecule causes better bonding with the surface and higher kinetics of reaction. It is thought that this effect can be related with the higher electron

density of the bigger molecules. Temperature has highly interesting effect on SAM formation. High or low temperature cause spoilt on organics and this can prevent SAMs formation on substrates (Diao et al. 2001). As a consequence of thermodynamics low temperature decreases the reaction kinetics. High temperature also damages the bond formation as well as increasing reaction kinetics. For example, after 100 °C for thiols sulphur bonds on gold surface are damaged (Ulman et al. 1996).

As the SAM formation highly sensitive to reaction conditions every condition affects the structure properties. It is possible to control structure formation by making the reaction conditions optimum. To work on optimum conditions cause low defects formation. So, it can be said that reaction conditions and their affects are the most important parameter. Among these conditions, some of them are clear but the some other not. The role of wetting properties, binding geometry and binding strength are not clear so far. Some experiments shows that wetting properties of the SAM solution can be related with the chain tilt but there has not been supporting evidence yet.

## **1.2. Nanolithography**

Nanolithography is the art and science of etching, writing, or printing at the microscopic level, where the dimensions of characters are on the order of tens of nanometers. It is also a term used to describe a number of techniques for creating incredibly small structures. The word lithography is used because the method of pattern generation is essentially the same as writing, only on a much smaller scale. This includes various methods of modifying semiconductor chips at the atomic level for the purpose of fabricating integrated circuits (ICs).

Lithography was introduced in 1798 as a printing tool by Alois Senefelder, who found that ink adsorbed to an image drawn with a greasy fluid onto limestone (Figure 1.4) and it could be used to transfer the image to a piece of paper pressed against the stone (Wouters et al. 2004).

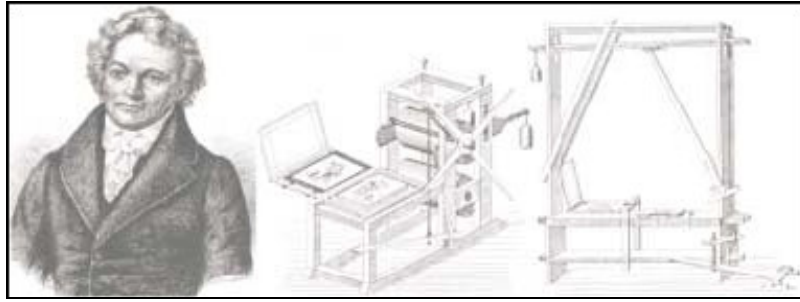


Figure 1.4. Lithographic stones were introduced by Alois Senefelder  
(Source: Wouters et al. 2004).

Since then, this printing technique has evolved dramatically and is nowadays not only used for printing but also for the (chemical) modification of substrates on a submicrometer scale, and is often referred to as microcontact printing.

Lithography is widely used in the semiconductor industry. The ongoing miniaturization in size and integrity of electronic and mechanical devices has led to an interest in the fabrication of nanometer-sized uniform structures on surfaces. With the development of (computer) chips and their increasing complexity, the requirement for techniques able to create smaller structures is ongoing. With downscaling device dimensions to the nanometer range, a current interest has been focused on the state-of-the-art lithographic development such as electron beam lithography, UV lithography, and scanning probe microscope (SPM) lithography.

One common method of nanolithography which is used particularly in the creation of microchips is known as photolithography. The size regime for devices produced by photolithographic techniques is limited. However, because if the wavelength of light used is made too small the lens simply absorbs the light in its entirety. This means that photolithography cannot reach the super-fine sizes of some alternate technologies.

An alternative technique that allows for smaller sizes than photolithography is that of electron-beam lithography. Using an electron beam to draw a pattern nanometer by nanometer, incredibly small sizes (on the order of 20nm) may be achieved. Electron-beam lithography is much more expensive and time consuming than photolithography, however, making it a difficult sell for industry applications of nanolithography (Lee et al. 2001, Bates et al. 2001).

New nanolithography technologies are constantly being researched and developed, leading to smaller and smaller possible sizes. Therefore, other patterning techniques have been intensively studied to create smaller structures. Scanning-probe-based patterning techniques, such as dip-pen lithography, local force-induced patterning, and local-probe oxidation-based techniques are highly promising because of their relative ease and widespread availability. With the application of probe-based techniques, control over position and direction is evident. In these techniques a small tip is used. Finally, not only patterns on substrates can be created, but also chemical modification reactions on specific substrates are accessible. The latter of these is especially interesting because of the possibility of producing nanopatterns for a broad range of chemical and physical modification and fictionalization processes. Both the production of nanometer-sized electronic devices and the formation of devices involving (bio) molecular recognition and sensor applications are possible.

SPM has demonstrated capabilities for atomic-level manipulation and also potentiality for local modification of various surfaces using different approaches such as exposure of organic thin films and a selective anodic oxidation of various substrates. Those investigations have largely been motivated to evaluate the potential use of a SPM in the fabrication of nanostructures in an atomic resolution. Especially, atomic force microscope (AFM) is a most promising method for fabricating organic thin films or substrates itself in nanometer scale (Lemeshko et al. 2001).

Instruments used in nanolithography include the scanning probe microscope (SPM) with the atomic force microscope (AFM). The SPM allows surface viewing in fine detail without necessarily modifying it. Either the STM or the AFM techniques can be used to etch, write, or print on a surface in single-atom dimensions.

### **1.3. Scanning Probe Microscope Lithography**

Creating structures having nanometer sizes is a scientific and technical challenge that has been addressed for terms of years. Clearly, physicists are able to combine atoms, chemists create molecules and biologists create biomolecules with sizes on the nanometer scale. A greater challenge is to engineer structures in the mesoscopic scale of 10 - 1000 nm. Methods for creating mesoscopic structures include optical lithography, and ebeam lithography. But, these techniques are limited in their use to few research

groups because of their expensive costs. With the Scanning Probe Microscopy (SPM), it is now possible to create mesoscopic size devices for a lower cost.

SPM is a technique that is used to study the properties of surfaces at the atomic level. A Scanning Probe Microscope scans with an atomically sharp probe on a surface, typically at a distance of a few angstroms or nanometers. The interaction between the sharp probe and surface provides a three-dimensional topographic image of the surface at the atomic scale. Lithographic techniques based on scanning probe techniques are the method of choice for applications in nanotechnology. There are two methods in Scanning Probe Microscopy: Scanning Tunneling Microscopy (STM) and Atomic Force Microscopy (AFM).

The period of SPM started with the scanning tunneling microscope (STM) in 1981. The first atomic resolution images were reported under ambient conditions. STM uses the quantum mechanical tunneling effect to determine the distance between the probe and the surface. Typically, the STM is set up to scan a surface at a constant distance away from the surface. Naturally, the probe will have to be moved up and down to follow the height of the surface, and this up and down motion can be used to make a three-dimensional image of the surface. Since the invention of the STM, development of various scanning probe instruments has been quite rapid. The AFM has been one of the most important and used techniques in the literature.

AFM was invented by Binnig, Quate, and Gerer in 1985 (Binnig et al. 1986). The AFM uses various forces that occur when two objects are brought within nanometers of each other. The basic AFM works by scanning a tip over a sample, and measuring the deflection of the tip by the repulsive force between the atoms of the tip and sample. The interaction force between a sharp probe and the sample surface is used to characterize the sample surface in atomic size range. An AFM can work either when the probe is in contact with a surface, causing a repulsive force, or when it is a few nanometers away, where the force is attractive. AFM has the potential to investigate numerous additional material properties, such as friction forces and adhesion between tip and sample surface, hardness and electrical properties of the sample, such as conductivity and magnetic properties (Richard et al. 1997).

In an AFM experiment, a small sharp tip (with a radius typically between 10-100 nm) is attached to the end of a compliant cantilever. The tip is brought into close proximity with a sample surface. Forces acting between the AFM tip and the sample will result in deflections of the cantilever. The cantilever bends vertically in response to

attractive and/or repulsive forces acting on the tip. These measurements can be performed in a variety of environments: ambient air, controlled atmosphere, liquids or ultrahigh vacuum. AFM is certainly the most versatile tool for nanotribology in terms of operating environment.

The field of probe lithography can be classified into two main areas: chemical (electrical) and physical (mechanical) surface modification

### **1.3.1. Electrical Surface Modification**

Electrical surface modification is also known as chemical surface modification. The category of chemical modification processes includes experiments that use local oxidation processes. This process was first observed in STM experiments, but has also been transferred to AFM and can be applied to conducting (metallic) substrates as well as to thin layers of nonconducting (organic) resists. Electrically conducting AFM probes can be used to chemically modify a surface to draw an image. Voltage bias between a sharp conductive oscillating AFM tip and a sample generates an intense electric field  $E$  at the tip. The oscillating high electric field desorbs the hydrogen on the surface and enables to oxidize exposed substrates in air very quickly. For example, applying an electrical bias between the conducting probe and a substrate can locally oxidize selected regions of the surface to form patterns. This method allows achieving sub-50 nm feature sizes.

With the help of the Voltage Lithography not only geometrical properties of the surface but also the local electro physical properties of the sample surface can be changed. For example, by application of voltage to conductive cantilever the electrochemical processes on the surface can be stimulated under the probe tip and metallic layer can be oxidized.

In air or other humid atmosphere the probe and the surface of the sample are covered by thin film of absorbed water. When the tip approaches sufficiently close to the surface, these absorbed layers come in contact and water bridge is produced because of capillary effect. With application of a corresponding electric field the electrochemical reaction in water-surface border, in water and in the probe will be initiated through that bridge. If the surface is positively charged and the tip negatively, then the tip and the

surface will interact electrochemically as anode and cathode correspondingly. Oxide will grow on the point right under the tip.

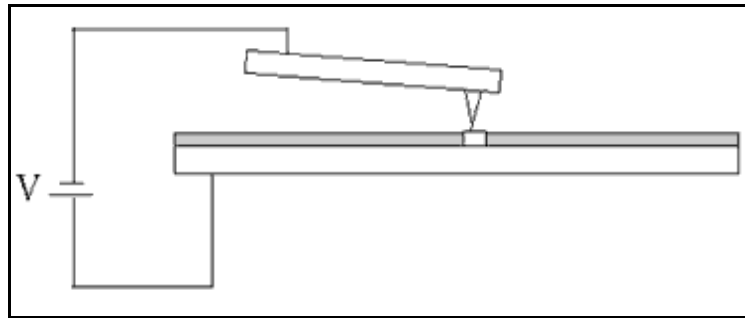


Figure 1.5. By placing a bias between an electrically conductive probe and a surface, the surface can be modified.

The resolution of the pattern obtained by electrically oxidation lithography depends on the following parameters:

- Diameter of the probe
- Voltage between probe and surface (applied bias voltage)
- Oxidation time
- Substrate temperature

Diameter of the probe is related with the pattern size. Since, pattern obtains by motion of the probe on the selective areas. Higher diameter prevents the better form. Because it effect more place this means to more oxide layer, debris and also unclear patterns. To increase applied voltage or oxidation time also make the same effect. But under convenient limited high voltage or time give better result for patterning. Since, it is needed to use enough voltage and convenient oxidation time to observe patterning. Substrate temperature has an affect on oxidation kinetics. To increase temperature increases the kinetics. On the other hand, much higher temperature can cause preventing patterning. Since high temperature can spoil the surface.

### 1.3.2. Mechanical Surface Modification

It is also known as force lithography or physical surface modification as the formation of patterns by the physical movement of material on a substrate (for example, by applying a high contact force). It is used for electron device fabrication. Moreover, dip-pen lithography, in which atoms and molecules attached by adhesion to a tip can be transferred to a substrate in a controlled fashion. In this process, chemical bonds are neither created nor broken.

The Atomic Force Microscope was initially developed to image the surfaces of insulating materials. However, it also was found useful since the AFM probe could cause mechanical modifications to a surface. Such mechanical modifications can now be used proactively to alter surface topography.

Force lithography is based on direct mechanical impact produced by a sharp probe on the sample surface. The probe tip pressure on the surface is sufficient to cause plastic deformation (modification) of the substrate surface. This type of modification has a range of applications in nanoelectronics, nanotechnology, material science, etc. It enables the fabrication of electronic components with active areas of nanometer scale, super dense information recording and study of the mechanical properties of materials.

Two types of mechanical surface modifications are possible; nanoindentation and nanoscratching techniques. For the first technique, the probe is pushed into the surface. In the second technique, a line is scratched on the surface (Figure 1.6). Both of two techniques consist of removing material from the surface leaving deep trenches and debris with the characteristic shape. Also for this techniques, there is no additional process is needed. Figure 1.6 shows how the mechanical surface modification occurs.

In nanoindentation technique the surface is modified by indenting it with a vibrating tip in the AFM semicontact mode. This method provides a lithography technique that is nearly free from problems due to cantilever torsion and permits to image the modified surface without any further modification.

Nanoscratching technique is the most common, the tip is scanned under strong loading forces to remove the substrate or resist. This technique utilizes the principle of scratching in the same way as the traditional tool: Material is removed from the substrate in a well-defined way, leaving behind deep trenches with the characteristic shape of the scratch used. The advantages of applying a nanoscratching for lithography

are obviously the precision of alignment, the no damaging definition process compared to electron- or ion-beam structuring techniques, and the absence of additional processing steps, such as etching the substrate. Nanoscratching was applied, for example to defining superconducting nanoconstrictions (Josephson junctions), surface quantum wells patterning.

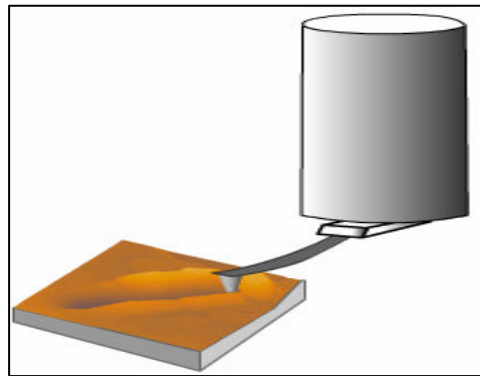


Figure 1.6. By means of applying a high contact force on a sample, patterns are created in mechanical surface modification

The size of the features made by scratching nanolithography technique depends on the following factors:

- Surface Material (hardness)
- Probe Diameter
- Probe Material (hardness)
- Force of the Probe on the Surface
- Probe Temperature

The hardness of the probe material shall exceed that of the sample. Also, the cantilever sticking and the material pickup shall be avoided. Small sample roughness is required. Moreover, the sample surface has to be clean. Force lithography is best performed on soft materials. Surface and probe material affect applied force on the probe surface. To use hard surface material causes increasing in force whereas to use hard probe material causes decreasing in applied force. To create pattern convenient force is necessary. Like oxidation lithograph, probe diameter is related with the patterns size, shape and debris. Probe temperature affects the patterning ability. It makes the process easy.

The force lithography can be carried out using two modes: raster and vector. In the case of vector lithography the influence is applied in single points or along the determined lines. The software provides a set of commands that permit to write lines of arbitrary length and direction with defined scan speed and oscillation amplitude.

In the case of raster lithography it is made from the already determined template. The image pattern scan mode is a synchronization of the raster scan mode with the desired pattern. The pattern can be constructed with a simple pixel-oriented paint program. In raster lithography method Set Point value clasified into two part; level1 and level2

Level 1 is the Set Point value when the probe moves from one template object to another. Typically, this value is equal to Set Point in scan settings for the contact mode and depends on the sample.

Level 2 is the Set Point value when the probe moves along the template lines and in its points. It determines the amount of force applied to the sample.

The advantage of vector lithography is a high speed while disadvantage is that the force is equal in each point. Raster lithography is slower, but it enables to change the force applied according with the template. Besides there are two ways to change the applied force when making vector lithography:

1. Changing of the beam bending by setting of the scanner displacement on defined distance along Z axis.
2. Changing of the beam bending, by setting of the SetPoint value. When doing raster lithography you can use only the first way.

Any atomic force microscope can be used for creating nanometer-sized patterns on a surface. However, the quality and complexity of the patterns depends on specific scanning probe hardware and software. The method of patterning is determined by the types of probes, substrates and the specific software performance capabilities used to drive the scanning probe tool.

The most critical hardware feature that is required is an X-Y calibration system. Because the piezoelectric ceramics used in AFM have unwanted characteristics such as creep and hystercics, calibration sensors are necessary to guide the motion of the probe. Without the calibration sensors, the probe moves in an unpredictable motion, and it is hard to write complex patterns. Because the instrumentation has X-Y calibration sensors, a higher quality pattern is possible.

Software is used for defining the pattern that will be drawn with an AFM and then for drawing the pattern on a materials surface. In this study *Nova 876 and Nova 914* were used as software. All parameters that related to the lithography and the others could be controlled easily.

#### 1.4. AFM Surface Characterization Techniques

Since its invention, the goal of AFM has been to image surfaces without causing surface damage. However, the imaging of soft (organic) materials in contact mode (with relatively hard tips and stiff cantilevers) leads to surface damage. Therefore contact-mode AFM for these kinds of samples is usually displaced by noncontact or semi-contact AFM to reduce tip-induced surface damage. The concept of the controlled mechanical deformation of substrates using standard AFM tips can be transferred to almost any substrate. The limiting factor in creating reproducible patterns is the stability of the tip itself, which has a tendency to deformation and contamination. To prevent excessive deformation, several groups have used diamond or diamond coated tips. Mechanical patterning (force lithography) has successfully been applied to substrates and films of soft metals

Before mentioned about its affinity on characterization, it is need to define some important parameters of AFM such as DFL, LF and laser. It is necessary for understanding to determine force calculations.

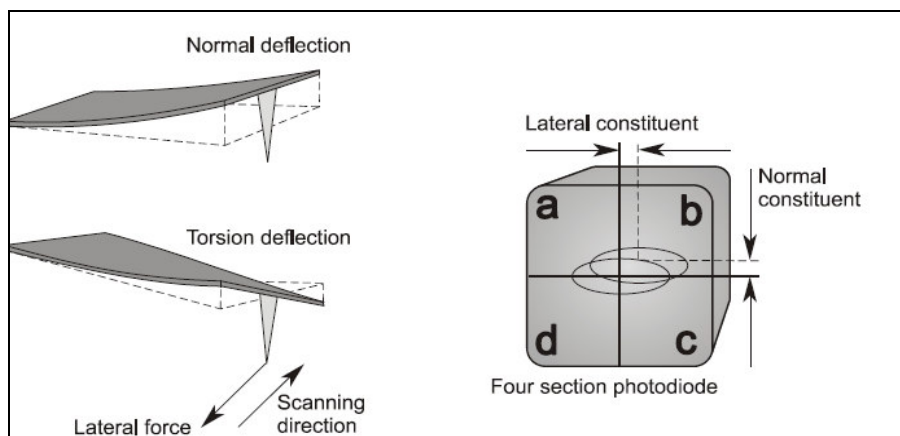


Figure 1.6. Demonstration of both deflection and detection of laser on tip and photodiode respectively

DFL is the signal related with the magnitude of deflection of the probe with respect to the normal. The DFL signal is the difference between signals from top and the bottom halves of the photodiode  $DFL = (A+B) - (C+D)$

LF is the signal related with the torsion deflection of the probe caused by lateral forces the torsion deflection of the probe causes the laser beam reflected from the probe to shift in the lateral direction. The corresponding signal LF is the difference between signals from the right and left sides of the photodiode.  $LF = (A+C) - (B+D)$ .

LASER is the integrated signal from all the four sections of the photodiode. This signal is proportional to intensity of the laser beam reflected from the probe.  $LASER = A+B+C+D$ .

Signals DFL and LF are used during alignment of the registration system to control the pointing of the laser beam at the tip of the probe. Once the laser beam is precisely at the probe tip, the values of DFL and LF are equal to 0. The value of signal intensity, LASER, should be set maximum.

Taken signals converted into images by the help of software. Beside topographic images, phase is also used. The Phase detector generates a signal, phase, whose value variations are proportional to variations of the probe oscillation phase shift with respect to the excitation signal. Signal phase is the sum of the probe oscillation phase shift with respect to the excitation signal and the phase shift between the excitation and reference signals (with accuracy to a constant). When scanning in the Phase Imaging mode, the tip of the oscillating probe periodically comes in touch with the sample surface. Its behavior is affected by the influence of various repulsive, adhesive, capillary and other forces. This can affect both the oscillation amplitude and phase. If the sample surface is inhomogeneous by its properties, this correspondingly results in some shift of the phase. The phase shift distribution over the sample surface visualizes distributions of characteristics of the sample substance. The Phase Imaging technique yields valuable information for a broad area of applications. In some cases it can uncover hidden contrasts in materials properties.

#### **1.4.1. AFM Surface Characterization with Contact Mode**

In Contact mode of operation the cantilever deflection under scanning reflects repulsive force acting upon the tip. Repulsion force  $F$  acting upon the tip is related to

the cantilever deflection value  $x$  under Hooke's law:  $F = -kx$ , where  $k$  is cantilever spring constant. The spring constant value for different cantilevers usually varies from 0.01 to several N/m. In our units the vertical cantilever deflection value is measured by means of the optical registration system and converted into electrical signal DFL. In contact mode the DFL signal is used as a parameter characterizing the interaction force between the tip and the surface. There is a linear relationship between the DFL value and the force. Too tight mechanical contact between the probe and the sample may cause damage to the conductive coating of the cantilever.

Contact methods of atomic force microscopy are based on surface topography measurements during contact scanning of the sample surface. It is classified into two groups; contact force and contact height methods.

In the Constant Force Method, which is the main technique, a constant value of contact force between the sample and the probe is maintained during scanning. The contact force constancy is performed by keeping the DFL signal constant and is maintained by means of a feedback system which controls vertical displacement of the probe. In this technique, the vertical driving signal, which is applied to the Z section of the piezo scanner, is used to build an image of the surface topography.

Constant Force mode has some advantages and disadvantages. Main advantage of Constant Force mode is possibility to measure with high resolution simultaneously with topography some other characteristics Friction Forces, Spreading Resistance etc. Constant Force mode has also some disadvantages. Speed of scanning is restricted by the response time of feedback system. When exploring soft samples they can be destroyed by the scratching because the probe scanning tip is in direct contact with the surface.

In Constant Height Method, the probe is in permanent contact with the surface. The probe's tip is maintained at a constant height, while the value of deflection of the probe contains information on the sample surface topography. The speed of surface topography measurements is limited in this method by resonance properties of the probe. This is unlike the Constant Force Method, which is limited by properties of the feedback system. Resonance frequencies of probes are much greater than the characteristic frequency of the feedback system, which is equal to several units of kHz. This gives an opportunity to scan samples at higher speed. Assume that the relationship between the value of the probe deflection versus the distance from the tip of the probe and the surface is known for a given probe (i.e. the relationship between the DFL signal

and the distance  $Z$  from the tip of the probe and the surface). Then an image of the DFL signal distribution can be converted into a topography image.

Constant Height mode has some advantages and disadvantages. Main advantage of Constant Height mode is high scanning speeds. It is restricted only by resonant frequency of the cantilever. Constant Height mode has also some disadvantages. Samples must be sufficiently smooth. When exploring soft samples they can be destroyed by the scratching because the probe scanning tip is in direct contact with the surface (Magonov 1996).

### **1.4.2. AFM Surface Characterization with Semicontact Mode**

During operations in the semicontact mode, the probe oscillation amplitude is used as a parameter to characterize the interaction between the probe and the sample surface. Operation with the scanning probe microscope in the mode when the probe oscillation amplitude is kept constant is the basis mode for topography measurements.

Measurements of the probe oscillation phase shift (signal Phase) are performed in this mode. When the oscillating probe comes in contact with the sample surface, it experiences both repulsive and also adhesive, capillary and some other forces. As a result of such interactions, a shift of both frequency and phase occurs. If the sample surface is inhomogeneous by its properties, the phase shift distribution will also be inhomogeneous. A distribution of the phase shift over the sample surface reflects distributions of properties of the material under study.

Possibility of scanning sample surface not only in attractive but also in repulsive forces was demonstrated in. Relatively small shift of oscillating frequency with sensing repulsive forces means that contact of cantilever tip with sample surface under oscillation is not constant. Only during small part of oscillating period the tip feels contact repulsive force. Especially it concerns to oscillations with relatively high amplitudes.

The Semicontact mode can be characterized by some advantages in comparison with Contact mode. First of all, in this mode the force of pressure of the cantilever onto the surface is less that allows working with softer and easy to damage materials such as polymers and bioorganic. The semicontact mode is also more sensitive to the interaction

with the surface that gives a possibility to investigate some characteristics of the surface distribution of magnetic and electric domains, elasticity and viscosity of the surface.

During operation in this mode, scanning is performed with a probe oscillating at the surface of the sample. The probe oscillates in the vertical direction at its resonant frequency (or close to it). Generation of mechanical oscillations of the probe is done by means of a piezo drive, which is in direct contact with the chip of the probe. Specifics of this technique are linked with the fact that the oscillating probe is so close to the sample surface that, while scanning, it slightly touches the surface. Most of the oscillation time the probe is not in contact with the surface and its interaction with the sample is relatively weak. Only on approach to the surface, up to the region where the interaction potential becomes repulsive, the interaction effect becomes significant. During this impact the probe loses the energy accumulated during the rest of the period. Depending on the character of interactions, such parameters as the main harmonic phase shift and, also, amplitudes and phases of higher harmonics can alter with respect to the excitation signal. The laser beam of the registration system is reflected from the oscillating in the vertical direction probe. These oscillations of the probe result in oscillations of the laser beam spot with respect to the top and bottom halves of the photodiode. This induces a variable electrical signal, at the probe oscillation frequency, at the output of the registration system. The amplitude of this signal is proportional to the oscillation amplitude of the probe. In the case under consideration this signal is the variable component of the DFL signal detected at the probe oscillation frequency. Therefore the registration system measures the probe oscillation amplitude and converts it into an electrical signal in the form of a variable component of the DFL signal. Then, processing of the variable component of the DFL signal takes place: filtering, amplification and detection.

### **1.4.3. AFM Spectroscopy**

In the ideal case, the probe is assumed to be terminated by a single atom, which implies that the AFM tip contacts directly the sample surface on an atomically small area. Many types of forces (attractive, repulsive, van der Waals, electrostatic) may be encountered when tip approaches the surface. There are different force regimes in which forces can be measured with AFM. Two force regimes can be distinguished; the

attractive regime, where interaction forces attract the tip to the sample but actual mechanical contact does not occur, and then the repulsive or contact regime, where the outer electronic configuration of tip and sample atoms provide electrostatic (Robert et al. 1997).

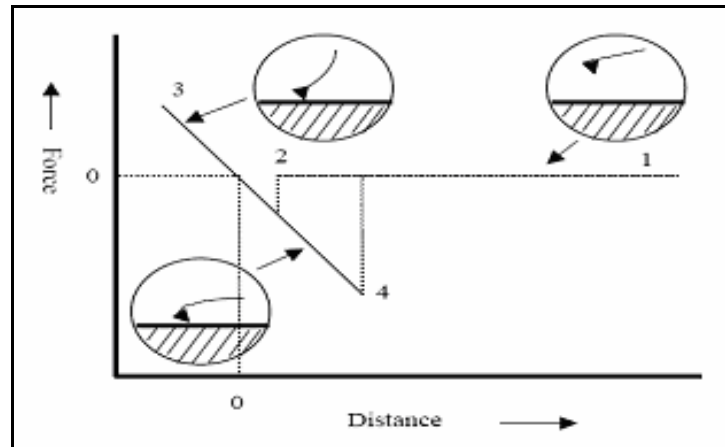


Figure 1.8. The typical force-distance curve with the tip position

Force-distance curves demonstrate the interaction between tip and sample. The typical force-distance curve is shown in figure (Figure 1.8).

At long distances between tip and surface, there are no interactions. The observed force is zero. (A straight line between 1 and 2, unless there are electrostatic forces). As the tip approaches the substrate, it jumps into contact due to attractive van der Waals interactions at the position 2. As the sample moves towards the tip (or the sample), the repulsive force dominates in total force (at position 3). When the sample is retracted, the force is reduced along the line from position 3 to 4. Under the zero force line in the graph, the net force acting on the cantilever becomes attractive by adhesion to hold tip on the surface. At position 4, as the tip (or the sample) is retracted further, the tip (or the sample) jumps off. For optimum AFM measurement, the force is usually set along the line between position 3 and 4 to minimize the contact force.

The direct modification of silicon and other semiconductor and metal surfaces by the process of anodization using the electric field from a SPM was the most studied subject of the literature. It was demonstrated that this procedure was the one promising method of accomplishing direct-writing lithography for the electron device fabrication. In most studies; the technique involved the application of an electrical bias to both the

conducting probe and the sample substrate to locally oxidize selected regions of a sample surface. SAM films consisting of organosilane, and bipolar amphiphilic, alkanethiol molecules show a great potential as ultra thin resist films. Such SAM films formed through the chemisorptions onto oxide and metal surfaces have excellent uniformity in molecular order and resistivity to various types of chemical reagents. Since most of lithographic works with organic resists have been exclusively carried out on silicon surface for practical application, so several organic resists with different function groups have been studied in order to investigate the surface group effect on the anodization using AFM and STM. The investigations from the literature showed that gold particles were particularly easy to modify among the all studies. (Mizutani et al. 1998, Xu et al. 1997, Liu et al. 2000).

## **1.5. Substrates and Organics**

### **1.5.1. Substrates**

Gold is the most used substrate and thiols are the most used organic groups. Gold is the most preferable substrate in literature because of its chains ability to interchange, ease of mobility and lack of oxidation. Since AFM does not require the substrate to be conductive, the choice of substrates is almost unlimited. In this study, setting off from the unlimited substrates ideas, a number of specimen supports have been used, among which the most important are silica, n and p type silicon, titanium thin film on silicon and mica. Also gold film that deposited on mica has been used to study scratching nanolithography technique on metallic surfaces.

#### **1.5.1.1. Mica**

Mica which is a non- conducting layered material is the most commonly used substrate for scientific researches. It is cheap and can easily be cleaved to produce clean, atomically flat surfaces up to even millimeters in size. The commonest form of mica is Muscovite  $\text{KAl}_2(\text{OH})_2\text{AlSi}_3\text{O}_{10}$ . It has hexagonal lattice with the hexagonal lattice constant within the layers, which can be used for calibration, is 0.52 nm. The root-mean-square roughness is  $0.06 \pm 0.01$  nm (Kindt et al. 2002). Mica has been

successfully used in numberless studies especially for AFM imaging of DNA studies. Highly charged properties of mica's surface leads the fact that it is always covered with a thin layer of water of approximately 0.5 nm when exposed to surrounding air. This water layer leads to a continuous adhesion between AFM tip and sample (Silva et al. 2002). Despite the common use of these substrates, the mechanism of adsorption is not well understood. For both glass and mica in hydrous area, it is known that positive ions tend to dissociate from the surface to make them negatively charged (Shao et al. 1996). Besides all this properties, the most important reason to use mica in this work is its firm structure. Under high forces mica deforms locally as a crack form. So it is impossible to scratch mica surfaces. In this study, however the value of applied forces reached 50.000 nN, there was no deformation on mica surface. This situation makes the mica convenient for this study.

### **1.5.1.2. Silica**

Glass otherwise silica is the most usable substrate in scientific researches. It has low cost in price and ease to find. Glass that has an amorphous structure is flat enough for imaging cells or other large and relatively high samples. On the other hand glass is generally too rough for reliable visualization of DNA. Besides this, glass is the best suited for all experiments in which visible light is transmitted across the sample, as in scanning near field optical microscopy or in the combined light- microscopy and SPM. Without cleaning some contaminations or defects can be observed. In this work; glass was cleaned by means of ultrasonic cleaner. In this method; glass rinsed into acetone and redistilled water respectively in ultrasonic cleaner then dried with argon spray. With this procedure glass surface unmodified or altered to change their physisorption or chemical properties. The surface should be almost featureless on the scale of macromolecular specimens.

### **1.5.1.3. Silicon**

Silicon is very important substrate in technology especially in semiconductor industry as well as thin film experiments. Since part of silicon wafers mostly used in semiconductor industry can be used as substrate. Economical reasons also have

important role for choosing silicon as a substrate. It is easy to oxidize silicon surfaces at room conditions. They have a thin oxide layer on their surface which makes them hydrophilic because of the OH groups on the surface. Silicon has diamond crystal structure with 0.357 nm in lattice constant. There are two types of silicon known as n and p type. Like other samples silicon substrates should be cleaned. In this study p type (111) silicon wafers polished one side type V\_DEL P.O. # B289160-6 models were used. n type silicon having orientation of (100) substrates were used.

In this study, besides mica, silicon (n and p type), glass, titanium on silicon and gold on mica and titanium were used as substrates. Gold surfaces can be easily prepared by vapor deposition onto glass and mica. Gold is chemically inert against oxygen and stable against radicals. It binds organic thiols or bifunctional disulfides with high affinity, which can be used to covalently attach biological macromolecules.

### **1.5.2. Organics**

In this work, thiols and amine groups were studied as organics. SAM of Decylmercaptan (DM), Octadecylamine (ODA) and Octadecanethiol (ODT) on different substrates such as n and p type silicon and mica are used. DM and ODT are a type of the thiols whereas ODA is amines. Difference between these two groups is their head groups. Thiols group is used as a head group where the bonding is done on sulfur atom whereas in amines amino group is used with the bonding through nitrogen. This difference in head groups affects surface selectivity. It is expected that DM and ODT make bonding with metals or positively charged samples, on the other hand, ODA can bond with negatively charged surface. It is also expected that ODA can bond with positively charged samples in a salt condition.

Competition of reactions using thiols and amines as nucleophiles show a clear thiols preference. The rate of replacement of molecules from SAMs by thiols are much faster than amines. This indicates that stability of thiols SAMs may be related with the electron density of the sulfur but there is no direct evidence supporting.

Due to the maximization of the van der Waals interactions between neighboring alkyl chains of the thiols and the over layer adsorption on surface (geometry), the thiols are tilted with respect to the surface normal. It is easy to assume that the ordering of thiols on related substrates is perfect, but this is not the case. Common defects are

pinholes, collapse site and mobile alkyl chains in the monolayer (chain length dependent of course). Thiols are generally easy to work with under normal laboratory conditions. They are very stable and in comparison to amines relatively harmless to the health.

Lateral cross binding of neighboring amines increases the stability of the SAM. Since most amines are very reactive, the SAM formation is more rapid than for thiols, the complete monolayer is established (equilibrium) usually within much earlier than the other organics. However, this reactivity is an apparent health hazard, which requires controlled handling. One of the other important properties of amines is their polarity. A polar amino group at the chain terminus results in a more disordered monolayer, probably as a result of acid-base interaction with the surfaces.

The thiols especially ODT involves an island formation and subsequent growth behavior while the amines have more random growth. The thiols are mostly used in dip pen lithography technique (mostly on gold surfaces) whereas the amines have been unsuccessfully in dip pen lithography so far. (Hong et al. 1999).

### **1.5.2.1. Octadecylamine (ODA)**

ODA is opaque, off-white liquid with ammoniacal odour. It is also insoluble in water however in some reactions it can be soluble in alcohol, ether, and benzene and very soluble in chloroform. Octadecylamine is not a volatilizing amine. It will not volatilize in a boiler below 350 °C. ODA is not soluble in water so when it falls out of the steam solution it lays down the passivating mechanism. A monomolecular film is formed when the hydrophobic ends of the amine molecule attach to the metal surfaces. This monomolecular film repels water creating a barrier between corrosive condensate and the metals. Excessive feed or too rapid of feed will cause the system to plug iron oxides removed from the metals. Incomplete film formation will cause localized corrosion. Extreme care and monitoring are required when using ODA. Octadecylamine has a number of disadvantages when used as a filming amine:

- it is highly viscous and can only be blended using high heat
- its viscosity limits the concentration that can be put in solution
- if overfed, it forms a slime or gum that builds up in steam traps

- if corrosion is already present in the system, it forms a gum with the corroded iron

- gum forming and viscosity limit the level of protection available, using this chemical

ODA has two form related with excess of HCl. Yet the salt form of ODA is done in HCl for the purpose of allowing extra bonding with hydrogen and chlorine atoms. Demonstrations of ODA are given below (Figure 1.8).

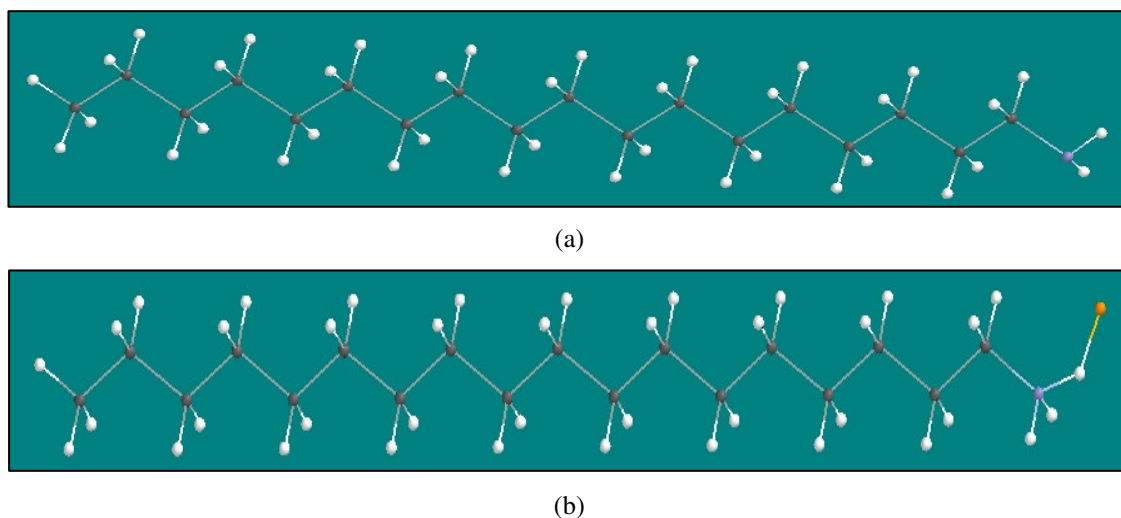
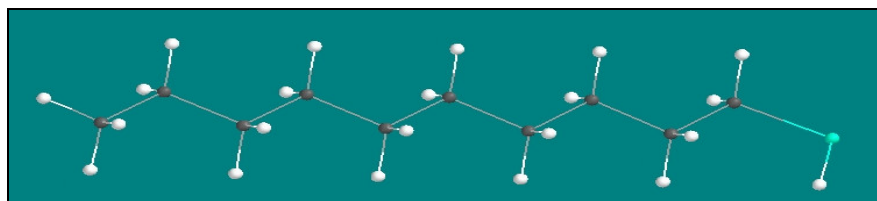


Figure 1.9. Demonstration of ODA molecules with  $(\text{CH}_3(\text{CH}_2)_{17}\text{NH}_2\text{-HCl})$  (a) and without  $(\text{CH}_3(\text{CH}_2)_{17}\text{NH}_2)$  (b) excess of HCl. The black atoms represent carbons, whites hydrogen blues nitrogen and the yellow one represent chlorine atom.

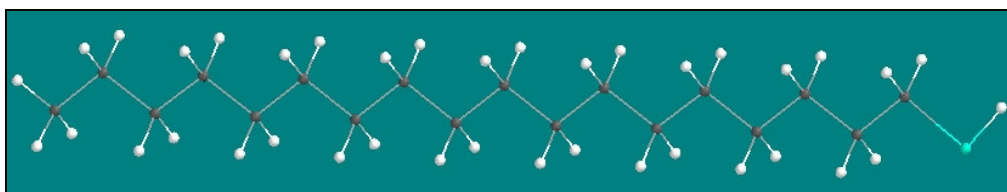
### 1.5.2.2. Decylmercaptan (DM) and Octadecanetiol (ODT)

DM and ODT, they are the most useful thiols with having difference in chain length. ODT is the longer one. They are also opaque with colorless liquid form. Like ODA, insoluble in water but soluble in ethanol. Other common properties of ODA and DM and ODT is having characteristic odour. It reacts with strong oxidants and strong bases. On the other hand, DM which has a boiling point  $241\text{ }^\circ\text{C}$  and melting point  $-26\text{ }^\circ\text{C}$  has some chemical dangerous properties like decomposing on burning producing highly toxic gases including sulfur dioxide. Figure 1.9 represents DM and ODT molecules. As it is seen from the Figure 1.9, difference between these two molecules is

their chain length. ODT is almost longer two times than DM. Their (DM and ODT) calculated molecular lengths are approximately 1.4 and 2.4 nm respectively.



(a)



(b)

Figure 1.10. Demonstration of (a) DM ( $\text{CH}_3(\text{CH}_2)_9\text{SH}$ ) and (b) ODT ( $\text{CH}_3(\text{CH}_2)_{17}\text{SH}$ ) molecules. The black atoms represent carbons, white hydrogen and green is sulfur atom.

ODT and DM form a hydrophobic SAM. ODT SAM nucleation sites eventually grow into larger domains. There is a relatively slow, initial nucleation process followed by a fast island growth process and then finally a slow saturation process. This is similar with the SAMs of shorter alkanethiol. There is not a directional influence on the SAM island growth process. This strongly suggests that these are measurements of the monolayer self-assembly process rather than tip-directed writing of a monolayer. The growth process for the SAMs is drastically different from the growth process for the ODT system. This difference is attributed to the very different hydrophobicities of the SAMs and their interaction with the water meniscus. In the most case, the adsorbate molecules are hydrophobic, but the SAM is hydrophilic. In the case of ODT, both adsorbate molecule and SAM are hydrophobic. In the case of ODT, the wettability of the surface decreases as the ODT is deposited thereby localizing monolayer growth and establishing well defined nucleation sites (Hong et al. 1999).

In this work, it is exclusively concentrated on SAMs of functionalized thiols (octadecanethiol (ODT), decylmercaptan (DM)) and amines (octadecylamine (ODA)) on different substrates such as n and p type silicon, glass, mica and titanium on silicon.

SPM of NT-MDT was utilized as a tool. Aim of this thesis is to achieve self assembly monolayer on chosen substrates and succeeding in nanopatterns SAM via atomic force microscope. Experimental facilities with characterization techniques and the obtained results are given the other chapters in details. In result and discussion part; all experimental results were examined in detail. At the final part of this thesis the results are concluded.

## CHAPTER 2

### EXPERIMENTAL PROCEDURE

In this chapter, the experimental procedure used in this study will be explained. In the first part, sample preparation including cleaning procedure, thin film deposition and self assembled monolayers (SAMs) preparation will be presented in details. The second part of the chapter is focus on AFM lithography on SAMs. Finally, characterization techniques that were used will be explained in summary.

#### 2.1. Sample Preparations

Nanometer-scale fabrication is a requirement for future microelectronic devices, and also has applications in high density data storage. Enormous efforts have been made in device technology and nanotechnology for reducing device sizes. The ongoing miniaturization in size and integrity of electronic and mechanical devices has led to an interest in the fabrication of nanometer-sized uniform structures on surfaces. Scanning probe microscopes (SPMs) are playing an important role in these fields. Self-assembled monolayers (SAMs) are expected to be used as a high-resolution resist, since the film thickness is uniform and the molecules are highly ordered. Patterning SAM films is therefore crucial for their applications. Obtaining well prepared organic SAM thin films, cleaning procedure is critical. Cleaning procedure has two parts, before SAM and after SAM. For bare substrates such as; n and p type silicon, mica and silica, sample preparations are done just three steps: cleaning procedure before and after SAM formation and SAM preparation. On account of SAMs are shaped on thin film such as titanium growth on silicon, sample preparation also consist of a thin film deposition step. Before SAM preparation step, film deposition is done. Gold surface was also used for investigating lithographic experiments. So in generally, sample preparation consists of four parts, these are:

- Cleaning Procedure I
- Thin Film Deposition
- SAM Preparations
- Cleaning Procedure II

## **2.1.1. Cleaning Procedure I**

All types of thin films need well cleaned substrates in order to growth fine films. Cleaning procedure is as important as film conditions. Some defects stem from dust or some other types of particles. Not enough cleaning can cause defects.

### **2.1.1.1. Cleaning Procedure for Silicon Substrates**

In this work, n and p type silicon were used as a substrate with appropriate cleaning procedure similar to described in the literature (Lee et al. 2001).

First, chemical etching was applied for both p and n type silicone substrates. This procedure includes holding the substrate at 1000C for 30 minutes in a solution contains; 10ml NH<sub>3</sub>+10ml H<sub>2</sub>O<sub>2</sub> and then drying the substrates with argon gas.

Acetone is the most usable cleaning chemical for nearly all sorts of materials. In this application, silicon substrates were wiped by acetone then parched with argon.

The best to all for cleaning silicon substrates was found as ultrasonic cleaner. Important parameter that must be taken into account is time. In detail, n and p type silicones were rinsed in acetone and redistilled water respectively in ultrasonic cleaner (Lee et al. 2001). During this process, rinsing time was applied as 5, 10 and 15 minutes for each part then dried with argon. For n type silicon even 5 minutes is given appreciable result however 10 minutes is the best one. Whereas for p type silicon substrate, there was no observed result with this procedure even increasing times. For p type silicon substrates, the best consequent was obtained with rinsing into 5 second hot piranha bath and 15 minutes into room temperature piranha bath solution than three times dipped into ethanol and redistilled water respectively and finally dried with argon (Lee et al. 2002). After all these experiments, it is understood and applied that for n type silicon substrates ultrasonic cleaner whereas for p type silicon room piranha bath with a formation of 3:1, %35 H<sub>2</sub>O<sub>2</sub>+ H<sub>2</sub>SO<sub>4</sub> is given the fine result as a cleaning procedure (Lee et al. 2001).

### **2.1.1.2. Cleaning Procedure for Silica**

For silica substrates ultrasonic cleaning was utilized for cleaning process. Silica substrates were rinsed in water in ultrasonic cleaner with 10 minutes and then they were dried with argon. The best result was obtained by using acetone with redistilled water in ultrasonic part. Glass samples were dipped into acetone and redistilled water respectively with 10 minutes for each dipping steps and then dried with argon.

### **2.1.1.3. Cleaning Procedure for Titanium**

Titanium differs from the other substrates. Piranha bath which is mostly used for gold surface was used for etching. Hot piranha bath solution was prepared as 3:1, %35  $H_2O_2 + H_2SO_4$ . After dipping into hot and room piranha bath with 5 seconds and 15 minutes respectively titanium was rinsed with ethanol and redistilled water before dried with argon. Alternatively dipping into hot piranha bath and then applying argon gas on the sample also gave good results. Piranha bath for titanium was found to be the appropriate method as a cleaning procedure.

### **2.1.1.4. Cleaning Procedure for Gold Surface**

Piranha bath is the mostly used procedure for gold surface in literature (Diao et al. 1999, Diao et al. 2000, Lee et al. 2001,). Piranha bath combining with hot and room temperatures has been given the most effective results. In this study, gold substrates were dipped into ethanol and water respectively before rinsing hot and room temperature solutions. Piranha bath was prepared based on the procedure of 3:7, %35  $H_2O_2 + H_2SO_4$ . Rinsing time plays important role on cleaning procedure. For hot solution, 5 and 10 seconds and for room temperature solution 10, 20 and 30 minutes were applied. Among these researches, most prominent conditions for piranha bath were found as 10 seconds for hot, 20 minutes for the room temperature solutions. After dipping piranha solutions the next step for gold substrates was rinsing into ethanol and redistilled water by three times respectively. Finally, argon was used for drying the substrate as final step of cleaning.

### 2.1.2. Thin Film Deposition

One of the aims of this project is to develop nanopatterns on SAMs. In order to make sure whether succeeding or failure in developing patterns, it is necessary to know capability of doing nanolithography. So as to improve ability of patterning and have a control on patterning, lithography was first done on metal surfaces especially on gold surfaces. First of all, lithography on gold and titanium surfaces was studied. Gold surfaces deposited on mica and titanium substrate, whereas titanium surface growth on p type silicon. Both gold and titanium samples were studied in this work as a patterning experiment.

Gold is the most preferable substrates for lithography because of ease to modify and lack of oxidation properties. To have control on modifying gold surface, it is needed to produce well deposited thin film. So as to obtain fine surfaces, gold thin films were deposited using thermal evaporation and sputtering systems.

Gold films were grown on cleaned silicon and glass substrates with thermal evaporation system at various conditions such as; 5 minutes at 160 Å., 10 minutes at 160 Å. and 10 minutes at 175 Å. The reason of using glass is to find approximate thickness value of the gold growth on silicon. Approximate thicknesses were found about 120 nm and 160 nm for respectively given conditions. The photography and schematic representation of thermal evaporation system that was used in this study is shown in Figure 2.1 and Figure 2.2 respectively.

Since this work needs to be done in downscale, even a dust particle gains a big importance. So, cleaning procedure is also significant after film deposition process. Due to the importance of cleaning, prepared gold substrates had been tried to clean base on suitable procedure given before. It was seen that the gold films separated from the substrates while the cleaning procedure had been performing. Growth another thin film as an interlayer between gold and substrate was thought as a solution to this problem. Since gold could not be attached the surface well to deposit much more powerful film for both gold and substrate in order to provide stronger connection. For this aim, chrome and titanium were tried as an interlayer because of ease to obtain and having less roughness titanium was preferred.



Figure 2.1. The photograph of thermal evaporation system used for deposition gold surface.

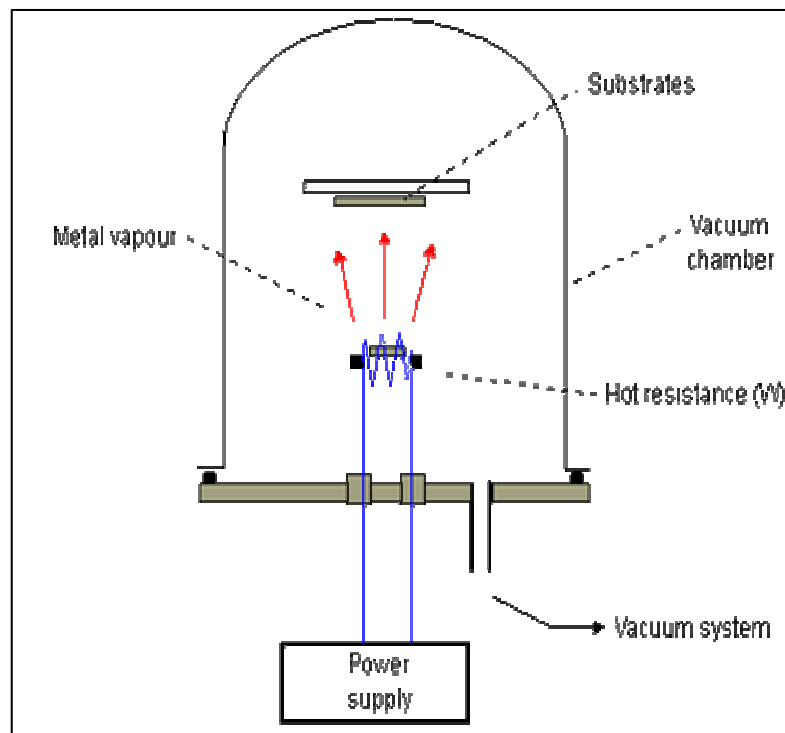
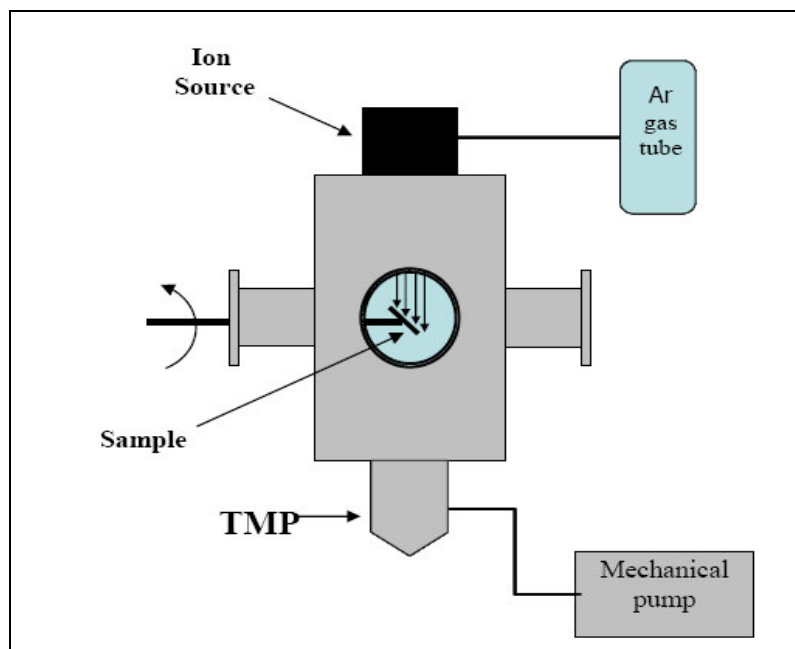


Figure 2.2. The schematic representation of thermal evaporation system

Titanium was deposited using ion beam system at certain conditions such as; 1000 V, 100 W, 0,1 A. Approximate thicknesses were found about 200 nm for given condition. The photography and schematic representation of ion beam system that was used in this study is shown in Figure 2.3.a and Figure 2.3.b respectively.



(a)



(b)

Figure 2.3. (a) The photograph of Ar-ion beam system. (b) Schematic representation of the same system

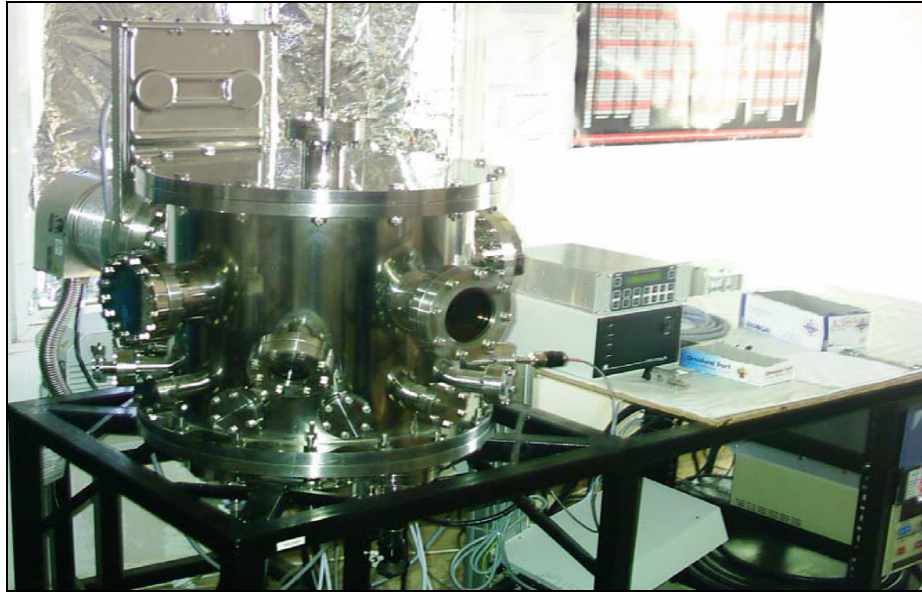
Titanium surface was also growth with magnetron sputtering system. The conditions of magnetron sputtering system during the titanium deposition were 23 W, 71 mA, 315 V. With both magnetron sputtering and ion beam systems it was succeeded to obtain fine titanium layer with the thickness about approximately 200 nm.

Using thermal evaporation system, gold film was deposited on cleaned titanium substrate growth on silicon at the given conditions (5 minutes at 160 A., 10 minutes at 175 A) with approximately thicknesses of 120 nm and 160 nm respectively. Gold layer was also deposited with magnetron sputtering system on cleaned titanium substrate which had been growth on silicon. The growth parameters are 399 V, 20 W and 47 mA. Obtained thickness for these conditions was approximately 100 nm. All experiments point out that gold deposition has given better result by using magnetron sputtering system. Parameters that were used in magnetron sputtering system both gold and titanium targets are given Table 2.1. The photography and schematic representation of magnetron sputtering system that was used in this study is shown in Figure 2.4.a and Figure 2.4.b respectively.

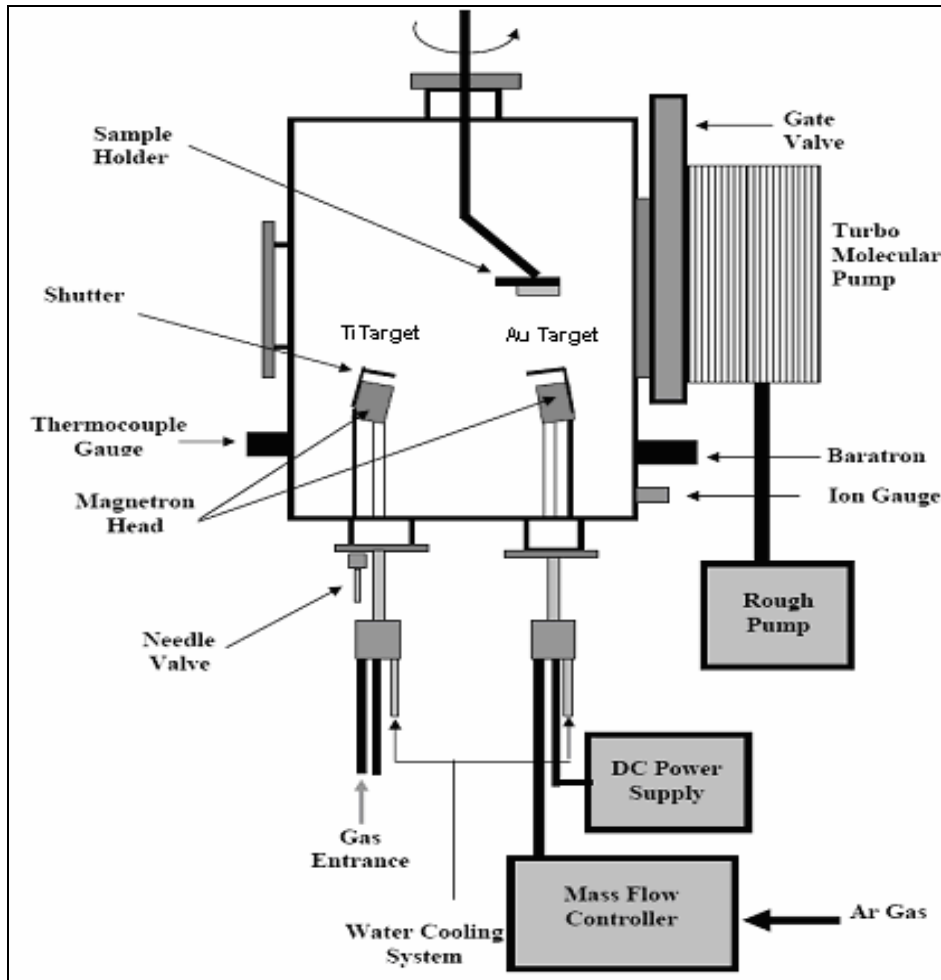
Table.2.1. Deposition conditions of thin films with sputtering system

<b>Target</b>	<b>Power (W)</b>	<b>Voltage (V)</b>	<b>Current (mA)</b>	<b>Gas Flow (SCCM)</b>
Ti	23	315	71	30
Au	20	399	47	40

Using titanium as an interlayer between gold and silicon substrate, peeling off problem was solved. This time another problem was observed; roughness. In order to overcome this problem annealing in different conditions such as 1hours at 500, 600 and 700 °C was applied. Annealed surfaces resembled to be separated. Some black areas appeared defects were observed. After searching with SEM it was understood that they were hole. Since, from edx data these black regions gave titanium peaks. Since the annealing did not encounter the roughness problem, etching with piranha bath was used. Piranha bath was prepared based on the procedure of 3:7, %35 H<sub>2</sub>O<sub>2</sub>+ H<sub>2</sub>SO<sub>4</sub> with hot and room temperature parts. After applying etching procedure according to the gold cleaning process, roughness problem was reduced as much as possible.



(a)



(b)

Figure 2.4. (a) The photograph of magnetron sputtering system. (b) Schematic representation of the same system

Gold film was also deposited on mica substrate with both magnetron sputtering and evaporation systems. However the film made at the same conditions, different from growing on titanium substrate, roughness problem was not observed on mica. Nanolithography was tried on prepared gold substrates, before applying on the surfaces of SAMs.

### 2.1.3. Preparation of SAM

The quality of SAM highly depends on preparation conditions. Since the monolayer formation occurs by dipping a substrate into a solution of surface active material. In this study, organics of amine and thiols groups consist of Octadecylamine, Decylmercaptan and Octadecanetiol were utilized. Important point in solution preparation is solvent concentration and molarities. Organics with prepared conditions are given at the Table 2.2.

Table 2.2. Organics of SAM used in the experiments with the preparation conditions

<b>ORGANICS</b>	<b>MOLARITIY (mM)</b>		<b>SOLVENT</b>
Octadecylamine-HCl (ODA-HCl)	0,1		Water
Octadecylamine-HCl (ODA-HCl)	0,1	1	Ethanol
Decylmercaptan (DM)	0,1	1	Ethanol
Octadecanetiol (ODT)	0,1		Ethanol

Different types of solutions of SAM were prepared according to the data given in the table. n and p type silicon, mica, silica and titanium deposited on silicon were used as substrates.

In order to obtain well formed SAMs, formation time must be taken into consideration. It is needed to be founded in the solution of SAM with enough time for being a layer. In this study for the aim of finding convenient time, different dipping

times starting with 24 hours were examined. The best monolayer formation was obtained with approximately 72 hours dipping time.

Chosen substrates were left into the organic solution given at the Table 2.2 at 72 hours, after applying cleaning procedure. Prepared substrates were exposed to another cleaning process, mentioned as cleaning procedure 2, before characterization and lithography.

#### **2.1.4. Cleaning Procedure II**

Prepared monolayers were exposed to second cleaning process as a last step of sample preparations part. In this procedure; substrates taken out from the solutions were dipped three times into ethanol and redistilled water respectively. Finally, cleaned substrates were dried with argon. Before any process such as lithography and characterization, prepared SAMs were cleaned carefully in this way.

## **2.2. AFM Lithography**

In this study, SPM solver pro was used as a lithographic instrument with the AFM modes. The photography and schematic representation of SPM system that was used in this study is shown in Figure 2.5.a and Figure 2.5.b respectively. Different types of tips are used based on experiments. In this project Otespa tip was preferred ( $f=200\text{-}400$  kHz,  $k=12\text{-}103$  N/m). The AFM was calibrated with height standards produced by Siloxane-MDT Ltd., Moscow, Russia. The automated AFM offers several features not common for conventional AFMs:

(i) Large sample holder and moving system for exact positioning of samples having diameters up to 5 cm,

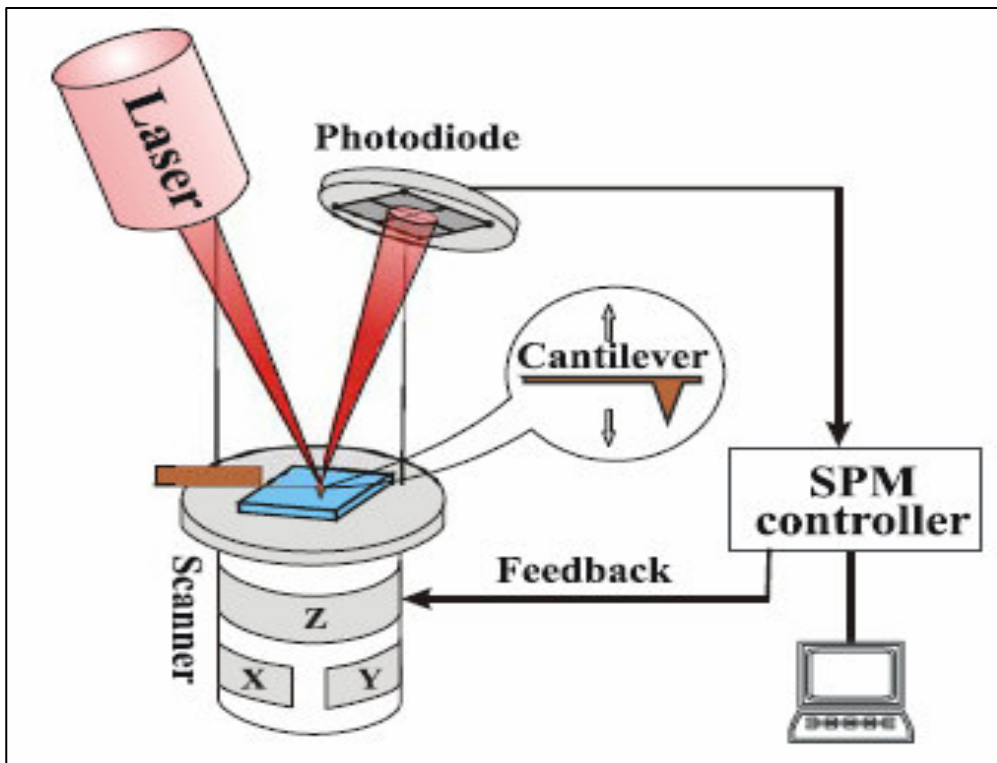
(ii) High-resolution optical microscope and integrated frame grabber for optical imaging of the sample,

(iii) Advanced control software (Nova 914 and Nova 876) allowing automated sample positioning and sample measurement using up to 16 different interaction/contrast modes simultaneously.

The AFM is thus capable of measuring an infinite number of sample positions, limited only by the amount of data-storage capacity.



(a)



(b)

Figure 2.4. (a) The photograph of SPM system. (b) Schematic representation of the same system

The AFM was used for automated imaging of the optical appearance, measurement of the surface roughness. AFM could be shown to represent an extremely powerful tool in materials research.

Simultaneous molecular displacement using an AFM tip can be used to fabricate nanostructures of SAMs. According to the organics that used in this study, basic procedure is simple. The van der Waals energy per CH<sub>2</sub> group is 2 kcal/mol. Therefore, under such imaging pressure, the AFM tip was in contact with the alkyl chains, which causes small local deformation. Increasing the local pressure would increase the deformation, disrupt the packing, and eventually displace thiols or amines molecules from their adsorption sites because the surface-head bond is the weakest at the interface increasing the load further would cause the substrates to deform.

First, the surface structure is characterized under low forces or load. Fabrication locations are normally selected in regions with flat surface morphology, e.g., Au plateau areas. The second step is patterning SAMs under high force. If the force is too low, molecules cannot be displaced completely in one scratch. Since the fabrication threshold varies with the geometry of AFM the fate of the displaced molecules depends on the structure of SAMs and the fabrication environment. Alkane thiols form an ordered structure without cross-linking among nearest neighbors. In air or water, where thiols exhibit little solubility, most of the displaced molecules often remain weakly attached to the substrate or SAMs in nearby locations.

For organics films, semicontact mode of AFM was preferred when taking a surface topography. As it was mentioned before semicontact mode is used for soft material for preventing deformation occurs from the scanning. After and before any type of lithographic experiment topographic images of the surfaces were taken to see the differences. For successful physical lithography, it must be known that how hard the tip should press into the sample. Since the force is the most important parameter on patterning, force calculation has been done as following.

Force is measured in an SPM by collecting a force curve, which is a plot of cantilever deflection signal, DFL, as a function of sample position along the z-axis known as height (i.e. towards or away from the probe tip; the z-piezo position). It assumes a simple relationship (i.e. Hooke's Law) between the force, F, and the cantilever deflection DFL:

$$F = -k \times \Delta z$$

$$F = -k \times b \times (\text{Set point of DFL} - \text{Initial DFL})$$

where  $k$  is the spring constant of the cantilever (N/m), and  $b$  is the slope obtained from DFL versus piezo  $z$ -position ( $b = \Delta Z \text{ (nm)} / \Delta \text{DFL (nA)}$ ).

Spring constant “ $k$ ” of the otespa tip at working frequency was obtained from a graph of spring constant versus frequency. In order to obtain constant  $b$  (slope  $b$ ), spectroscopy contain topographic image of the working area in semicontact mode with DFL (nA) versus height (nm) was done. The graph obtained from the spectroscopy gives information about force since it is a graph of cantilever bend versus the set point value. Set point is the parameter which is related with the distance between substrate and the tip. Since the force is related with the distance by changing set point parameter, it is possible to change applied force. Tip-sample interaction under DFL approach or retracting motion is presented in the figure below.

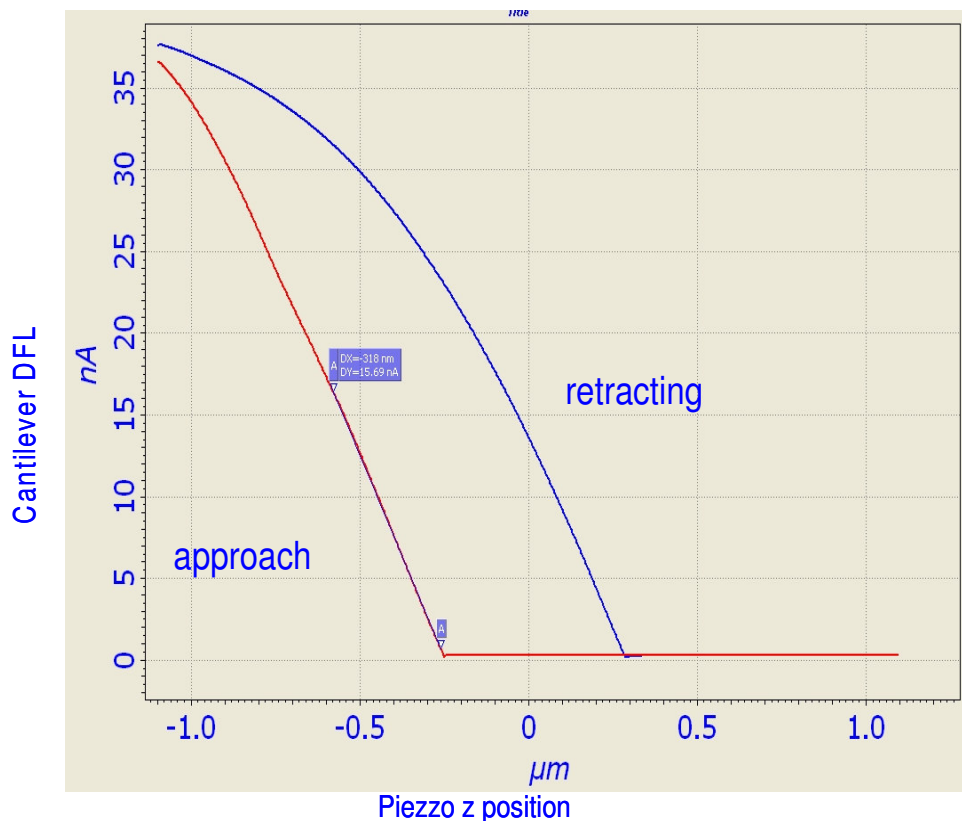


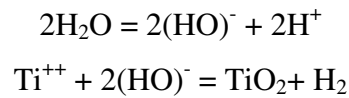
Figure 2.5. Tip-sample interaction under DFL approach or retracting motion

The curve consist of two parts; horizontal (load) and tilted (unload) related with the tip motion on the surface during the indentation. From the slope of the second part, it is possible to find slope “b” for any sample

Before starting lithography, it is needed to determine convenient force limit for each substrate. It is necessary for defining working force and making a comment about surface. These limits were investigated by making both patterning and nanoindentation on the surfaces. During the experiments applied force were being increased. It was done almost every part of the substrate. Determining force limits procedure applied on bare substrates. It was seen that; except for mica, all type of bare substrates couldn't deform under high force values. Mica substrate affected the force values over 50.000 nN (approximately 57.000 nN) by locally cleaving. For the lithographic experiment made for SAMs, convenient applied forces chosen below this value. As the organics deform less higher than 50.000 nN, it is necessary to work on convenient force limits. All lithographic experiments were examined under 50.000 nN. The criteria of determining the convenient force for organics was the same with defining force limits. Simply the procedure is to start with the low force and than increasing it with little steps until the determined force limits. Since it was examined that between these limits bare substrates didn't effect. If any deformation obtains, it must belong to organics. As it was mentioned before that set point is the parameter related with the force. Set point was used for controlling increasing force values. The force was increased by increasing set point. Deformation force was defined as a set point value. After finding convenient set point to increase force was lasting. The depths of obtained patterns were measured simultaneously with increasing forces. The end of the force limits for organics was determined by obtaining the same depth with increasing forces. Since, it means to scratch all layers from the surface. The defined end point was also preferred as a right value for raster lithographic experiments. Shapes of the patterns were usually chosen line because of noticing the differences in relations between the applied forces and the depth. As it comes to raster lithography, all conditions were determined with a chain of experiments before doing. It does with certain values and images.

For oxidation nanolithography conductive AFM tip was used. Titanium surface that was deposited on silicon with magnetron sputtering system was used as a substrate. Lithographic experiments were used at room temperature at the 90% humidity with changing voltage values. Voltage bias between a sharp conductive oscillating AFM tip and a sample generates an intense electric field  $E$  at the tip. The oscillating high electric

field desorbs the hydrogen on the Ti surface and enables to oxidize exposed Ti in air very quickly. Chemical reaction under oscillating electric field:



The thickness of the oxide increases with increasing voltage. There is no oxide growth obtained less than 5 V even at 90% relative humidity. The width of the oxide patterns depends on the curvature of the conductive tip, relative humidity, voltage and temperature. The curvature of the tip used here is 70 nm coated with conductive carbon. The thickness of the oxide with changing oxidation time and applied voltage were examined. With oxidation lithography, not only geometrical properties of the surface but also the local electro physical properties of the sample surface can be changed. Reliable titanium oxide patterns with high accuracy can be obtained with SPM oxidation Lithography. For complex pictures Raster Lithography can be executed by introducing JPEG-file to SPM controller software. Difference between minimum and maximum tone voltage will be applied proportionally to brightness and, correspondingly. Anodizing oxide will grow to a different height according to the contrast of topographical image.

### **2.3. Characterization Method**

After nanolithography, except for SPM system some characterization process was done. Examined samples were investigated by FTIR (Fourier Transform Infrared Spectroscopy), XRD (X-ray Diffraction), SEM (Scanning Electron Microscopy) and EDX (Energy Dispersive X-ray Analysis).

First, AFM was used as characterization technique. It is used for obtaining more detail images of the surfaces. It also provides to take three dimensional topographic surface images. Furthermore, the height analysis and surface roughness measurements were done by using atomic force microscope.

To understand that any chemical bonding whether occurred or not on the substrates' surfaces FTIR was used. FTIR analysis was done with FTS 300 MX DIGILAB Excalibur Series system with both transmitted and pike 80 spectrum

techniques. Both in these two techniques absorbance of the beam are measured. Lost in intensity was measured as absorbance. Difference between these FTIR techniques is just usage. In transmitted method substrates put directly on the source. At pike 80 spectrum method some other apparatus are used for measuring absorbance beam. For the substrates used in this study by eliminating bare substrates and air effect measurement was done. By comparing the surfaces information of bare and immersed into SAMs solutions substrates sample surface's examined. In this method, further chemical bonding that occurs on the surfaces are observed as an extra peak different from the surfaces' peaks.

XRD characterization was done with Phillips X'pert Pro system. It was used for examining any crystal structure whether form or not on the surfaces. It is expected that if any crystal structure forms, it can be observe as a peak.

Besides these, substrates surfaces were examined with SEM and EDX. The analyses were done with Phillips XL-30S FEG. Using EDX it is possible to see surface materials that are found on the structure with ratios.

## CHAPTER 3

### RESULT AND DISCUSSION

This chapter includes characterization results, which were obtained from SPM with AFM, FTIR, SEM, EDX, and XRD techniques. In order to support the consequences obtained from AFM, other methods were utilized.

#### 3.1. SPM Results

Using AFM, samples surface can be examined much more details. Besides viewing the surface as topographic, it was also used for both thickness measurements and nanolithography. Before any experiment, bare substrates were investigated by means of AFM for the aim of understanding their hardness properties. Having capacitance to high forces is wanted properties for suitable substrates. It is advantage for both determining monolayer thickness and eliminating substrates affect. AFM images of the bare substrates before applying SAM procedure are given in Figure 3.1. The measurements were done with semicontact mode. The color differences in the AFM images indicate the height difference. The bright areas correspond to the high height, while dark areas correspond to the low height. It was seen that surfaces were very smooth even at 80nm scale.

Before any lithography it is needed to define convenient parameters. For the aim of determining applied force, deformation limits of the substrates were examined. The average suitable force value of the SPM device that is convenient for any type of samples is about 60.000 nN. Organics are the soft material and they deform under small force values than metallic surfaces. While working on organics, this point was taken into account. All substrates were examined before monolayer formation for finding convenient force limits. After monolayer formation, nanolithography work on the substrates above determined force value. Nanopatterning was used as an examination procedure. The method was applied based on AFM lithography technique consist of contact and semicontact modes. By changing contact force convenient value was found.

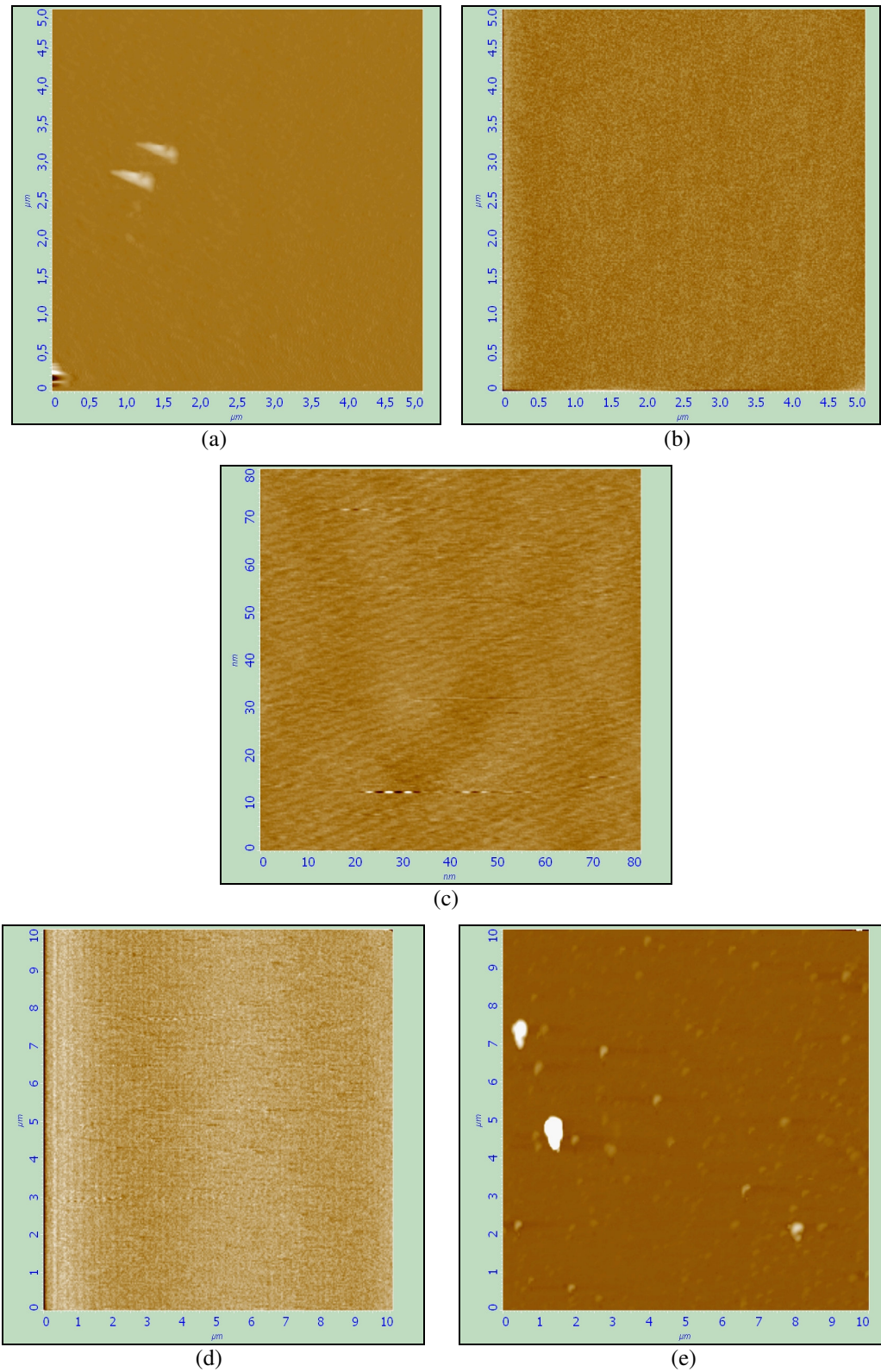
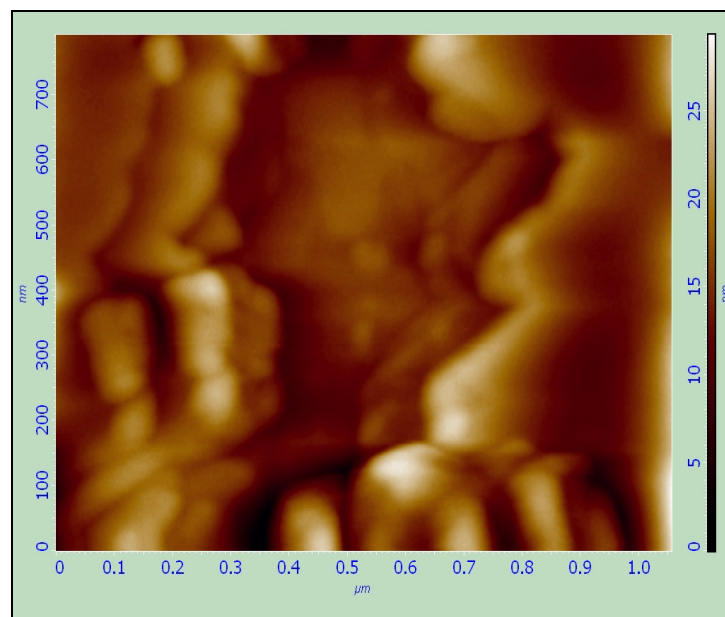
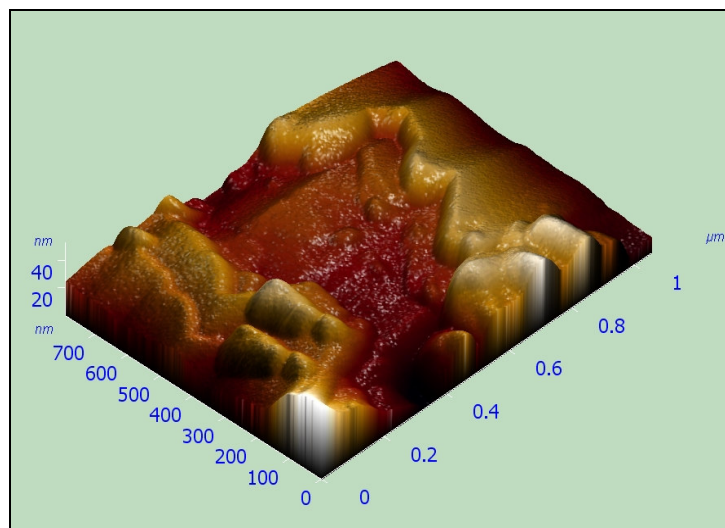


Figure 3.1. Topographic images of substrates taken from AFM with semicontact mode (a) and (b) n and p type bare silicon substrates images respectively at the scale of 10X10  $\mu\text{m}$ , (c) silica surfaces at 80X80 nm scales, (d) and (e) mica and titanium surface images at the 10X10  $\mu\text{m}$

Force affect was investigated by comparing the images taken before and after modification. As it was expected, the bare substrates except for mica couldn't be deformed under high force values (even at 60.000 nN). When it comes to mica, it didn't affect forces until the values of 50.000 nN. Mica didn't deform under that rate whereas over that value it cracked locally (above 55.000 nN). Figure 3.2 demonstrates the deformation of mica under high deformation force value. To avoid substrate deformation, 50.000 nN was chosen as a convenient limit for monolayer experiments.



(a)



(b)

Figure 3.2. (a) Two and (b) three dimensional topographic image of mica taken with AFM under 55.000 nN applied force.

AFM was used first step of the determining monolayer formations. After applying SAM procedure on mentioned substrates, nanolithography based on mechanical surface modification techniques especially nanoscratching method was applied. By applying increasing forces to surfaces, it was tried to give some comments about existence of monolayers formation on the substrates. If the monolayers exist on the samples, it is expected to be observed this formation with thickness measurement. Since, the bare surfaces couldn't deform at the organics deformation values. At the lack of monolayers situation, deformation must not be observed. According to this idea, it is possible to eliminate substrates either with existence or lack of formation. It was observed from the experiments that were made, there wasn't any apparent deformation on SAM that was growth on n type silicon and silica even with any organics and at any conditions. On the other hand, there were some deformations having a thickness related with organics molecular length observed. Molecular length of the organics that were used as SAM solutions were calculated by PROGRAMME SPARTAM 02 LINUX – UNIX (copy right 1991-2001), with semi-empirical model (version 113) with PM3 method. Calculated molecular lengths of the organics are given Table 3.1.

Table 3.1. Calculated molecular length of the organics

<b>Organics</b>	<b>Molecular Length</b>
Octadecylamine-HCl (ODA-HCl) (CH <sub>3</sub> (CH <sub>2</sub> ) <sub>17</sub> NH <sub>2</sub> -HCl)	2,59-2,76 nm
Decylmercaptan (DM) (CH <sub>3</sub> (CH <sub>2</sub> ) <sub>9</sub> SH)	1,35-1,48 nm
Octadecanetiol (ODT) (CH <sub>3</sub> (CH <sub>2</sub> ) <sub>17</sub> SH)	2,37-2,47 nm

As it is seen from the Table 3.1 data is given as range. This is related with the bonding geometries. Organics can be bonded to the surface with or without last elements, since the molecular length either include or not the last bonds. First values consist of lacking of situation whereas second parts represent existence of last bonds. In the other words; these ranges are related with maximum and minimum bonding positions. The other important point here, the molecular length of the organics can take

any values between this range according to the bonding geometries occurred between surface and the organics. Bonding geometries consist of contact angle between surface and the organic.

Before studying on organics, nanolithography was done on gold and titanium surfaces. Since it is easy to modify gold molecules and lacking of oxidizing, made gold surfaces preferred. Most physical surface modifications were studied on gold surfaces. Titanium surface was examined for oxidation lithography. Ease to obtain make the titanium substrate preferred.

### 3.1.1. Physical Surface Modification

Gold surfaces deposited on mica and titanium substrates were investigated with AFM in nanolithography. Before physical surface modification, gold surfaces were investigated. Figure 3.3.(a) and 3.3.(b) represent topographic images of gold substrates growth on mica by evaporation and magnetron sputtering systems with 800X800 nm. Difference from images (a) and (b) is their grain size originated from distinct deposition methods.

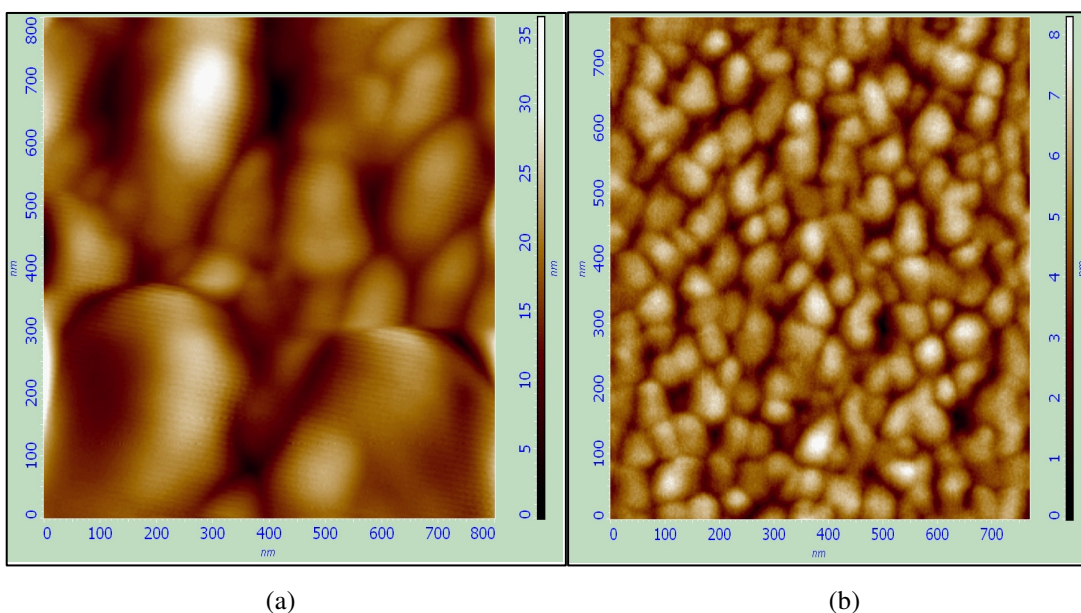
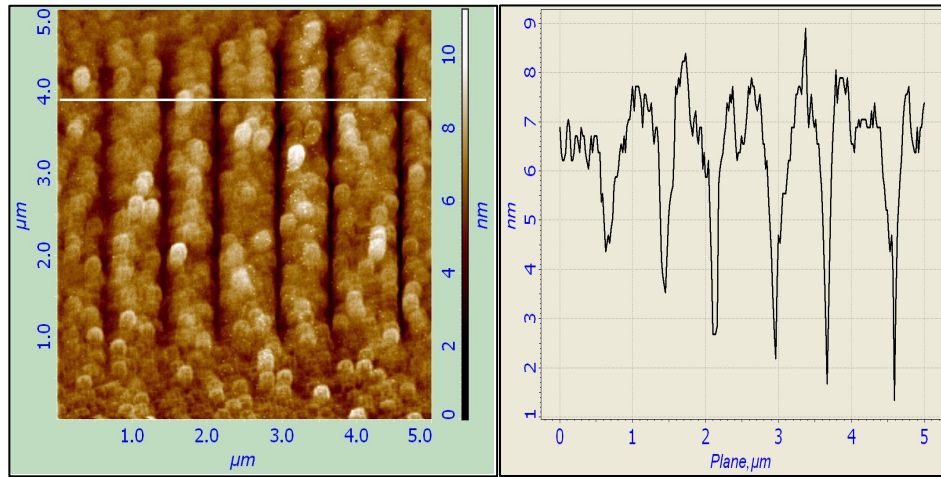


Figure 3.3. Gold substrate growth on mica by (a) evaporation (b) magnetron sputtering systems with 800X800 nm

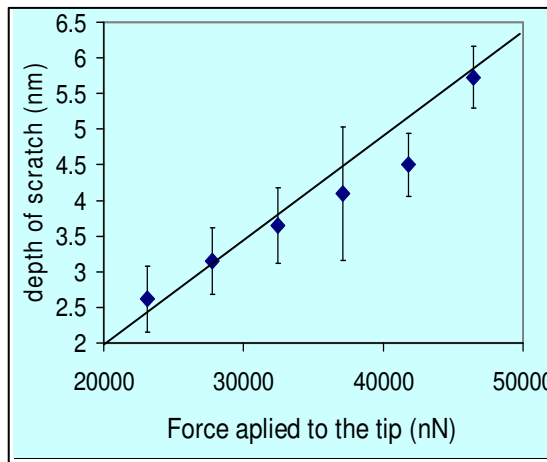
Taken images show that grain sizes of the gold surface that was prepared by sputtering system are smaller than evaporated gold surface. Having smaller grain sizes means better deposition technique and smoother surface. This is derived from better controllability properties of the sputtering system. Giving better results made the sputtering system preferred for preparing substrates for nanolithography. Physical surface modification with nanoscratching and nanoindentation methods was studied on gold surfaces as shown in Figure 3.4. By doing this modification, vector lithography method was used. In this method shape of the pattern is chosen from the software. Applying force that is determined with given set point value deformation obtains. Set point defines the distance between surface and the tip. In contact mode to increase set point means how push the tip to the surface. In semicontact mode, set point represents the differences between tip and surface. So, increasing means increasing the distance and applied force on the substrates.

Nanoscratching technique was applied with increasing force values on each line. Cross-section of the scratched lines that are pointed out the Figure 3.4.(a). It illustrates that lines depth increase with increasing applied forces. The graph of the force applied to tip versus scratch depth shows that the relation between force and depth are almost linear (Figure 3.4.(b)). Nanoindentation technique was done using decreasing force values. The cross-section of the demonstrated line on the figure shows that indent depths decreasing with decreasing applied forces. So, it was understood that size of the depth of nanopatterns are related with the applied force to tip. Figure 3.4 shows that nanopatterns depth is increasing with increasing applied force values. Since, both nanoindentation and nanoscratching techniques give the same results and nanoscratching also contain indentations experiments, scratching preferred as a convenient method.

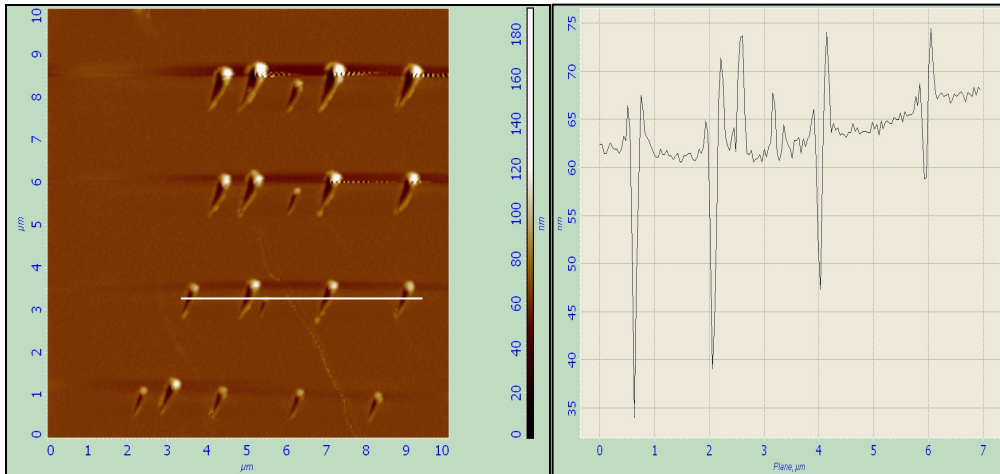
Like other AFM measurements, differences in height demonstrate with color contrast. Dark regions represent deeper areas whereas brighter regions show higher places. From this point, it is seen from Figure 3.4 that, there are some color differences in nanoscratches. So, from the increasing darkness of the nanopatterns it is understood that line depth is increasing. It is also the same for nanoindent patterns. Brighter points in nanoindent patterns represent debris of the surface that is observed after modification. Since, at any surface modifications surface disturbs like indentation or scratching and some collapses stem from debris obtained because of surface deformations. Part of the surface deformations collapse near region of the pattern where change from tip motions



(a)



(b)



(c)

Figure 3.4. Physical surface modification of gold thin film deposited on mica substrates (a) nanoscratches with line depth and (b) applied force versus depth graph in 5X5  $\mu\text{m}$  scale and (c) nanoindentation with indent depth graph of chosen line with 10X10  $\mu\text{m}$  scales

Physical surface modification can also be applied on complex pictures with raster lithography method. In this method complex pictures can be executed by introducing JPEG file to SPM controller software. By using this method logo of İzmir Institute of Technology (IYTE) was made. Figure 3.4.(a) represents topographic image whereas Figure 3.4.(b) represents phase image of the same figure. Different from phase and topographic image, phase image isn't real. It demonstrates just surface. Whereas topographic image is the real one and it contains everything on the surface. For example a dust particle can't be observed on phase image since it isn't a part of surface. It is observed on topographic image since it illustrates everything such as dust or same other materials come from surroundings on the surface.

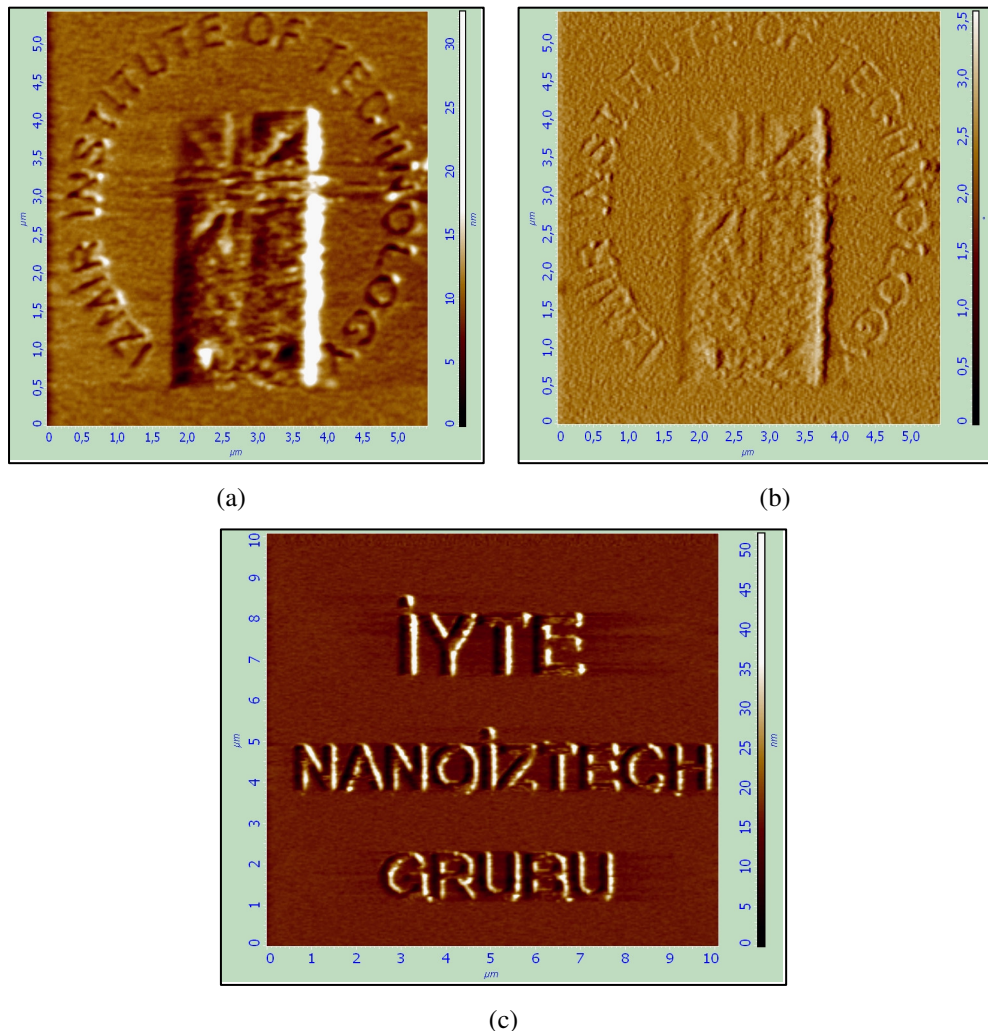


Figure 3.5. Raster lithography on gold film on mica made by using sputtering method with (a) topographic and phase image of the patterns in 5X5 μm scales and (c) writing with raster lithography on gold films on mica in 10X10 μm

Figure 3.5.(c) represents another type of raster lithography contains a documents not a picture. In this study characters name of a group was done by raster lithography. Bright regions in both two experiments illustrate the debris of surface material which appears after scratching a surface. While scratching a surface, the scratched surface materials are left according to the tip motion. Mostly, end or near of the characters debris of the work left.

The same nanolithography was also done on gold substrate growth on titanium that deposited on silicon by using sputtering method (Figure 3.6).

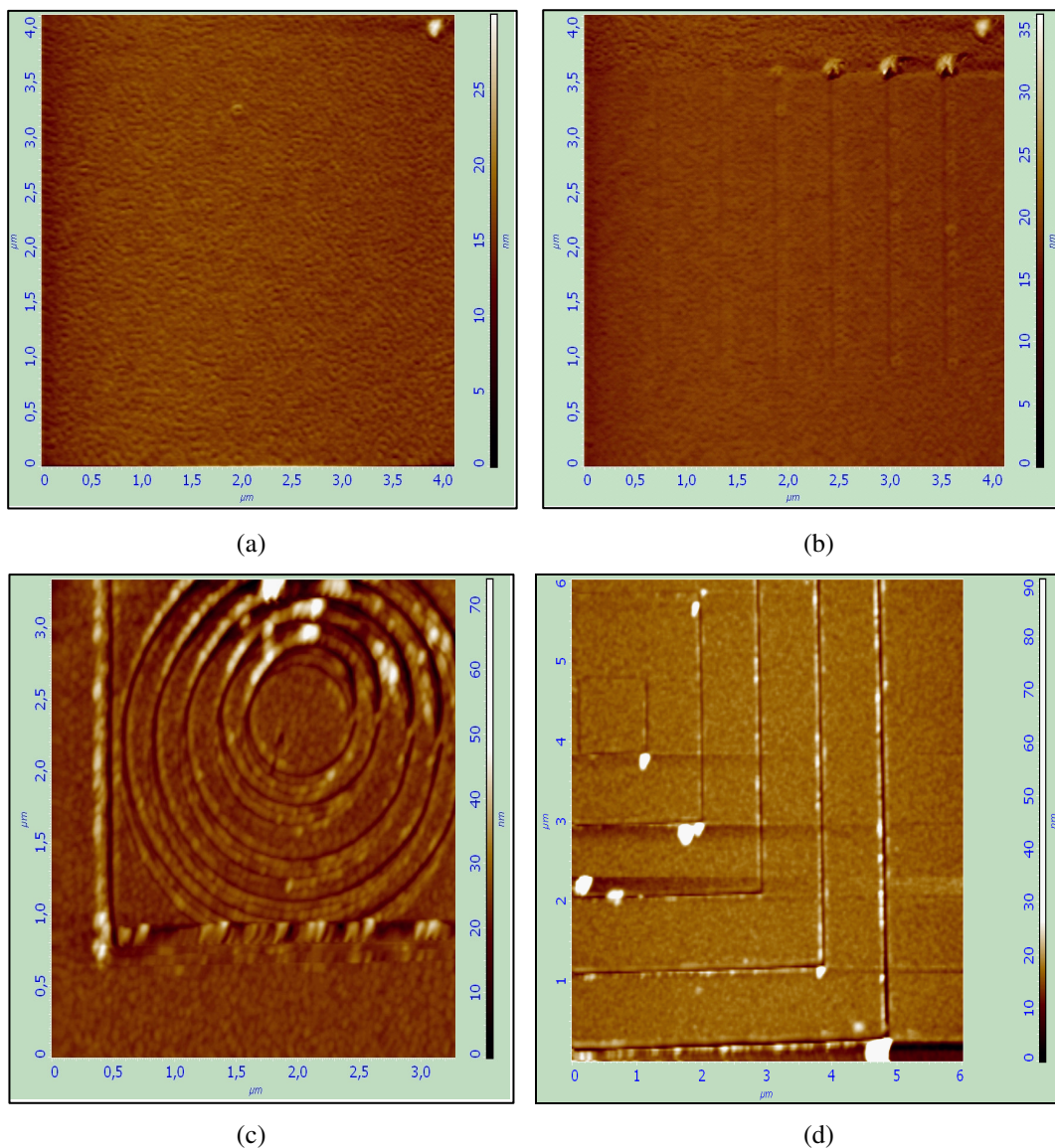


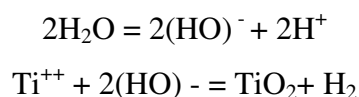
Figure 3.6. AFM surface images of (a) gold on titanium deposited on silicon made by using sputtering method, (b) applying nanoscratching lithography technique, (c) and (d) lithographic patterns on gold

In Figure 3.6.(a) an AFM image of gold surface is shown before any nanolithography. Whereas at Figure 3.6.(b), (c) and (d) vector lithography applications did on the gold surface with nanoscratching technique is demonstrated. The made nanopatterns are also illustrated. Smooth thin film surface was obtained by using the same growth conditions with prepared on mica. Patterning with vector lithography consists of nanoscratching was done with the scale of  $4 \times 4 \mu\text{m}$  Force and depth measurement wasn't done since it was just done demonstrated that lithographic patterns could also be done on this substrate too. With applying increasing force values on surface nanoscratches were done. It does not seem as clear as the gold surface on mica. Because the experiments were done at lower force rate just seeing that the patterns could be observed. Lithographic patterns shown on Figure 3.6.(c), it was done by drawing each pattern more than one cycle. Because of this extra lines observe at the image. The other effect of drawing more than one time is to have increasing debris collapse around the patterns. The other lithographic image is demonstrated at Figure 3.6.(d).

### **3.1.2. Chemical Surface Modification**

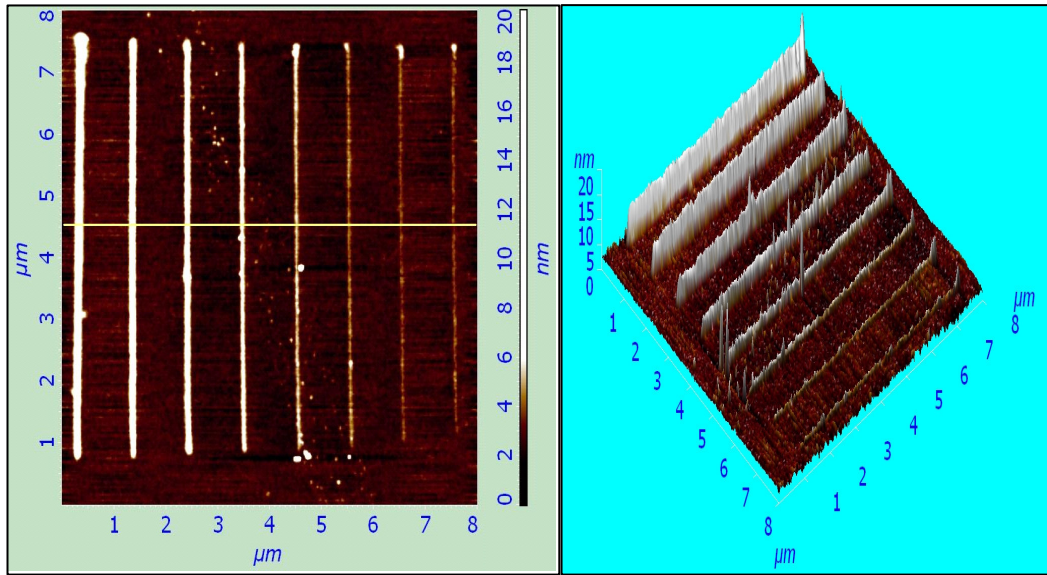
Chemical surface modification was applied on titanium surface that was deposited on silicon surface with sputtering system. Oxidation procedures were done at room temperature ( $27^{\circ}\text{C}$ ) with 90% relative humidity. Conductive tip was used. The curvature of the tip used here is 70 nm coated with conductive carbon. To find convenient voltage value, different voltage degrees were tried. For this experiment -10 V was found convenient value. Negative voltage was used to the oxidize titanium surface (because of applied negative voltage hydroxyl ions hit the surface and this causes oxidation on the surface). Voltage bias between a sharp conductive oscillating AFM tip and a sample generates an intense electric field  $E$  at the tip. The oscillating high electric field desorbs the hydrogen on the titanium surface and enables to oxidize exposed titanium surface in air very quickly.

Applied electric field  $E$  causes a chemical reaction. This reaction consists of two parts. First part is electrolysis of the water obtained from the humidity and the oxidation part occurred on the surface. The chemical reaction under oscillating electric field is given below:

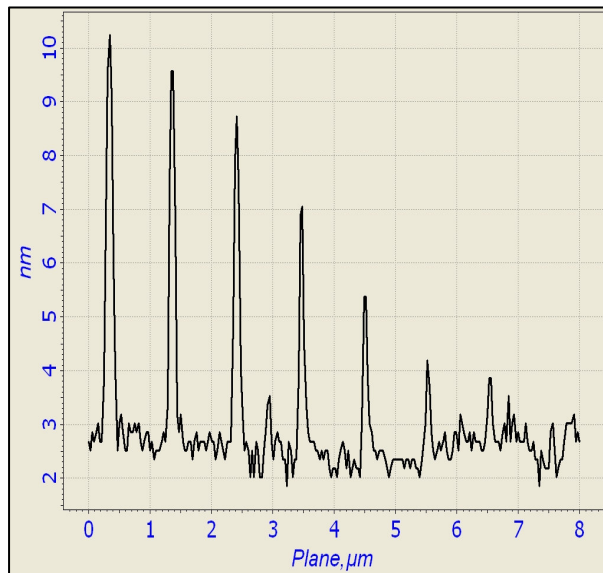


During the experiment, it was seen that the thickness of the oxide increases with increasing voltage. There was no oxide growth obtained less than convenient voltage values (5V) even at 90% relative humidity. The relation between oxidation time and oxide layers was utilized. Two and three dimensional AFM images of oxide layer with decreasing oxidation time are given in Figure 3.7 with 8X8  $\mu\text{m}$  scales. In the figure, cross-section of pointed line which is represented thickness of oxide layer according to changing oxidation time is observed.

The thickness of the oxide increases very quickly with oxidation time, then it saturates due to insulation of tip current with oxide grown under the tip. The width of the oxide patterns depends on the curvature of the conductive tip, relative humidity, voltage and temperature. Difference between minimum and maximum tone voltage will be applied proportionally to brightness and, correspondingly, anoding oxide will grow to a different height according to the contrast of topographical image.



(a)



(b)

Figure 3.7. Oxidation lithography on titanium thin film deposited on silicon substrates (a) two and three dimensional AFM images of oxide layer with decreasing oxidation time (b) cross-section of pointed line which is represented thickness of oxide layer according to changing oxidation time in  $8 \times 8 \mu\text{m}$  scales

After doing nanolithography on gold and titanium surfaces using SPM lithography techniques, nanopatterning on self assembled monolayers has been investigated.

### 3.1.3. SPM Results of SAM

Prepared SAM substrates were examined. SPM was used first investigating method. SAM of amines and thiols were utilized for nanopatterning of physical surface modification methods as a first elimination technique. Organics are soft materials; they can be deformed under even low forces. From this point, SPM lithography was used as a first way to observe SAM formation. All force values applied on prepared substrates. Among the used substrates, n type silicon and silica didn't deform even under high forces and with all type of organics used in this study. This means that monolayer formation didn't occur on silica and n type silicon. So, these substrates were eliminated and the others were used for nanopatterning. Also deformed substrates were examined with other methods in order to support the idea of monolayer formed.

### 3.1.4. SAM with Amines

ODA-HCl was preferred from amine group. It was examined with different molarities in water (0,1 and 1 mM) and with 0,1 mM in ethanol. Silicon with n and p type, silica, titanium substrate deposited on silicon and mica were used as substrates. Among these substrates mica, titanium and p type silicon were examined. Since it was thought that monolayer formations occurred just on these substrates. Table 3.2 shows the organics of SAM with the substrates on which monolayers were formed. Related substrates are explained below

Table 3.2. SAM of amines with the substrates on which monolayers were formed

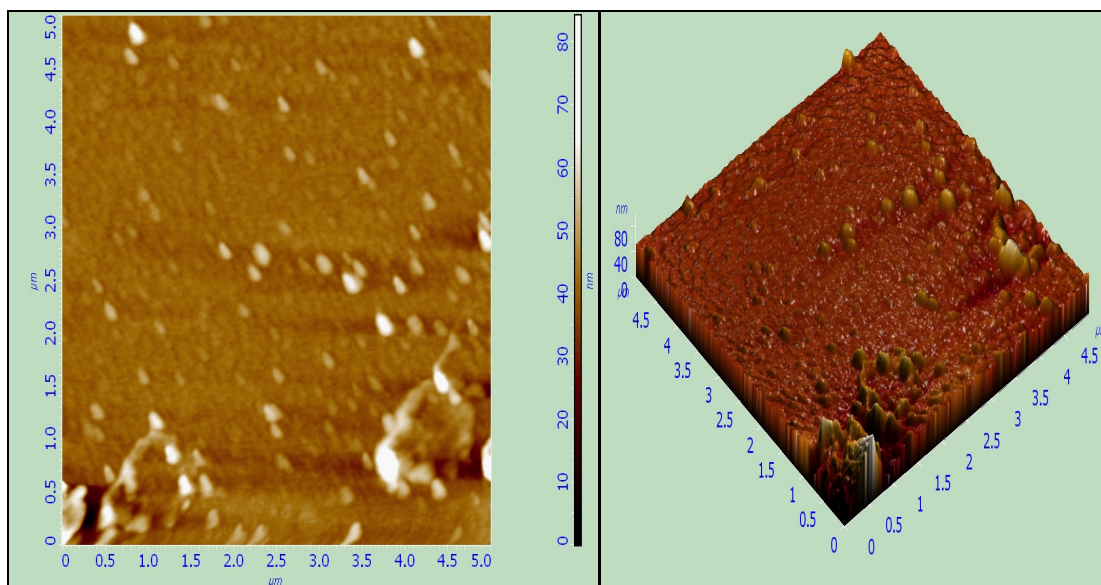
<b>ODA-HCl 0,1 mM in water</b>	<b>ODA-HCl 1 mM in water</b>	<b>ODA-HCl 0,1 mM in ethanol</b>
mica	-	mica
p type silicon	-	p type silicon
-	Titanium on silicon	Titanium on silicon

### **3.1.4.1. ODA-HCl with 0,1mM in Water**

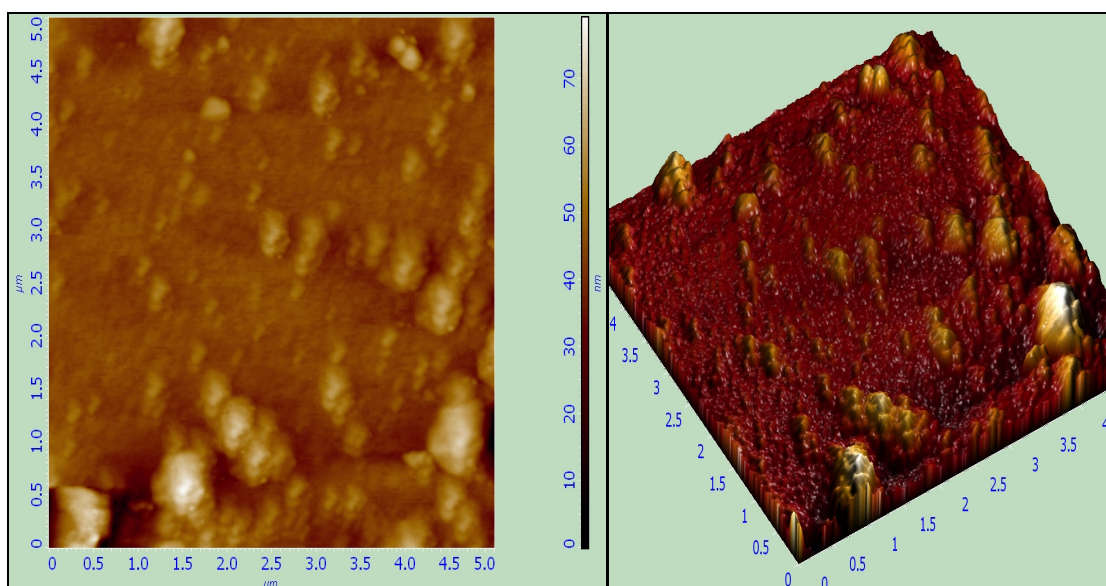
SAM solution of ODA-HCl was prepared with water solvent in 0,1 mM. All substrates were immersed into solution but monolayer formation was just observed on mica and p type silicon. Before nanolithography, surfaces were examined with atomic force microscopy mode of SPM. The results are given below.

#### **3.1.4.1.1. SAM of ODA-HCl with 0,1mM in Water on Mica**

In Figure 3.8, two and three dimensional topographic AFM images of SAM consist of ODA-HCl with 0,1mM in water on mica with different regions are illustrated. As it is seen from the figure, there are some particles on the surfaces. Some of them reach nearly 80 nm thicknesses. These big particles can be dust or something from out of surface that comes from environment. Since, the AFM investigating is done in the air. Some particles could stick on the surface during the experiment. After SAM preparation steps all substrates were cleaned organics molecules on the surface from the remains.



(a)



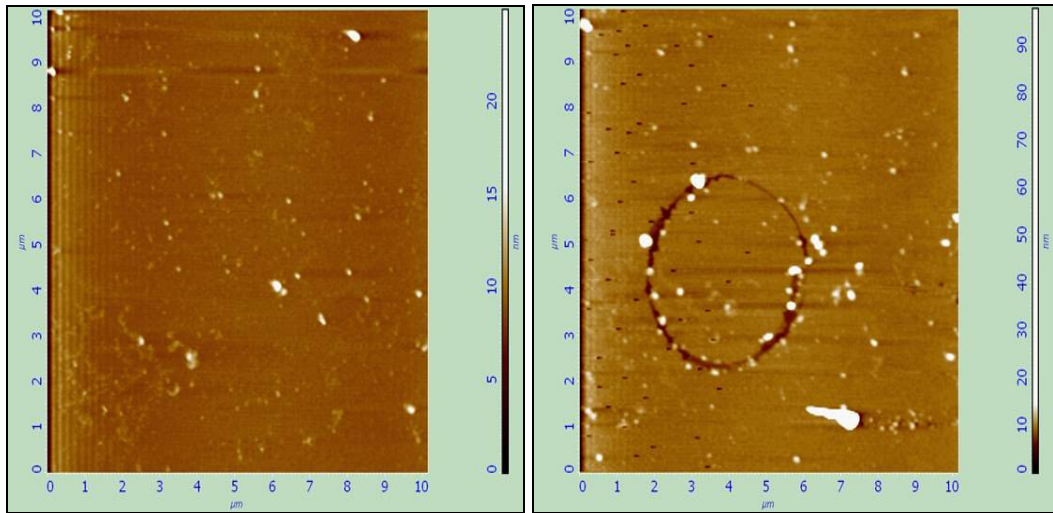
(b)

Figure 3.8. Two and three dimensional topographic AFM images of SAM consist of ODA-HCl with 0,1 mM in water on mica with represented (a) and (b) from different regions with the scale of 5X5  $\mu\text{m}$

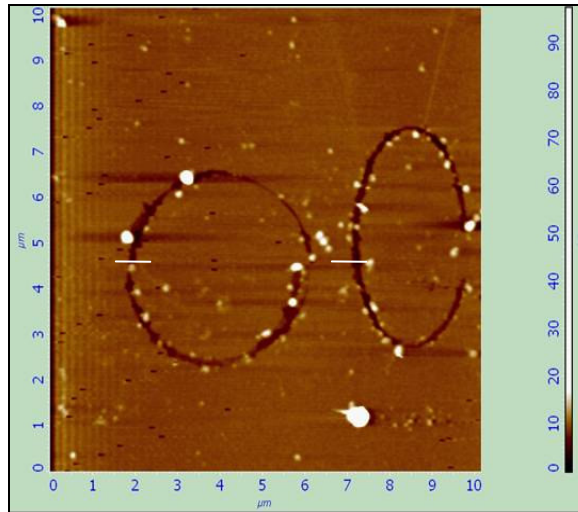
After viewing surfaces in details, nanolithography was done for the aim of both observing monolayer formations and developing nanopatterns on the surface. Figure 3.9 represents the results of this experiment. After taking an image from the suitable area which was the smooth part of the observed place, a circle was drawn as a nanopattern. Taken image shows that the circle could be done. It is seen that, there are some

differences between the images taken before and after. There is a white particle seen on the right at the bottom. It could be dust. Beside this, there are also some other bright things on the surface near the circle. These stem from the debris of the surface material. Since during the scratching, the surface is deformed. Scratched material is left beneath the patterns. The observed white regions come from this left scratched materials. At Figure 3.9.(b) another pattern was done. Different from the debris of the surface material, it is seen that the white region on the right at the bottom was getting smaller. This is because of the effect of the scanning. While scanning the surface consecutively, the particles out of the surface like dust can leave substrates.

Both of two patterns were done with increasing force values. 20.000 and 30.000 nN force values were applied on the respectively on patterns. During the modification, it was seen that thickness of the patterns didn't change. Before finding the convenient force values, it was also seen that the same thickness was observed along the patterns. Thickness measurements of the patterns are given the graphs at the Figure 3.9.(c). First graph belongs to first pattern whereas the second one belongs to the other pattern. It is seen that thickness of the patterns about 2,5 nm. Measurements match with the calculated values of the organics molecules of the SAM. Obtaining the same thickness values demonstrate that monolayer formation occurs at the surface. On the hand, bare substrates couldn't deform under applied forces.



(a)



(b)



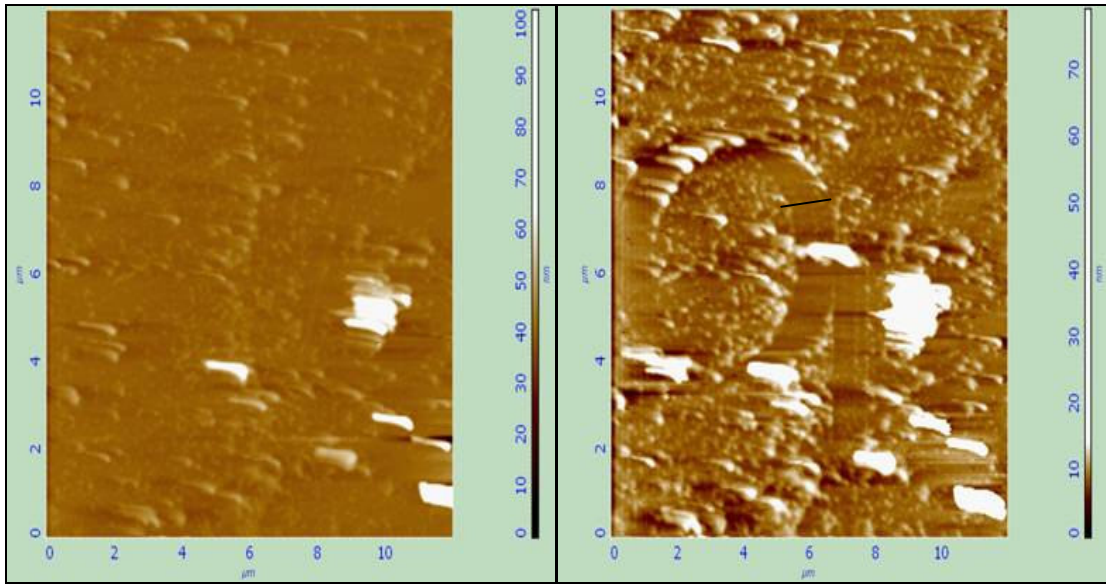
(c)

Figure 3.9. AFM images of SAM consist of ODA-HCl with 0,1 mM in water on mica with (a) before and after nanolithography (b) and after second nanolithography (c) with thickness measurements

### **3.1.4.1.2. SAM of ODA-HCl with 0,1mM in Water on p type Silicon**

In Figure 3.10, two dimensional topographic AFM images of the p type silicon with thickness measurements are illustrated. They are taken after immersing the SAM solution of ODA-HCl at stated conditions. As it is seen from the figure, there are some particles on the surfaces. Bigger white particles could be dust but the others don't seem to dust. They seem something else like surface materials. After patterning, it was observed that number of particles increased and they were also more prominent. It could be because of the patterning. Since this procedure include debris formation. Nanolithography was done with 30.000 nN applied force value. After nanolithography, thickness measurement was done (Figure 3.10.(b)). The thickness of the pattern measured roughly as 2,5 nm. This value matches calculating range of the organic.

Roughness is the common properties of mica and p type silicon substrates. On the other hand, from the AFM images it was seen that pattern made on mica substrate was clearer than the silicon. This can stem from difference electronic properties of the substrates. Mica has negative surface charge whereas p type silicon has positive. This difference can cause dissimilarity in binding geometries. Beside electronic properties, the different could be because of SAM properties. While scratching SAM on any substrate, two conditions are possible. These are removing the material completely on the surface or bending the organics. For silicon surface applied force could cause bending the organic molecules. Yet, for mica applied force can remove the material on the surface. So, pattern on mica can be observed clearer because of this difference.



(a)

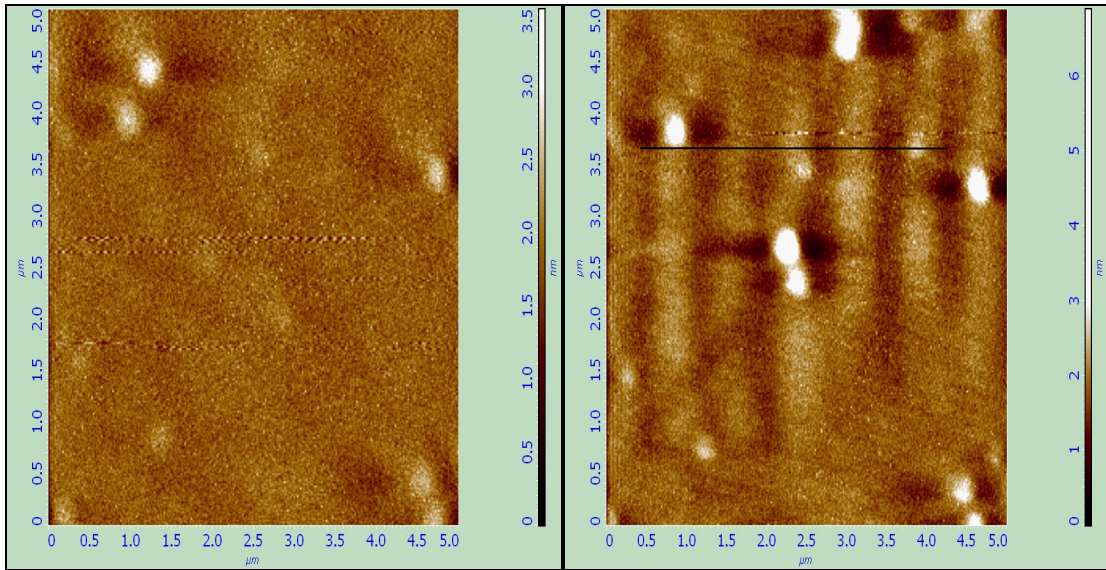


(b)

Figure 3.10. Topographic AFM images of SAM consist of ODA-HCl with 0,1 mM in water (a) on p type silicon and (b) thickness measurement of the surface with the scale of 10X10  $\mu\text{m}$

### 3.1.4.2. SAM of ODA-HCl with 1mM in Water on Titanium

The SAM formation of ODA-HCl (1 mM with water solvent) was only observed on titanium that was deposited on silicon. In Figure 3.11, topographic images of the titanium surface with nanoscratches and thickness measurement of the surfaces are illustrated with the scale of 5X5  $\mu\text{m}$ .



(a)



(b)

Figure 3.11. Topographic AFM images of SAM (ODA-HCl with 1 mM in water) on titanium deposited on silicon (a) after and before lithography and (b) thickness measurement of the surface with the scale of 5X5  $\mu\text{m}$

Nanoscratching was done as nanopatterns. This time patterns couldn't be as clear as the other substrates that had been observed before. Distinction both in solutions and surface properties can cause dissimilarity in bonding geometries. Titanium surface had deposited on p type silicon. To applied SAM procedure on deposited surface can also affect formation. Figure 3.11.(b) demonstrates the thickness measurement of

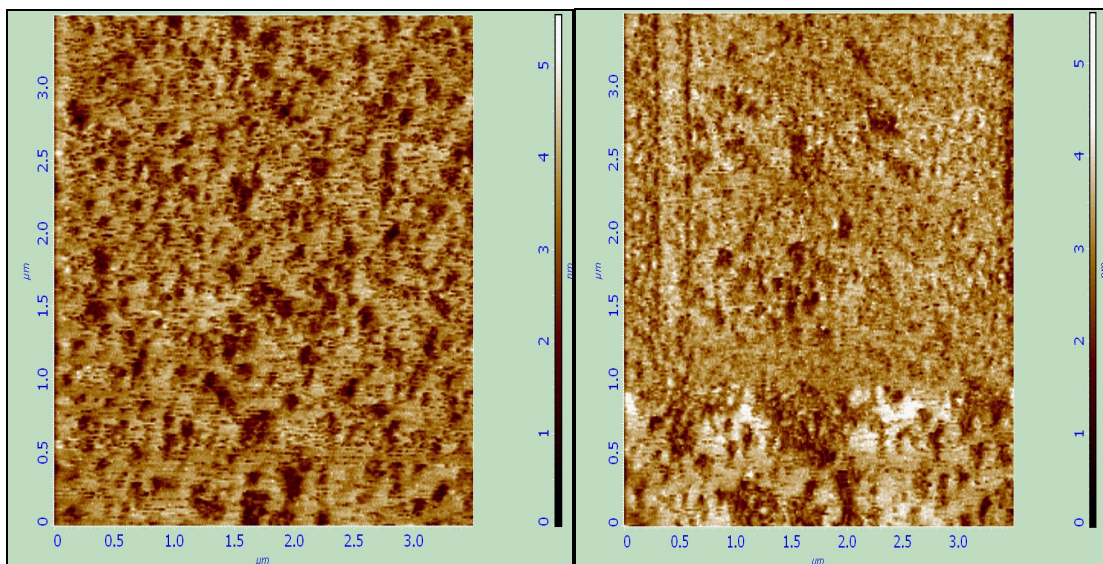
nanoscratches. Thickness measurements of the patterns are almost the same values about 1nm; however increasing forces values applied (increasing between 40.000 and 50.000 nN force limits). Thickness values didn't match to calculated results. But, bare titanium surface doesn't deform under force. So, occurrence of deformation could be related with SAM. To apply force may just bend the organics. The diversity could stem from the bending or bonding geometries. Since, the organic molecules can bond to surface angular.

### **3.1.4.3. SAM of ODA-HCl with 0,1mM in Ethanol**

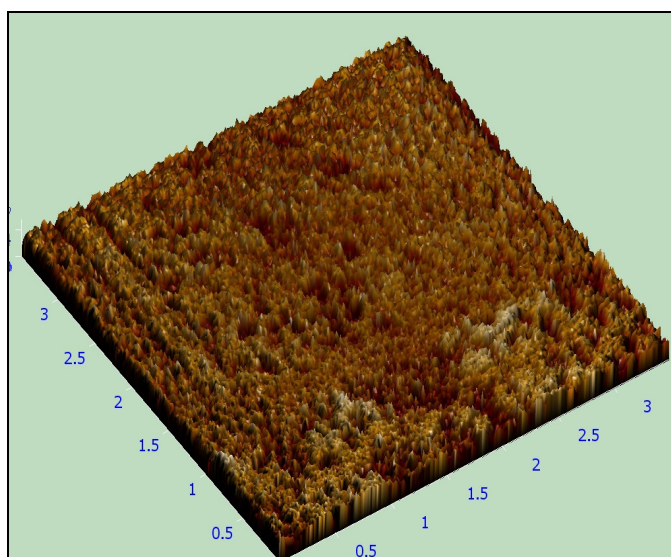
SAM solution of ODA-HCl was prepared with ethanol solvent using 0,1 mM concentration. Monolayer formation was observed only on mica, p type silicon and titanium surfaces among the substrates.

#### **3.1.4.3.1. SAM of ODA-HCl with 0,1mM in Ethanol on Mica**

In Figure 3.12, two and three dimensional AFM topographic surface images of mica consist of ODA-HCl solution are illustrated. As it is seen from the figure, there are some holes on the surfaces. They must be pinhole defects. Different from the examined substrates dust particles wasn't be observed even at three micrometer. Beside lack of dust particles, formation on the surface is seen clearer. Using ethanol as a solvent in the SAM solution can affect the formation this way. After examined the surface nanolithography was used on the surface. The logo of IYTE was tried with raster lithography method. Yet, the surface area was small for patterning, it couldn't be seen clearly. Changing in surface is distinguished but the shape is not. This can stem from using small surface. Since, surface area couldn't be enough for the patterning.



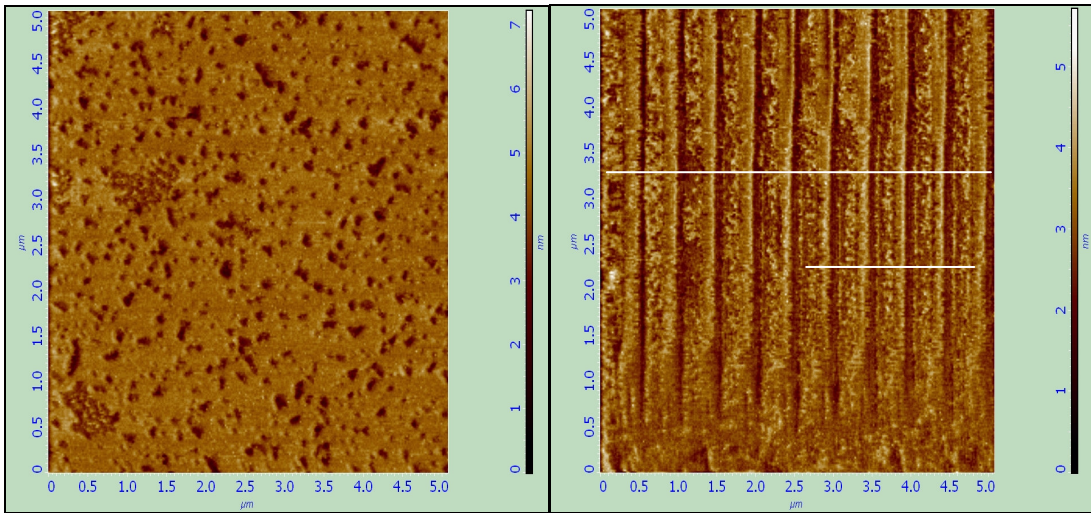
(a)



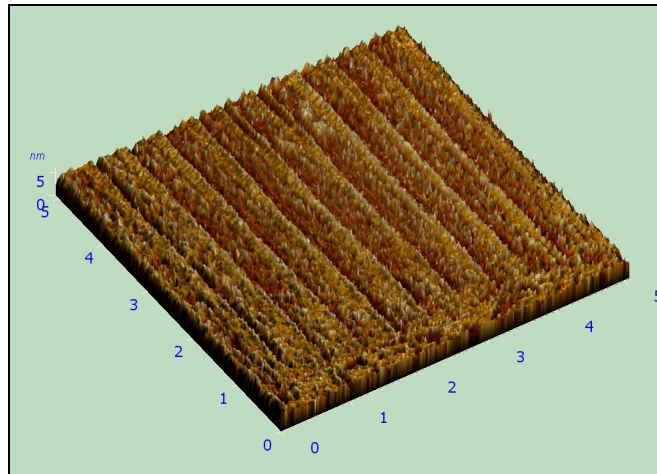
(b)

Figure 3.12. Topographic AFM images of SAM consist of ODA-HCl with 0,1 mM in ethanol on mica with (a) two and (b) three dimensional with the scale of  $3,5 \times 3,5 \mu\text{m}$

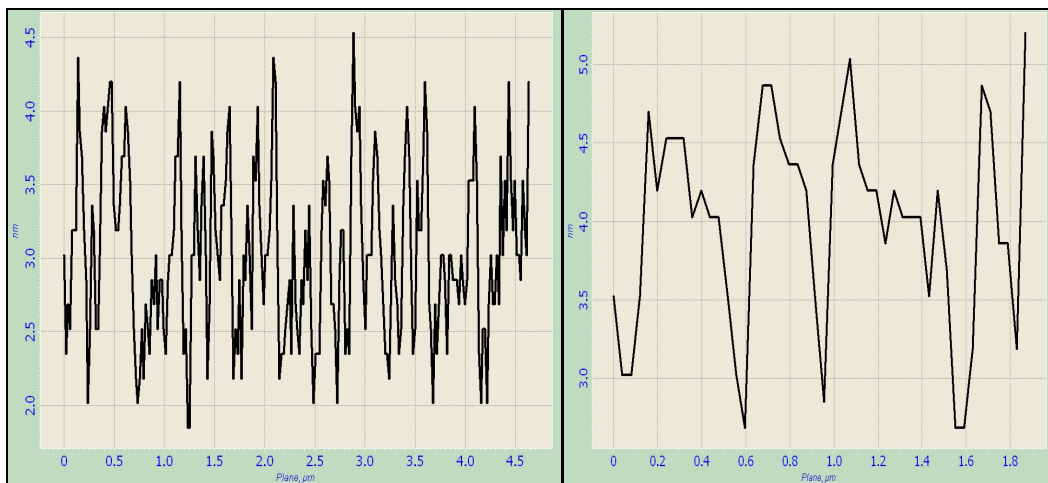
Bigger area was used for patterning at Figure 3.13.(a), (b) and (c). It is seen that holes are observed much clearer. Nanoscratching was done with increasing force values (increasing between 40.000-50.000 nN). Two and three dimensional images at the figure show these nanopatterns. Thickness measurements were taken first through the whole surface but since it wasn't seen clearly, it was taken from limited area.



(a)



(b)



(c)

Figure 3.13. Topographic images of the surface consist of organics (ODA-HCl with 0,1 mM in ethanol) on mica with (a) two and (b) three dimensional and (c) thickness measurement with the scale of 5X5  $\mu\text{m}$

Thickness measured roughly about 1,5 nm. Despite of the increasing force, thickness is the same nearly all scratches (Figure 3.13.(c)). This value is less than calculated one. This might be due to bonding geometries of SAM on mica surface. The organics could make angular bonding to the surface. Since the ODA-HCl is longer molecules and the longer molecules cause diversion from the tilted angle. This diversion could be observed reducing in the thickness. It is also possible that the dissimilarity in thickness can stem from the bending of the organic molecules.

The logo of IYTE was examined with raster lithography as shown in Figure 3.14.(a). In raster lithography force limited applied figure parts are given the software. The force value of the restricted figure area could be enough for leaving the monolayer from the surface. In raster lithography the force magnitude applied and the tip is proportional with the contrast of the JPEG picture introduced to the nanolithography software. A complicated picture even in gray scale can not be written on a SAM monolayer film. The picture should be in black and white. This effect can be observed clearly on Figure 3.14 (a) and (b). All the lithographic parts of the picture couldn't be observed, since the monolayer formed very thin.

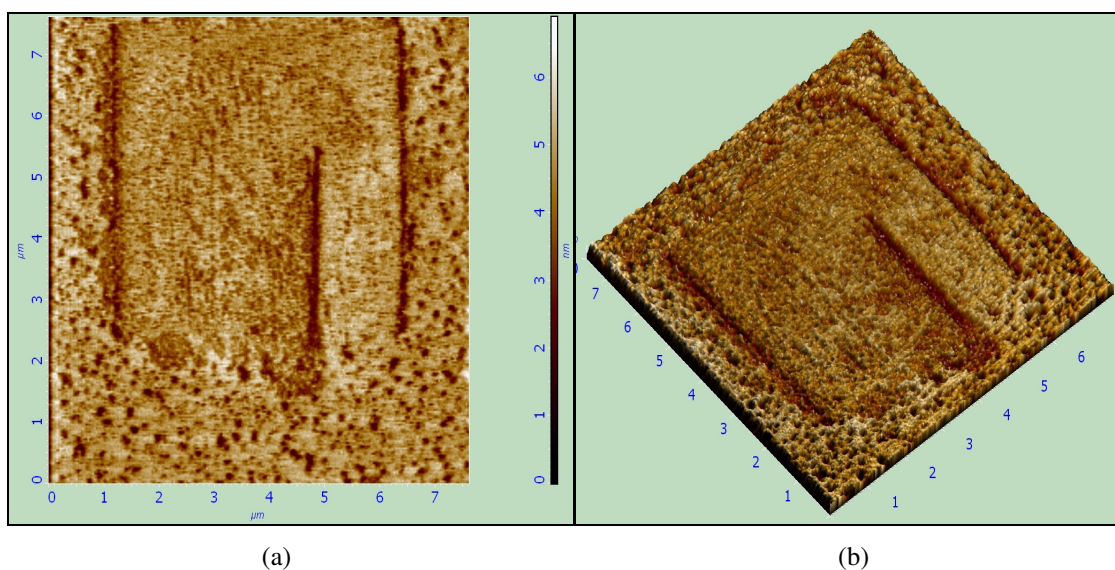


Figure 3.14. (a) Two and (b) three dimensional nanolithography images of logo of IYTE on mica surface containing ODA-HCl (with 0,1 mM in ethanol) within 7X7  $\mu\text{m}$

### 3.1.4.3.2. SAM of ODA-HCl with 0,1mM in Ethanol on p type Silicon

In Figure 3.15, two dimensional topographic images of p type silicon surface prepared by the solutions of ODA-HCl with 0,1 mM in ethanol are illustrated. As it is seen from the figure, there are some particles on the surfaces. Beside these particles, a number of pinholes are observed. Nanolithography was done on the surface. Even at high force values, deformation couldn't be observed. But the holes were thought that monolayer formed. Since the used substrate was bare silicon and has smooth surface.

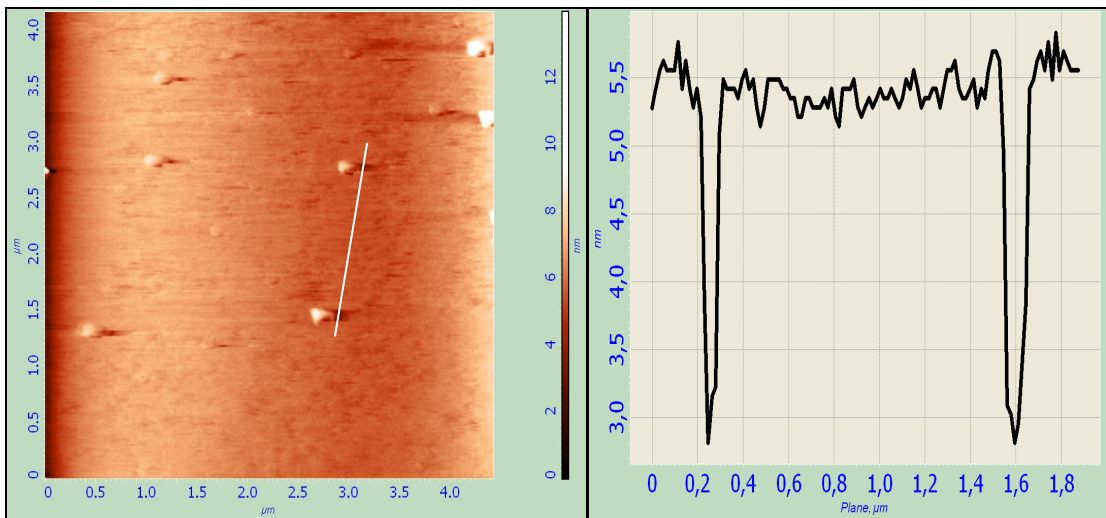


Figure 3.15. Two dimensional topographic AFM images of surface prepared by ODA-HCl with 0,1 mM in water on p type silicon with the thickness measurement in the scale of 5X5 μm

Thickness measurement of defects matches with the organic length. At the Figure 3.15 measurement of two of them is illustrated. As it is seen the thicknesses are about 2,5 nm. This value matches the length of ODA-HCl.

### 3.1.4.3.3. SAM of ODA-HCl with 0,1mM in Ethanol on Titanium

In Figure 3.16.(a) and (b), two dimensional topographic images of titanium deposited on silicon surface with the SAM solution of ODA-HCl with 0,1 mM in ethanol are illustrated. In Figure 3.16.(a), before and after nanopatterning surface images are shown. As it is seen from the figure, surface viewing in nanolithography was

used on the surface. Even at high force values, patterning couldn't be seen clearly. Thickness measurements of the nanoscratches patterns are almost the same values about 1nm; however increasing forces values applied (increasing between 30.000 and 50.000 nN).

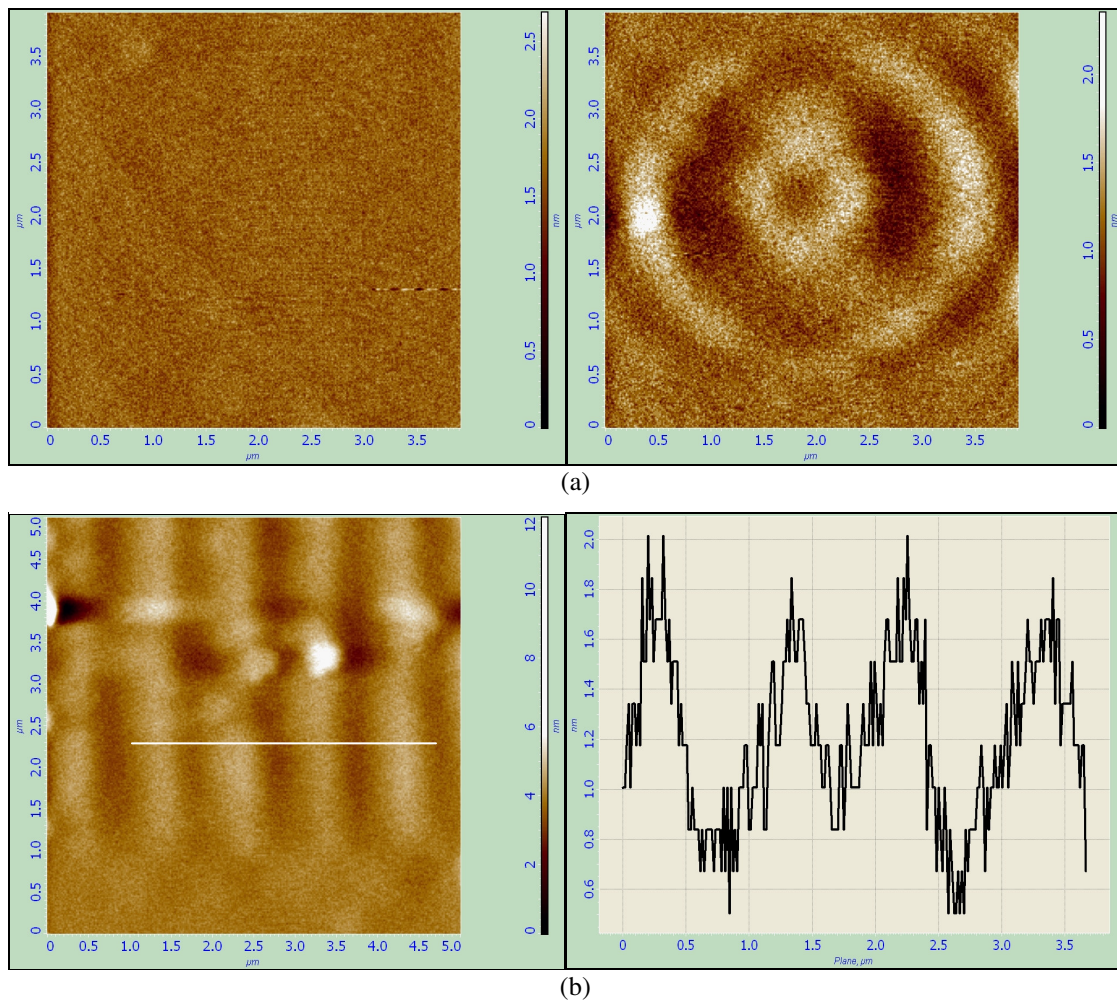


Figure 3.16. Topographic AFM images of titanium deposited on silicon with SAM of the solutions of ODA-HCl with 0,1 mM in ethanol (a) before and after nanopatterning surface image with the scale of 3,5X3,5  $\mu\text{m}$  (b) and nanoscratching with thickness measurement at 5X5  $\mu\text{m}$

Thickness values didn't match to calculated degrees. But, bare titanium surface doesn't deform. So, occurring deformation could be related with the something that out of the surface like SAM. The angular bonding between organic and surface could be

occurred. It is also possible that the molecules bended under force and this could cause observing as less thickness.

### 3.1.5. SAM with Thiols

DM and ODT were examined as SAM organic molecules with different molarities in ethanol (0,1 and 1 mM). Silicon with n and p type, titanium thin film on silicon and mica were used as substrates. Among these substrates mica and titanium were chosen. Since, it was thought that monolayer formed only on these substrates. Table 3.3 shows the organics of SAM with the substrates on which monolayers were formed. Before nanolithography, surfaces were examined with atomic force microscopy.

Table 3.3. SAM of thiols with the substrates on which monolayers were formed

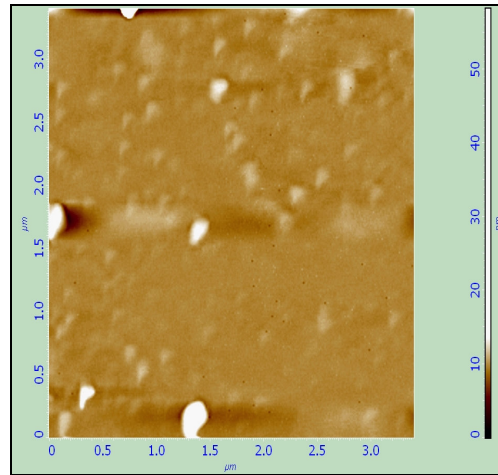
<b>DM 0,1 mM in ethanol</b>	<b>DM 1 mM in ethanol</b>	<b>ODT 0,1 mM in ethanol</b>
-	-	-
mica	-	mica
-	-	Titanium on silicon

#### 3.1.5.1. SAM of DM with 0,1mM in Ethanol on Mica

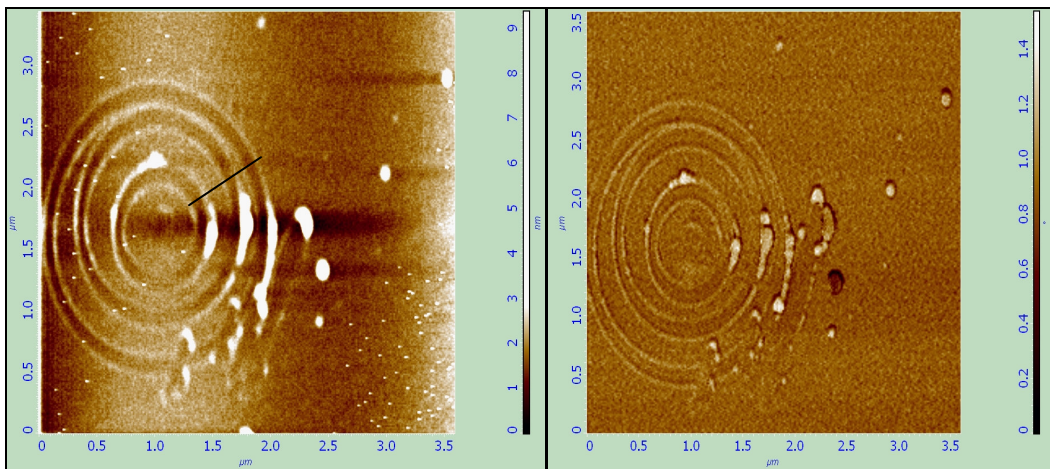
SAM solution of DM was prepared with ethanol solvent with 0,1 mM concentration. All substrates mentioned before were immersed into DM to form on them. But monolayer formation was observed only on mica. The results are given as following.

AFM images of surface with nanolithography patterns are given in Figure 3.17. Thickness measurement is given in Figure 3.17.(c). Bigger particles represented as brightening part those brightened areas could be dust. The others are organic molecules formed as SAM. Topography and phase images of surface are shown in Figure 3.17.(b). In this figure, each circle was done at the same force value (35.890 nN), but different number of cycles. First circle was done by after 5 scratching cycles and the others were done with 10 and 15 cycle of scratching respectively. The thickness measurement shows

that patterns thickness is the same for all of them, in spite of increasing scratching cycles. The thickness of the patterns was measured less than 1 nm. Calculated value is around 1nm. Similar thickness results obtained. So, this means that the deposited monolayer thickness is the same everywhere on film. There is very small difference between calculated and measured thickness. This difference might be due to the tilt angle. On the other hand, there is some debris due to collection of SAM organic material due to scratching the surface. It should be carefully during thickness measurement close to debris. The thickness should be measured as difference in height between the scratched well and normal surface that represents the global film surface. It Brighter regions represent the left debris from scratching nanolithography process as demonstrated in Figure 3.17.(c).. The amount of debris depends pretty much on the film thickness and the depth of the scratch due to higher tip force magnitude. Some times the left material (debris) can reaches up to 3nm in height on organic SAM films. The patterns are observed clearly. The surface materials (organics) could be removed completely from the surface. Having too much debris can also stem form removing of the molecules completely. Since, at the other substrates that have differences in thickness debris of the material couldn't be observed.



(a)



(b)



(c)

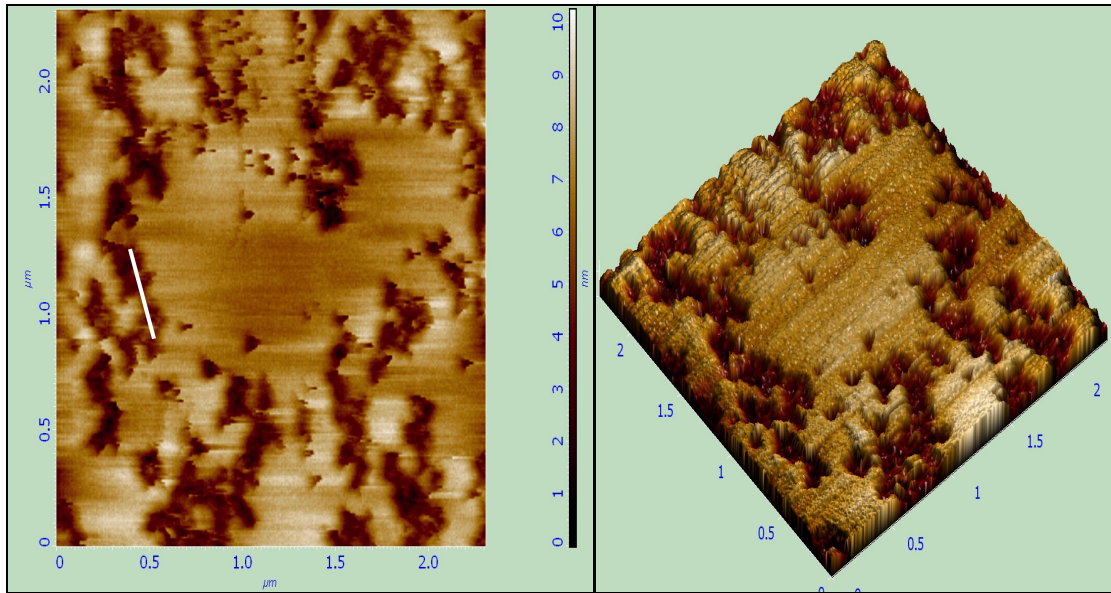
Figure 3.17. AFM topography images of SAM of DM with 0,1 mM in ethanol on mica: (a) bare DM film, (b) topography (right side) and phase (left side) images of surface after nanolithography in  $3,5 \times 3,5 \mu\text{m}$  and (c) thickness measurement

### **3.1.5.2. SAM of ODT with 0,1mM in Ethanol**

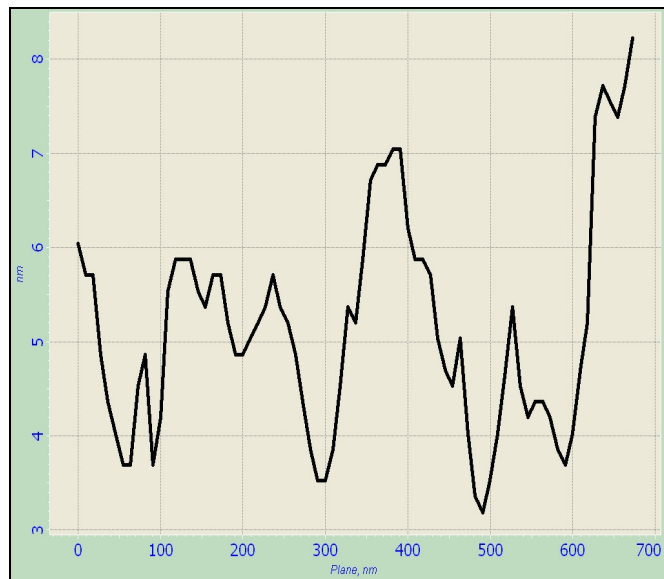
SAM solution of ODT was prepared with ethanol solution with 0,1 mM concentration. SAM formation was observed only on mica and titanium surfaces.

#### **3.1.5.2.1. SAM of ODT with 0,1mM in Ethanol on Mica**

In Figure 3.18, two and three dimensional topographic AFM images of SAM of ODT with 0,1 mM in ethanol on mica are illustrated. As it is seen from the figure, some formations with pinhole defects on the surfaces are clearly visible. It is known that pinholes defects are mostly observed on thiols groups. Even 2  $\mu\text{m}$  scales the formation that occurred on the surface is seen clearly (Figure 3.18). The AFM thickness measurement on one of the defects is around 2nm (Figure 3.18 (b)). This value almost matches calculated thickness result. So, it is possible that these holes are the pinholes defects of the SAM molecules.



(a)



(b)

Figure 3.18. (a) Two and three dimensional topographic AFM images in  $2 \times 2 \mu\text{m}$  and (b) thickness measurement on one of the defects on mica with the SAM of ODT having the concentration of  $0,1 \text{ mM}$  in ethanol

Nanolithography was tried on the SAM of ODT on mica surface as shown in Figure 3.19. Circular patterns were drawn with force values between  $35.000\text{-}45.000 \text{ nN}$  below critical sheet collapse value of mica. Thickness measurement couldn't be done since the patterning cause increase in the surface roughness. The left debris on the surface which increases surface roughness prevents the thickness measurement.

However the shape of the pattern is seen from the image that shows a rough ODT SAM film formation on mica.

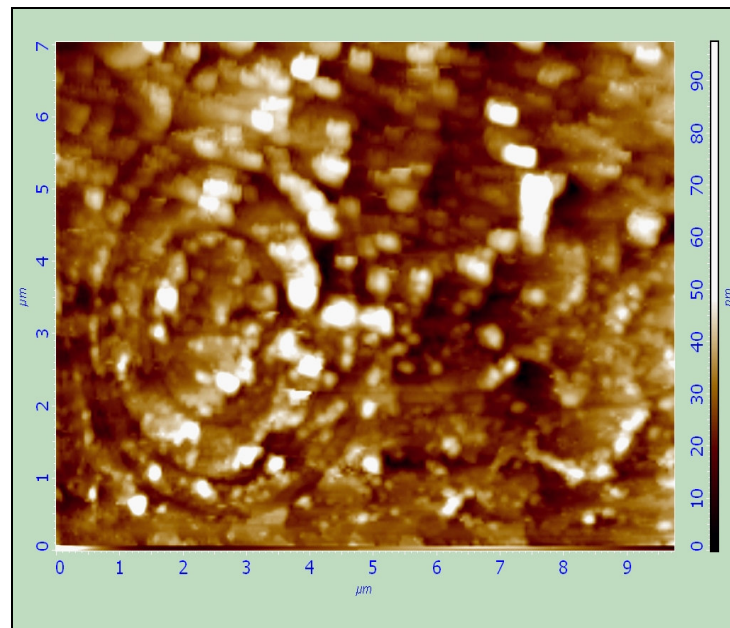


Figure 3.19. Nanolithography on mica prepared with the SAM of ODT with 0,1 mM in ethanol

Another nanolithography trial is illustrated in figure 3.20. Circle was chosen as a pattern. During the patterning 24.380 nN contact force applied on the surface. The pattern couldn't be observed clearly. Since the applied force couldn't be high enough for deformation, surface deformed just locally. Lacking of debris can be stem from bending of the molecules. The applied force can just cause bending on some of the surface area.

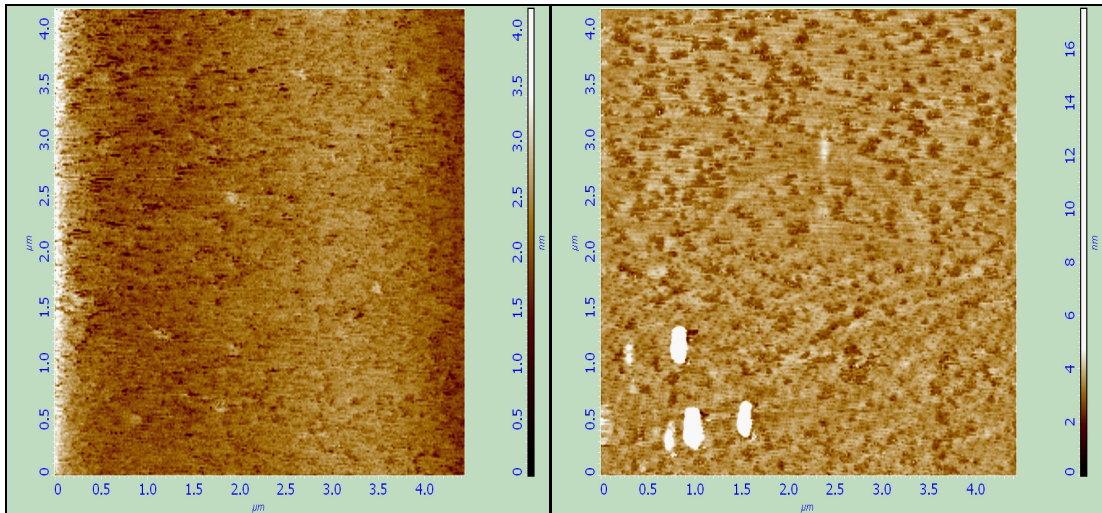


Figure 3.20. Two dimensional topographic AFM images with nanolithography of mica with the SAM of ODT having the concentration of 0,1 mM in ethanol at the scale of 4X4  $\mu\text{m}$

### 3.1.5.2.2. SAM of ODT with 0,1mM in Ethanol on Titanium Substrate

In Figure 3.21 two dimensional topographic images of titanium deposited on silicon surface with the SAM of ODT having the concentration of 0,1 mM in ethanol at different scales are illustrated. From the color differences it can be said that some formation is observed on the surface. Beside the brighter particles which are thought a dust, some other formations are seen. (Figure 3.21). They are also observed at nanometer scales.

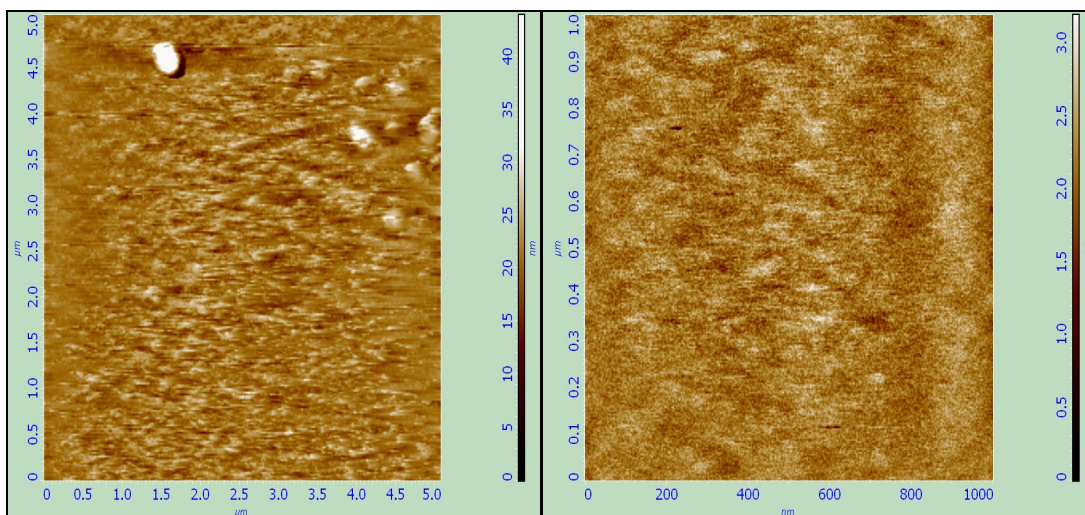
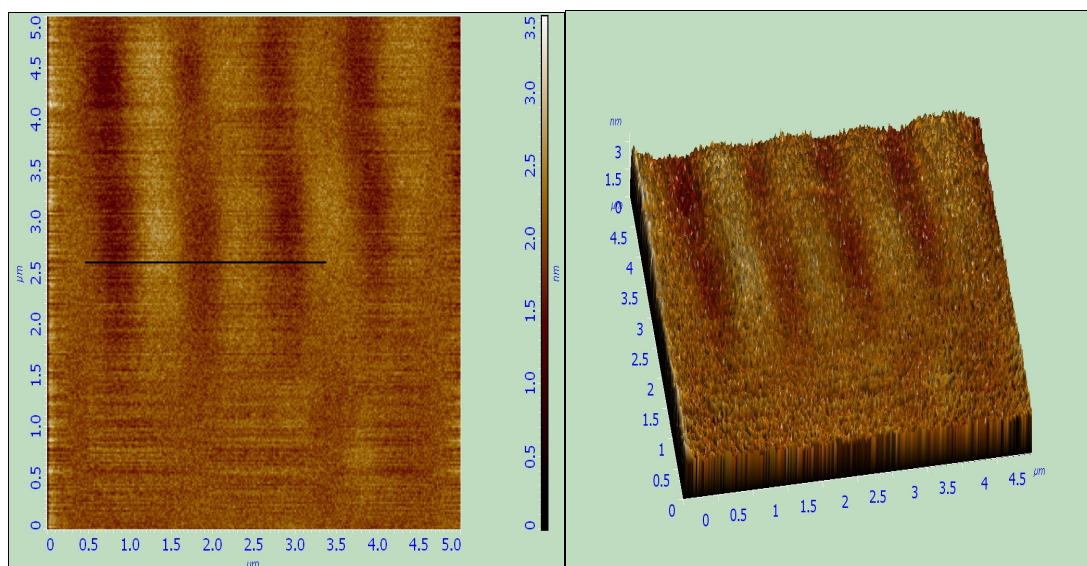
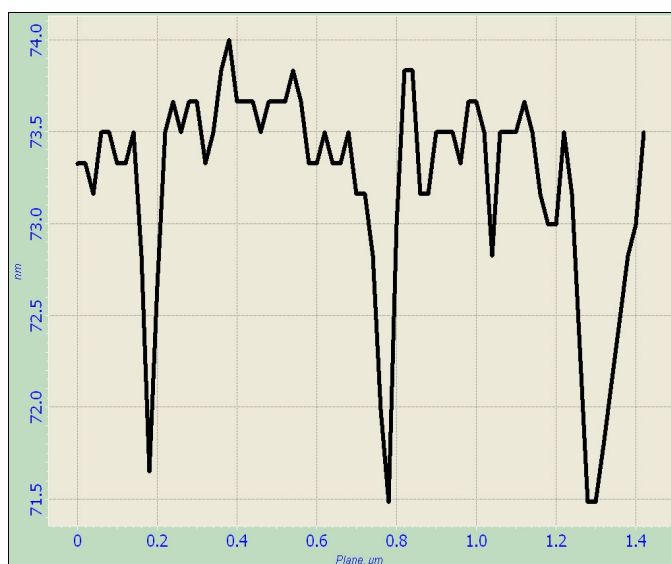


Figure 3.21. Topographic AFM images of titanium surface with the SAM of ODT having the concentration of 0,1 mM in ethanol at different scales

Scratching nanolithography was done on the titanium surface with the SAM of ODT as shown in Figure 3.22. Scratches were done increasing forces (increasing between 30.000-40.000 nN). However applying high forces, the patterns couldn't be seen clearly. The pattern debris couldn't be observed. The organic molecules could bend under high forces. Thickness measurements of the patterns are almost the same value about 2nm, however unclear patterning. Measured thickness is a bit different from the calculated one. The differences may originate from both bending of the molecules and surface roughness. To deform surface increases the roughness. The surface roughness could be added to the thickness of the pattern. Monolayer could be form on the surface. Since, the bare substrate doesn't deform and however unclear patterns, thickness were the same for all scratches.



(a)



(b)

Figure 3.22. (a) Two and three dimensional topographic AFM images at 5X5  $\mu\text{m}$  in scales and (b) thickness measurement of represented area of titanium surface with the SAM of ODT with 0,1 mM in ethanol

### 3.2. SEM and EDX Results

Scanning Electron Microscopy (SEM) and Energy Dispersive X rays (EDX) were used other characterization techniques. SEM was used for viewing the surfaces in details. EDX was preferred for investigating materials that stayed on the surface. By

using this technique it is possible to understand whether the surface has organic molecules or not.

### 3.2.1. ODA-HCl with 0,1mM in Water

After AFM characterization technique, substrates that were thought monolayer formed were examined with SEM and EDX. Mica and p type silicon substrates prepared with SAM of ODA-HCl was investigated for the aim of supporting the idea of monolayer formation. The results are given below.

#### 3.2.1.1. SAM of ODA-HCl with 0,1mM in Water on Mica

Figure 3.23 represents SEM images of the SAM consist of ODA-HCl with 0,1 mM in water on mica with 2X2  $\mu\text{m}$  and 500X500 nm scales. As it is seen from the images, there are some formations on the surfaces. This is probably monolayers formations. They are even observed at nanometer scales.

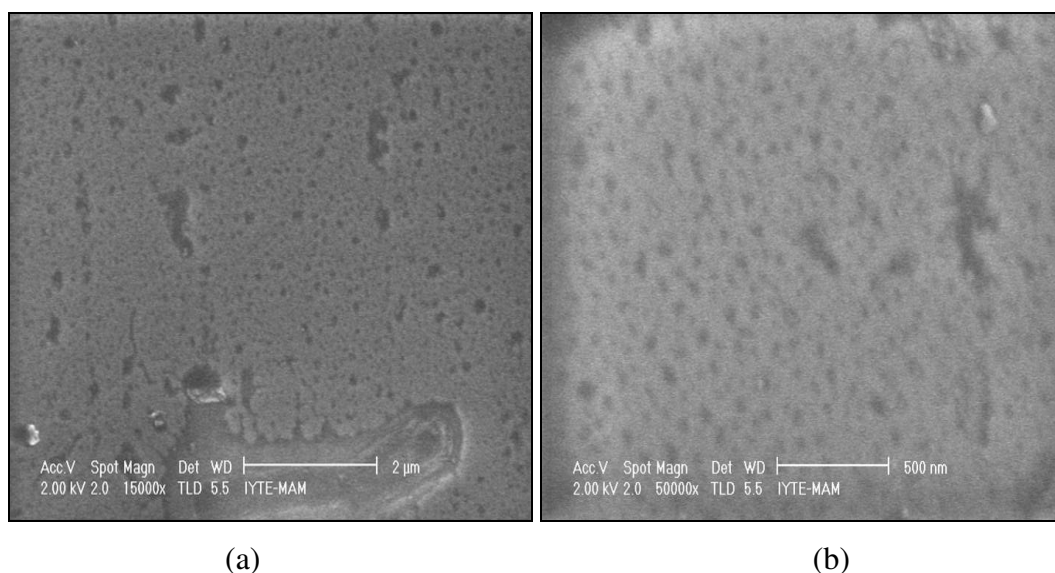


Figure 3.23. SEM images of ODA-HCl with 0,1 mM in water on mica with (a) 2X2  $\mu\text{m}$  and (b) 500X500 nm in scales

The EDX data shows that there are organics on the surface (Figure 3.24). Besides mica's structural components, carbon and nitrogen atoms which belong to ODA-HCl structure were observed on the surface. This illustrates that SAM formation occurred on the surface. There are some black regions which are probably the type of defect of pinholes.

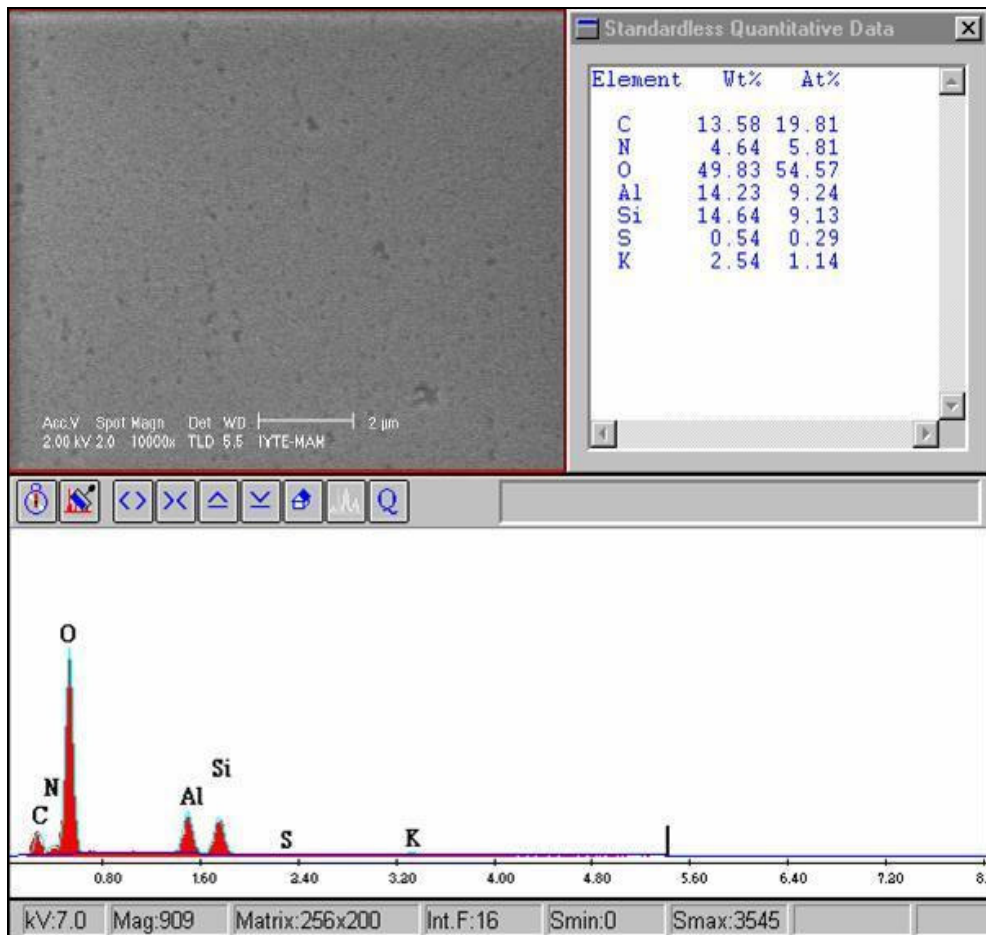


Figure 3.24. EDX results of SAM consist of ODA-HCl with 0,1mM in water on mica

### 3.2.1.2. SAM of ODA-HCl with 0,1mM in Water on p type Silicon

SEM images of SAM consist of ODA-HCl with 0,1 mM in water on p type silicon with EDX data are given in Figure 3.25. As it is seen from the image, except for silicon surface some other atoms belong to organics of SAM are observed. Among these atoms carbon, nitrogen and chlorine comes from the ODA-HCl. Oxygen, can originate from the surrounded area. The surface could be oxidized. These atoms show that there

are organics related with the ODA-HCl on the surface. But the ratios of the molecules are at low range. The formation could be little or the ratio of the organics is small beside silicon material. There are some black points on the surface. These areas can represent the pinholes, uncovered surface parts.

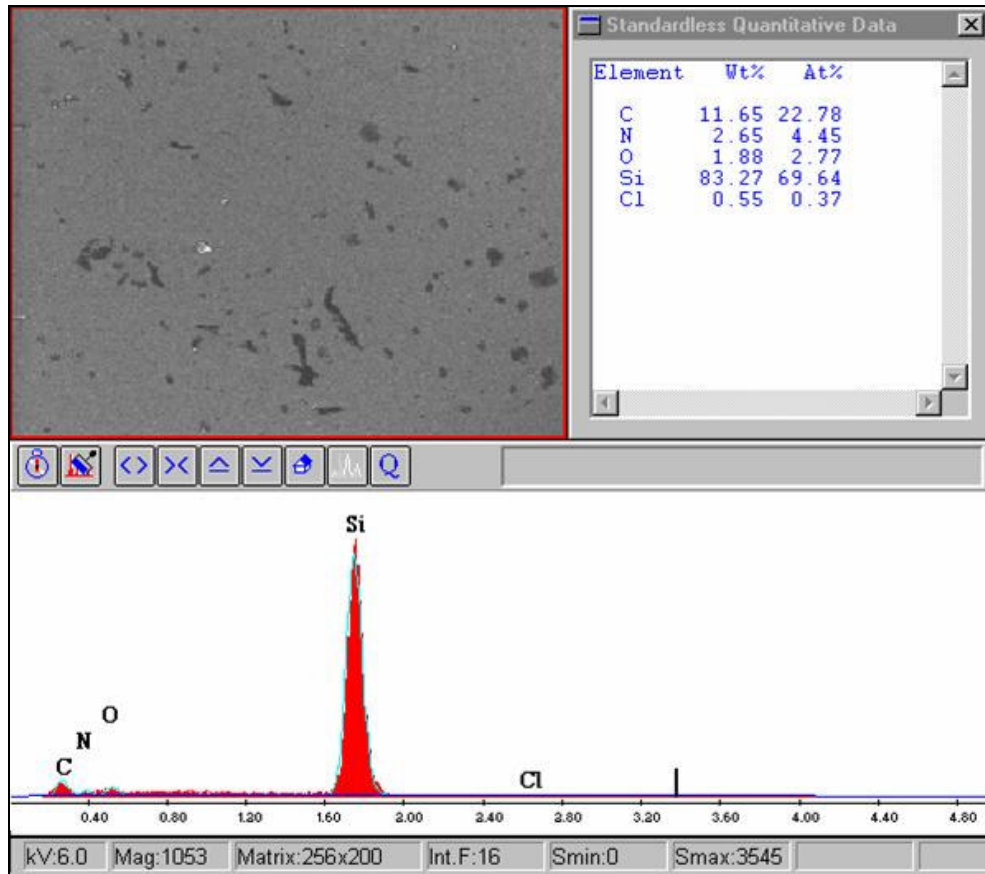


Figure 3.25. SEM with EDX results of SAM consist of ODA-HCl with 0,1 mM in water on p type silicon

### 3.2.2. SAM of ODA-HCl with 1mM in Water on Titanium

SEM images with EDX data of SAM consist of ODA-HCl with 1mM in water on titanium is given at Figure 3.26. There are some islands and brighten areas on the surface. Brighten areas are stuck particles. The islands seem organic surfaces. Since the EDX data demonstrate that, there are some organic atoms on the surface. On the other hand, these atoms belong to ODA-HCl which is thought that had been deposited on the surface.

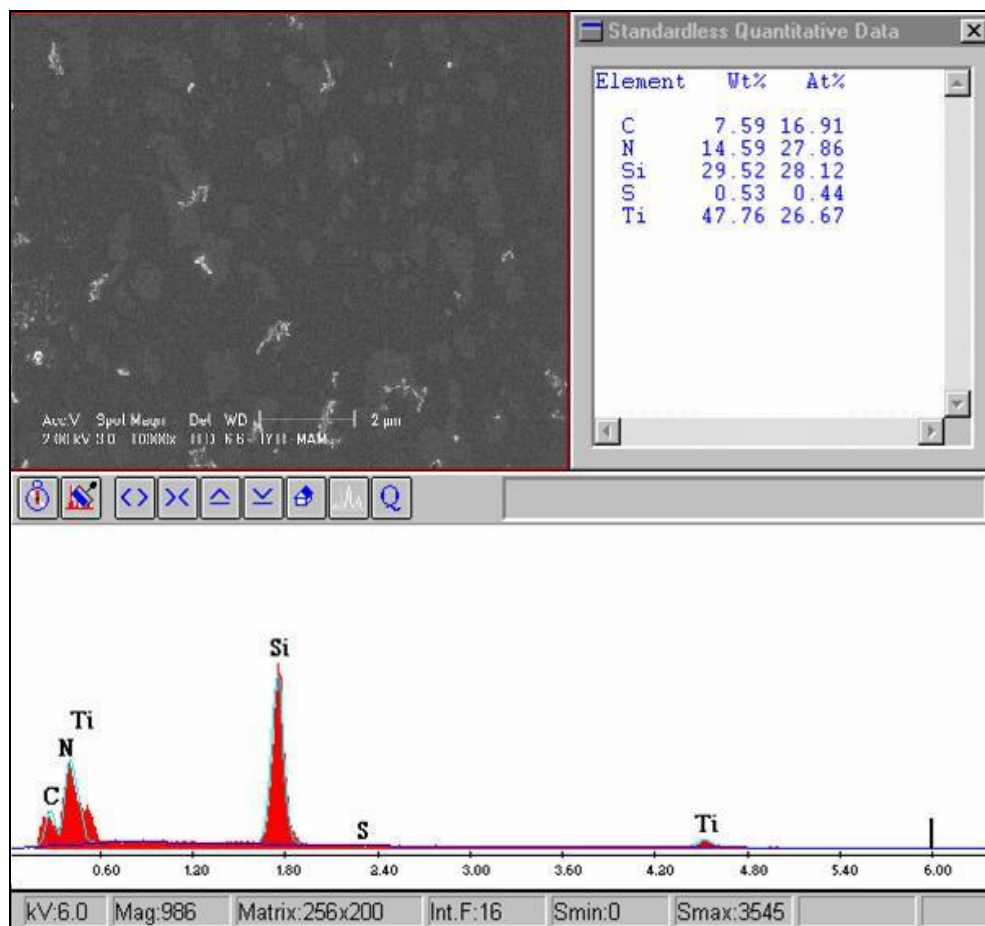


Figure 3.26. SEM with EDX results of SAM consist of ODA-HCl with 1 mM in water on titanium

### 3.2.3. SAM of ODA-HCl with 0,1mM in Ethanol

After AFM characterization technique, monolayer formation was observed only on mica, p type silicon and titanium surfaces. For the aim of supporting the idea of monolayer formation, mentioned substrates were examined with SEM and EDX. The results are given below.

#### 3.2.3.1. SAM of ODA-HCl with 0,1mM in Ethanol on Mica

SEM images of the surface with EDX data are given in Figure 3.27. The surface seems to be very smooth. But organic molecules of ODA-HCl were observed on the surface. The rate of the organics seems to lower rate than the surface molecules.

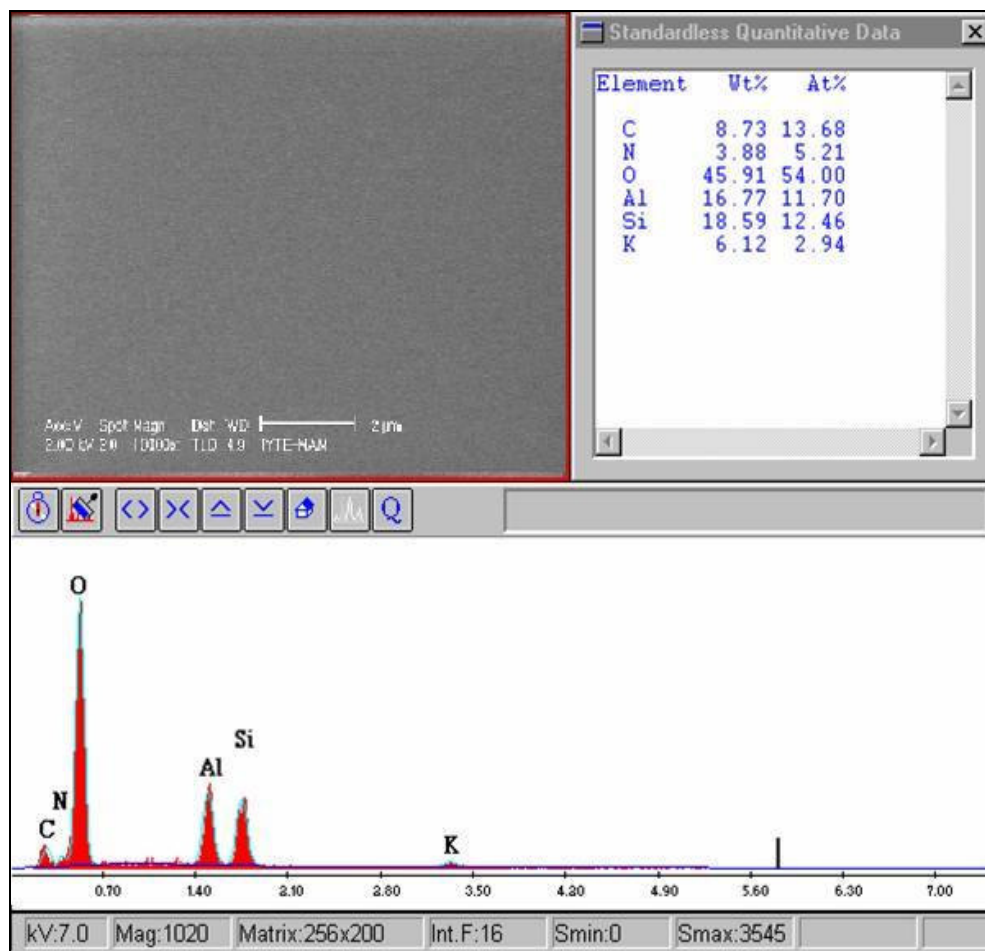


Figure 3.27. SEM with EDX results of SAM consist of ODA-HCl with 0,1 mM in ethanol on mica

### 3.2.3.2. SAM of ODA-HCl with 0,1mM in Ethanol on p type Silicon

SEM images of the surface with EDX data are given in Figure 3.28. The surface seems to be very smooth. There isn't any prominent sign observed from the SEM image except for some of the brighten parts. Also the EDX data of the surface shows that carbon and chlorine elements are on the surface (Figure 3.28). These atoms could come from organics because used solution consists of these. On the other hand, different from the others nitrogen didn't observe with EDX. This can be cause of either lower rate of finding on the surface for observing or boding over chlorine atoms to the surface.

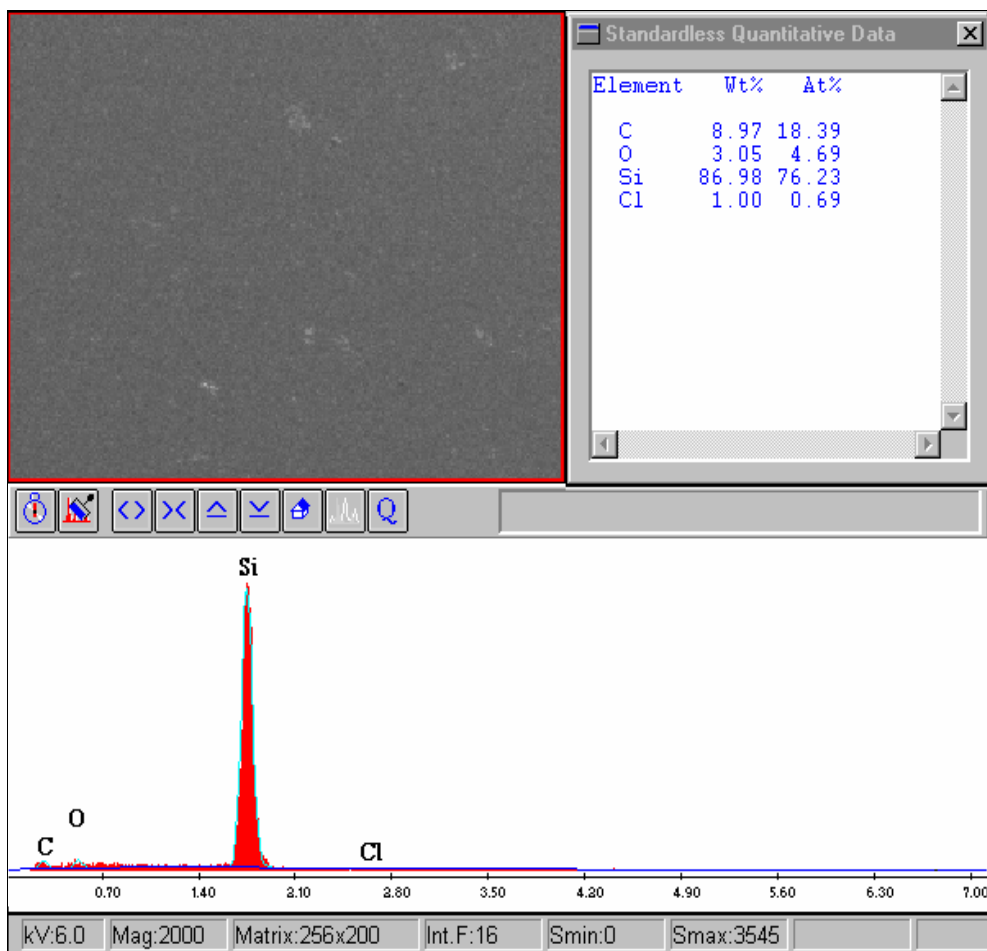


Figure 3.28. SEM with EDX results of p type silicon prepared by the solutions of ODA-HCl with 0,1 mM in ethanol

### 3.2.3.3. SAM of ODA-HCl with 0,1mM in Ethanol on Titanium

Figure 3.29 represents SEM with EDX results of titanium on silicon prepared by the solutions of ODA-HCl with 0,1 mM in ethanol. It is seen from the SEM image that some white points observe even at 200 nm. It is observed that there is an organic formation on the surface. Since the EDX data shows that there are organic molecules of ODA on the surface (Figure 3.29).

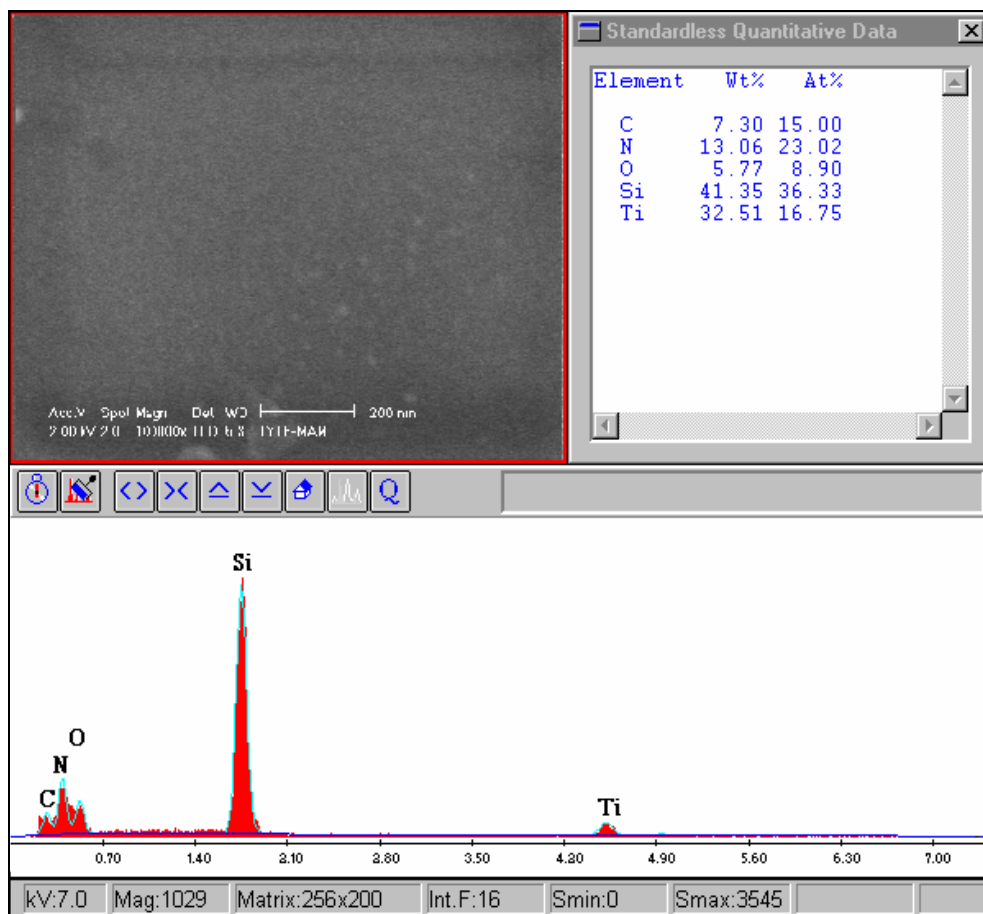


Figure 3.29. SEM with EDX results of titanium on silicon prepared by the solutions of ODA-HCl with 0,1 mM in ethanol

### 3.2.4. SAM of DM with 0,1mM in Ethanol on Mica

Figure 3.30 represents SEM with EDX results of mica prepared in the solutions of DM with 0,1 mM in ethanol. The EDX data demonstrates that there are some organics on the surface since carbon and sulfur atoms representing SAM of DM were observed on the surface besides mica's structural components as substrate. But the atomic rate of SAM molecules obtained from EDX data is small compared to atomic rate of mica due to thickness of SAM film around 2 nm. It is known that thiols have higher electron density. Since sulfur is a big atom and has more electrons, higher electron density prevents viewing the surface at low scales. So, low scale images couldn't be taken.

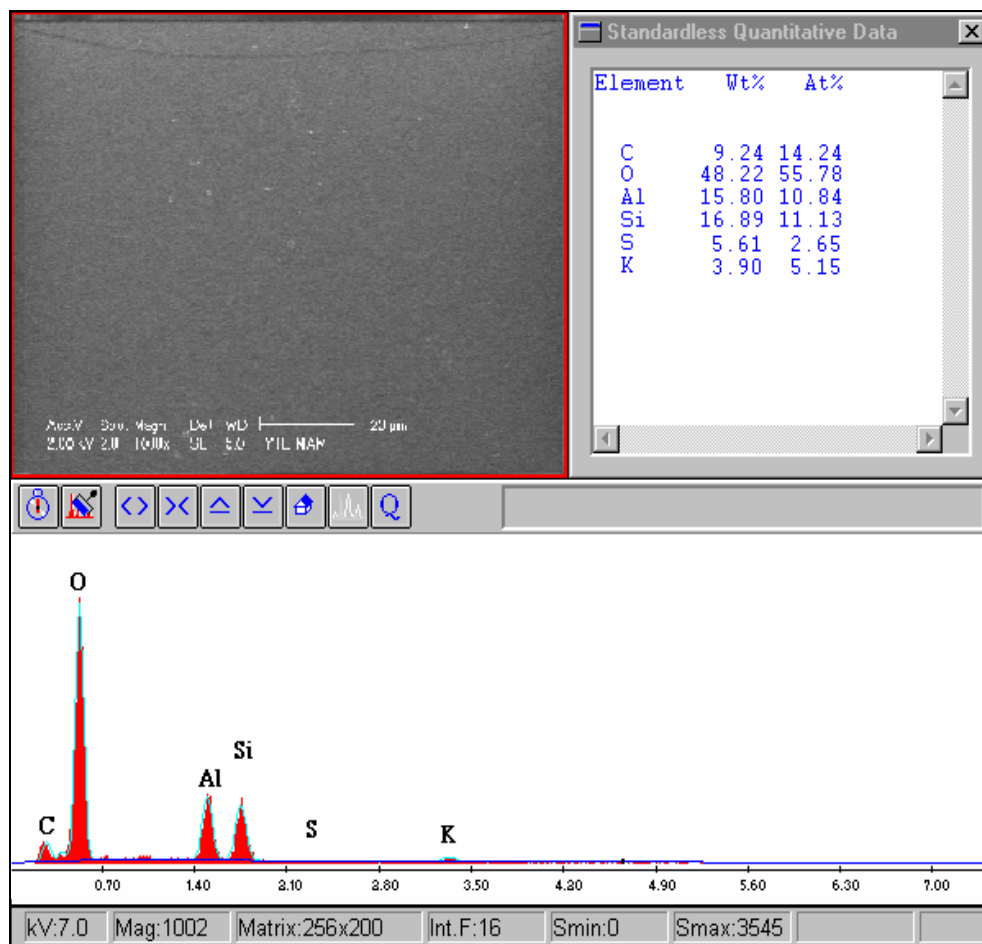


Figure 3.30. SEM with EDX results of mica prepared in the solutions of DM with 0,1 mM in ethanol

### 3.2.5. SAM of ODT with 0,1mM in Ethanol

SAM solution of ODT was prepared with ethanol solution with 0,1 mM concentration. SAM formation was observed only on mica and titanium surfaces with AFM characterization technique. For the aim of supporting the idea of monolayer formation, mentioned substrates were examined with SEM and EDX. The results are given below.

#### 3.2.5.1. SAM of ODT with 0,1mM in Ethanol on Mica

Figure 3.31 illustrates SEM and EDX data of mica with SAM of ODT. SEM image demonstrate that there are two holes on the surface which are pointed out. These

can be two pinholes defect on the film. The EDX data shows that there are also some organics films on the surface besides structural components of mica substrate. Observed atoms; carbon and sulfur, belong to ODT SAM film deposited on mica. The ratios of the SAM molecules are as high as the surface component of mica substrate.

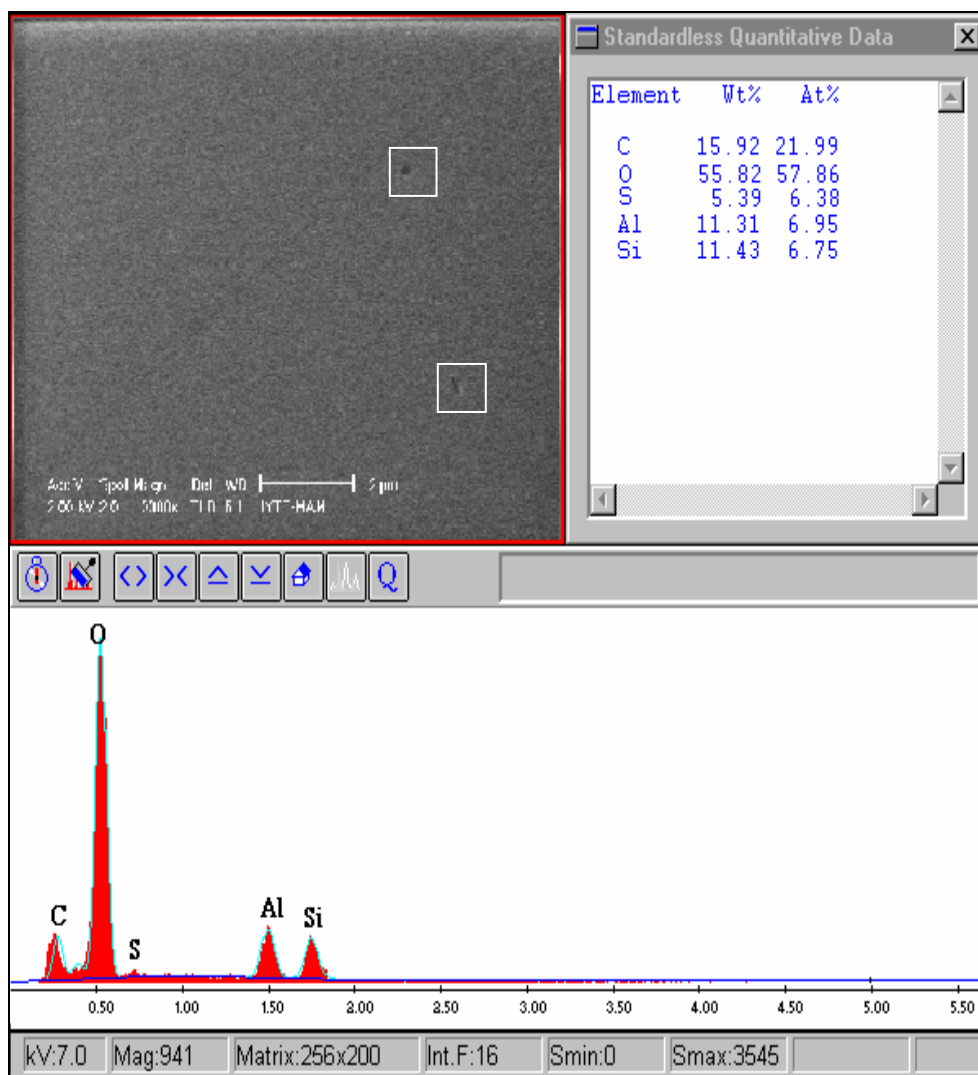


Figure 3.31. SEM with EDX results of mica contains SAM of ODT with 0,1 mM concentration in ethanol

### 3.2.5.2. SAM of ODT with 0,1mM in Ethanol on Titanium

Figure 3.32 illustrates SEM and EDX data of titanium with SAM of ODT. There isn't any prominent sign observed from the SEM image except for some of the brighten parts. The EDX data shows organics existence on the surface besides titanium.

Observed atoms; carbon and sulfur, belong to ODT. This illustrates that SAM formation occurred on the surface. The ratios of the molecules are as high as the surface component of mica substrate

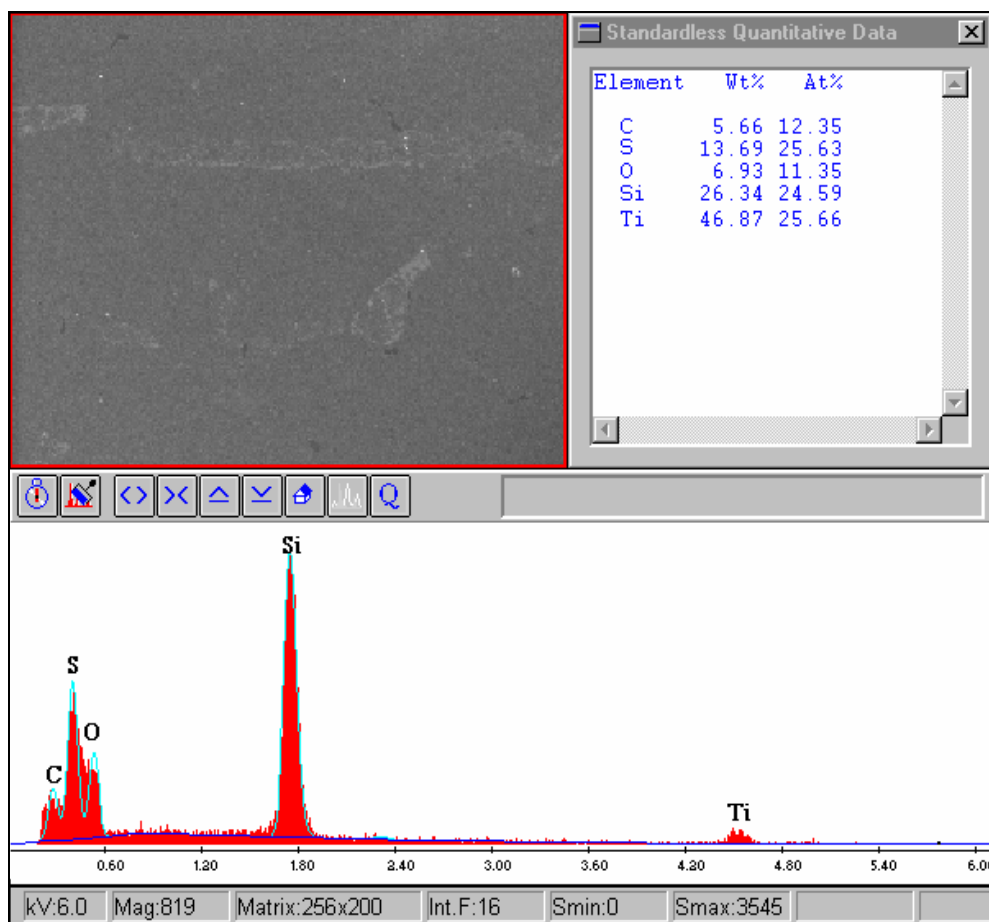


Figure 3.32. SEM with EDX results of titanium contains SAM of ODT with 0,1 mM concentration in ethanol

### 3.3. FTIR Results

Examined samples were also investigated by FTIR (Fourier Transform Infrared Spectroscopy) as a characterization technique. To understand that any chemical bonding whether occurred or not on the substrates' surfaces, FTIR was used. FTIR analysis was done with FTS 300 MX DIGILAB Excalibur Series system with both transmitted and pike 80 spectrum techniques (80 spectrums). Both in these two techniques absorbance of the beam are measured. Lost in intensity was measured as absorbance. Difference between these FTIR techniques is just usage. In transmitted method substrates put

directly on the source. So, it can't use for all type of samples. It is mostly used for transparent substrates. The beams send to the sample and differences into incoming and outgoing beams give the absorbance. This method measured directly absorbance beams. At pike 80 spectrum method some other apparatus are used for measuring absorbance beam. In this technique the beams can't measured directly. For the substrates used in this study by eliminating bare substrates and air effect measurement was done. By comparing the surfaces information of bare and immersed into SAMs solutions substrates sample surface's examined. In this method, further chemical bonding that occurs on the surfaces are observed as an extra peak different from the surfaces' peaks. Examination results are given below.

### **3.3.1. ODA-HCl with 0,1mM in Water**

Mica and p type silicon substrates prepared with SAM of ODA-HCl was investigated with FTIR. This characterization technique was used for supporting the idea of monolayer formation. The results are given below.

#### **3.3.1.1. SAM of ODA-HCl with 0,1mM in Water on Mica**

FTIR analysis of the substrate demonstrated that there was an organic formation on the surface. At Figure 3.33 FTIR results of the substrate are given. A peak around the wavenumber of  $3500\text{ cm}^{-1}$  belongs to OH. Since, the FTIR analysis demonstrates chemical bonding observed over the surface. Mines peaks come from background otherwise substrate and the other peaks represent newly formed chemical bonds. When the figure examined in details; it is seen that there are some peaks between the wavenumber of  $500\text{-}1450\text{ cm}^{-1}$  and above  $3500\text{ cm}^{-1}$ . These peaks belong to organics. The peaks about  $1380\text{ cm}^{-1}$  and  $1450\text{ cm}^{-1}$  wavenumber belong to  $-\text{CH}_3$  and  $-\text{CH}_2$  functionalize groups respectively. As comes to broad peak around  $3500\text{ cm}^{-1}$ , it belongs to OH groups. It can come from water content. It shows that organic bonded to surface from the salt form and this means that bonding occurs over whole molecule via chemically. Sharp cut part of the peak demonstrates broadening in intensity. There are also some noises and unknown peaks are observed. These can come from the

environment. However the background effect of substrate and the air was eliminated, during the experiment because of the humidity they can observe.

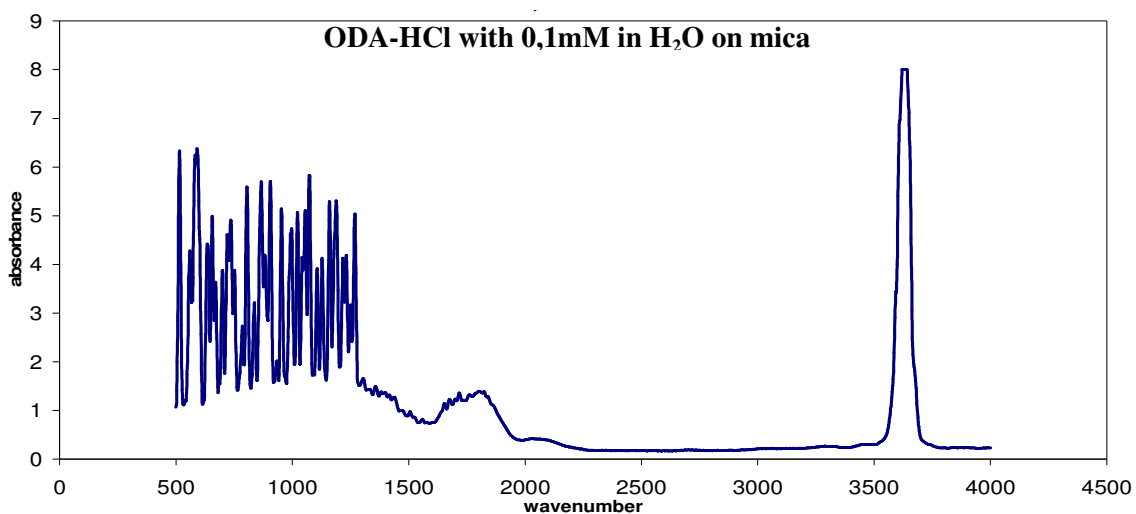


Figure 3.33. FTIR results of transmitted method of SAM consist of ODA-HCl with 0,1 mM in water on mica

FTIR analysis was done with difference methods such as transmittance and 80 spectroscopy for the substrates prepared on mica. Obtained data from each technique gave the same information. They supported the reliability of the methods. An FTIR result of 80 spectroscopy method is given at Figure 3.34. It is seen from the image like transmittance methods  $\text{-CH}_3$  and  $\text{-CH}_2$  functionalize groups are observed between the wavenumber of  $500\text{-}2000\text{ cm}^{-1}$  and to broad peak of OH is seen around  $3500\text{ cm}^{-1}$ .

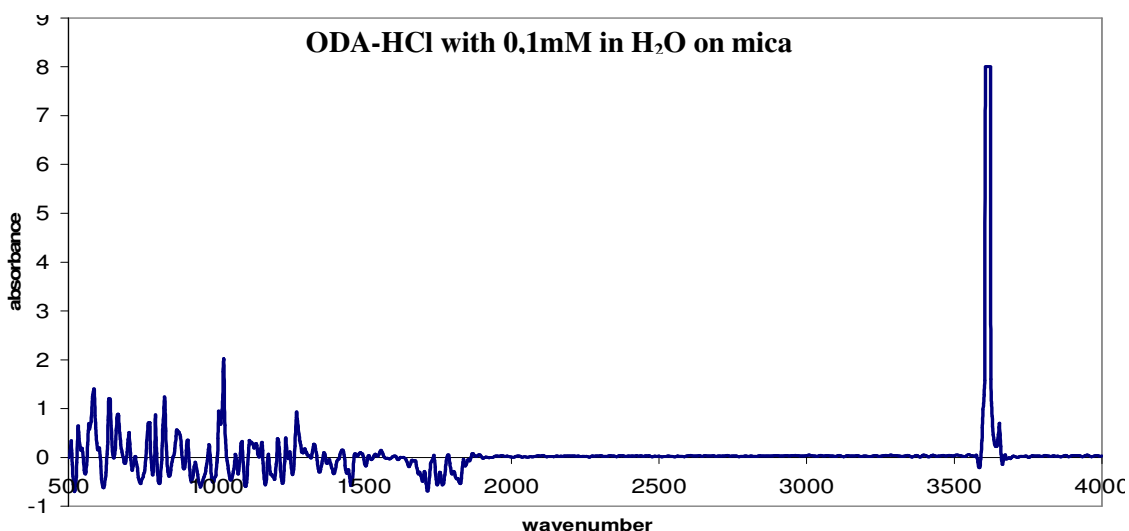


Figure 3.34. FTIR results of 80 spectroscopy method of SAM consist of ODA-HCl with 0,1 mM in water on mica

### 3.3.1.2. SAM of ODA-HCl with 0,1mM in Water on p type Silicon

FTIR analysis of the SAM consist of ODA-HCl on p type silicon demonstrated that there was an organic formation on the surface (Figure 3.35). Peaks observed around the wavenumber of 1050-1120, 1380, 1450 and 3500  $\text{cm}^{-1}$  belongs to ODA-HCl. When the figure examined in details; the peaks about 1050-1120  $\text{cm}^{-1}$  represents  $-\text{C-N}$  bonds, around 1380  $\text{cm}^{-1}$  and 1450  $\text{cm}^{-1}$  wavenumber belong to  $-\text{CH}_3$  and  $-\text{CH}_2$  functionalize groups respectively. And the peak around 3500  $\text{cm}^{-1}$ , it belongs to OH. Peaks have lower absorbance intensities because of the thin film formation. There are also some noisy peaks observed. These are originated from the environments affect like humidity. It is seen that the organic peaks are observed clearly on mica substrate than silicon. It can stem from bonding geometries of the surfaces. Organics could bond the silicon with deviation from the tilt angle. This makes the film formation thin. At FTIR analysis thin film affect observed as smaller peaks.

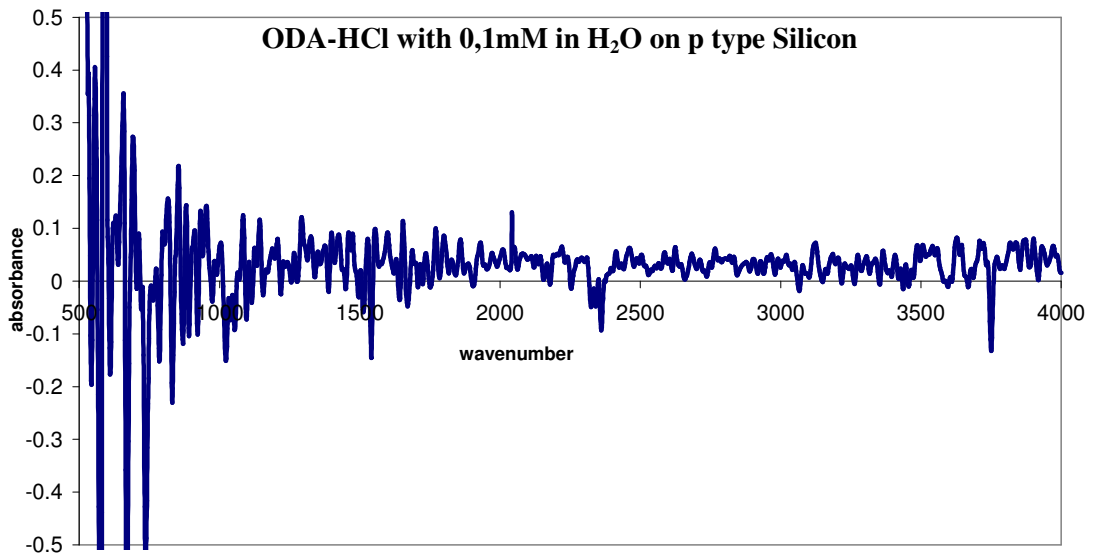


Figure 3.35. FTIR results of 80 spectroscopy method of SAM consist of ODA-HCl with 0,1 mM in water on p type silicon

### 3.3.2. SAM of ODA-HCl with 1mM in Water on Titanium

FTIR analysis of the substrate of titanium with SAM consist of ODA-HCl is illustrated at Figure 3.36. It is seen that there is an organic formation on the surface at the very low intensity values. Having lower absorbance intensities stem from the thin film formation. Peaks observed around the wavenumber of 1050-1120, 1380, 1450 and 3500  $\text{cm}^{-1}$  belongs to ODA-HCl. Like the other amines substrates, these peaks represent  $-\text{C}-\text{N}$ ,  $-\text{CH}_3$  and  $-\text{CH}_2$  functionalize groups and OH which is showed the organic bonded to surface in salt form. Because of the different substrates peaks are distinct from each other.

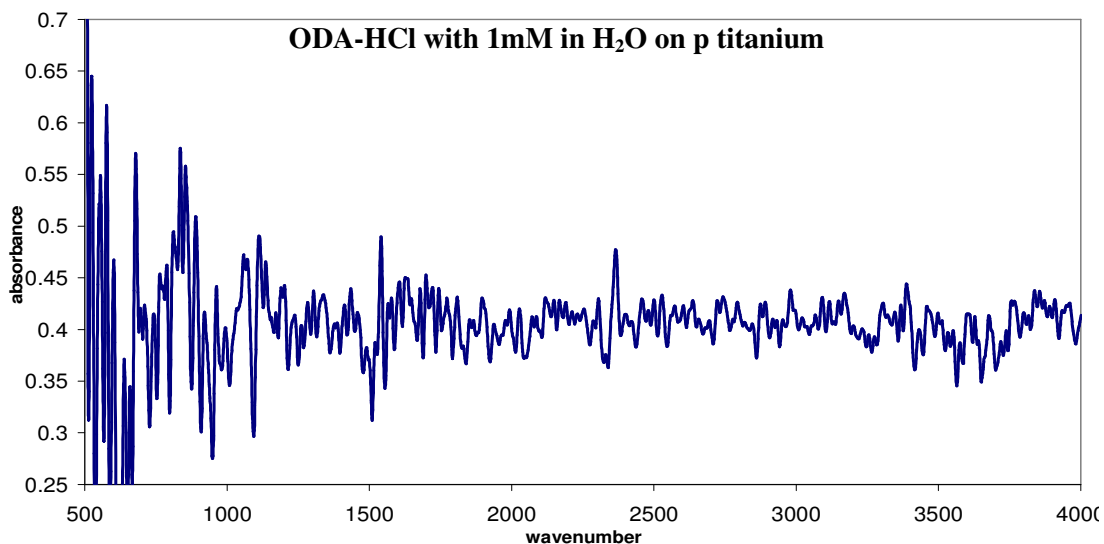


Figure 3.36. FTIR results of SAM consist of ODA-HCl with 1 mM in water on titanium deposited on silicon

### 3.3.3. SAM of ODA-HCl with 0,1mM in Ethanol

After AFM and SEM with EDX characterization technique, monolayer formation was observed only on mica, p type silicon and titanium surfaces. For the aim of supporting the idea of monolayer formation, mentioned substrates were examined with FTIR. The results are given below.

#### 3.3.3.1. SAM of ODA-HCl with 0,1mM in Ethanol on Mica

At Figure 3.37 FTIR results of the substrate are given. The peaks about  $1380\text{ cm}^{-1}$  and  $1450\text{ cm}^{-1}$  wavenumber belong to  $-\text{CH}_3$  and  $-\text{CH}_2$  functionalize groups respectively. Broad peak around  $3500\text{ cm}^{-1}$  belongs to OH groups. It shows that organics bonded to the surface are in salt form, e.g. chemical bonding. The cut of the highest peak demonstrates broadening in intensity, which means that there is a new formation of SAM organics on the surface. Similar results obtained in water and alcohol solvent show that they are bonded to mica surface with the same way. So, solvent type doesn't affect the bonding type of adsorption of amine groups on mica surface.

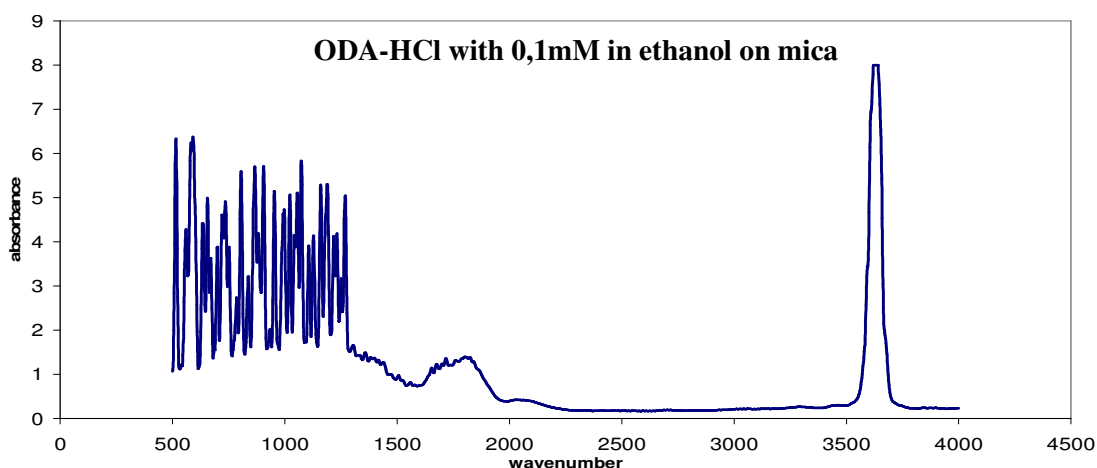


Figure 3.37. FTIR results of SAM consist of ODA-HCl with 0,1 mM in ethanol on mica

### 3.3.3.2. SAM of ODA-HCl with 0,1mM in Ethanol on p type Silicon

FTIR analysis of the substrate of p type silicon prepared by the solutions of ODA-HCl is illustrated at Figure 3.38. Peaks observed around the wavenumber of 1050-1120, 1380, 1450 and 3500  $\text{cm}^{-1}$  belongs to ODA-HCl. Like the amines on the other substrates, these peaks represent  $-\text{C}-\text{N}-\text{CH}_3$  and  $-\text{CH}_2$  functionalize groups and OH groups. The other peaks on the surface can be impurities coming from the surrounding environments. Different from the other substrates the peaks wasn't as clear as pointing out the formation.

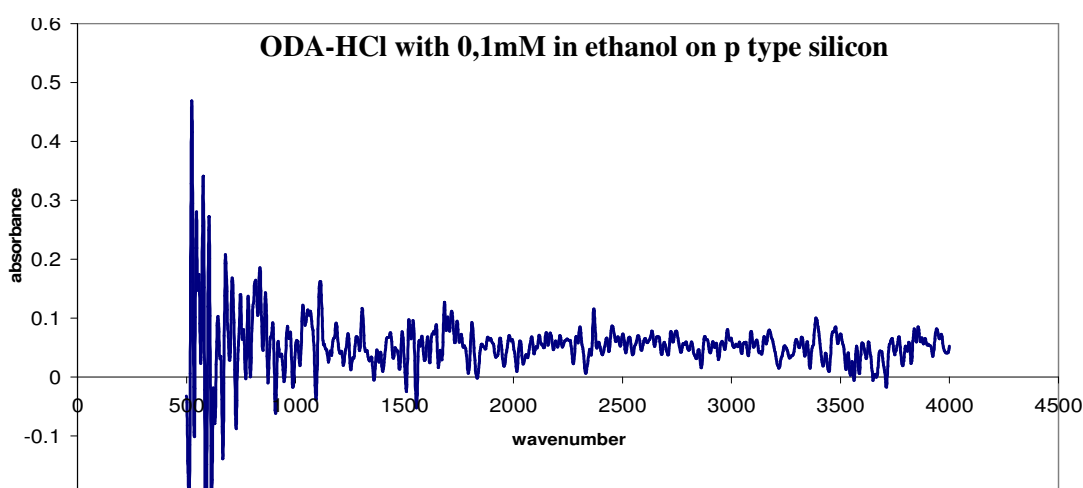


Figure 3.38. FTIR results of p type silicon prepared by the solutions of ODA-HCl with 0,1 mM in ethanol

### 3.3.3.3. SAM of ODA-HCl with 0,1mM in Ethanol on Titanium

FTIR analysis of titanium on silicon with the SAM solution of ODA-HCl is illustrated in Figure 3.39. It is seen that there is an organic formation on the surface at the very low intensity values. Having lower absorbance intensities stem from the thin film formation. Peaks observed around the wavenumber of 1050-1120, 1380, 1450 and 3500  $\text{cm}^{-1}$  belongs to ODA-HCl. Like the other amines substrates, these peaks represent  $-\text{C}-\text{N}$ ,  $-\text{CH}_3$  and  $-\text{CH}_2$  functionalize groups and  $\text{NH}_3^+$  which is told the organic bonded to surface from the salt form. As it is examined in detail, there are some other peaks on the surface. These can be impurities occurred into organic solution during the experiments. Stem from the surrounding area. Also these peaks can stem from the titanium defects. Since from these defects area organics could bond to silicon surface and this bond can seem as a new peak.

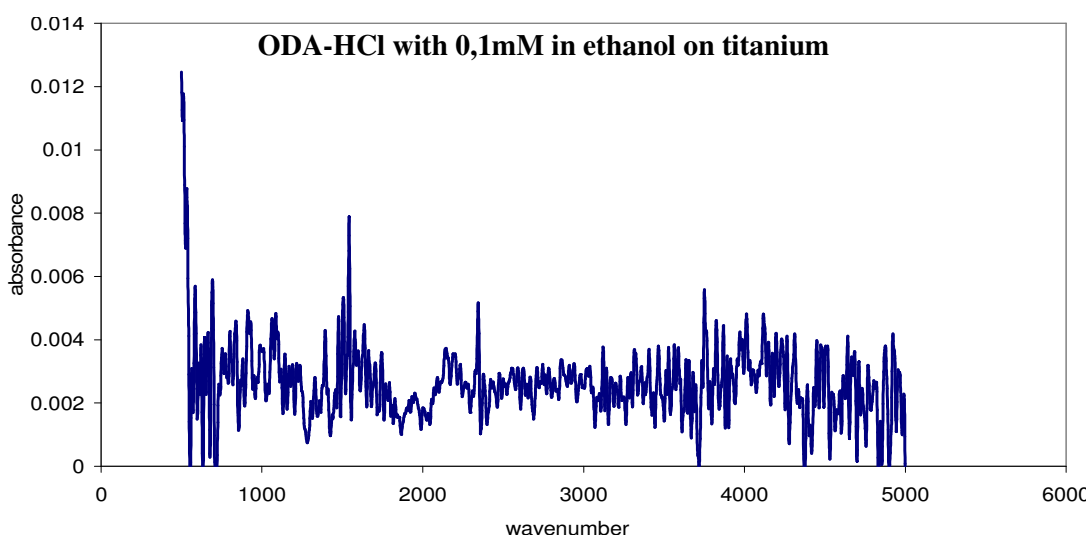


Figure 3.39. FTIR results of titanium on silicon with the SAM solution of ODA-HCl with 0,1 mM in ethanol

### 3.3.4. SAM of DM with 0,1mM in Ethanol on Mica

FTIR results of mica with the SAM solution of DM with 0,1 mM in ethanol are given in Figure 3.40. The thiols of DM have a weak S-H bond between the wavenumber of 2500 and 2600  $\text{cm}^{-1}$ . When the SAM formation is completed, this bond is broken and the organics are bond to the surface from the sulfur atom (Colthup et al. 1990). Beside

this broken bond, C-H,  $-\text{CH}_2$  and  $-\text{CH}_3$  strong bonds also observed around 1355-1470, 1450 and 3500  $\text{cm}^{-1}$ .

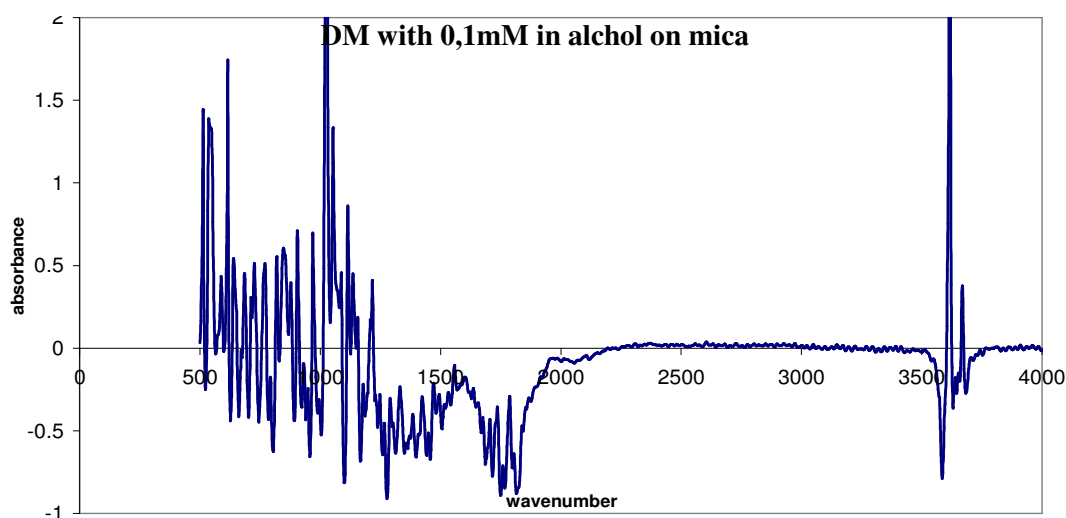


Figure 3.40. FTIR results of mica with the SAM solution of DM with 0,1 mM in ethanol

### 3.3.5. SAM of ODT with 0,1mM in Ethanol

SAM solution of ODT was prepared with ethanol solution with 0,1 mM concentration. SAM formation was observed only on mica and titanium surfaces with AFM and SEM with EDX characterization technique. For the aim of supporting the idea of monolayer formation, mentioned substrates were examined with FTIR. The results are given below.

#### 3.3.5.1. SAM of ODT with 0,1mM in Ethanol on Mica

FTIR analysis of the SAM of ODT on mica is illustrated in Figure 3.41. The weak S-H bond between the wavenumber of 2500 and 2600  $\text{cm}^{-1}$  isn't observed like DM either. This means that sulfur atom organic bonded to surface. The other peaks belong to thiols such as at around 1355-1470, 1450 and 3500  $\text{cm}^{-1}$  -C-H,  $-\text{CH}_2$  and  $-\text{CH}_2$  strong bonds respectively also observed. So, it is clear that the organic bond to surface.

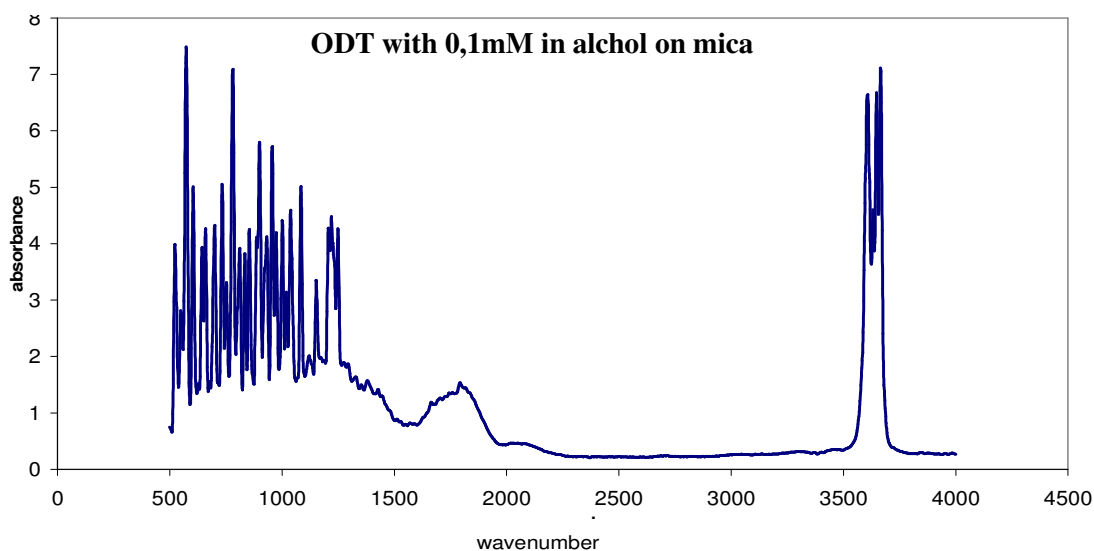


Figure 3.41. FTIR results of mica with the SAM solution of ODT with 0,1 mM in ethanol

### 3.3.5.2. SAM of ODT with 0,1mM in Ethanol on Titanium

FTIR analysis of the substrate of titanium with the SAM solution of ODT is illustrated at Figure 3.42. It is seen that there is an organic formation on the surface at the very low intensity values. Having lower absorbance intensities related with insufficient film thickness to measure with FTIR. Peaks observed around the wavenumber of 1355-1470, 1450 and 3000  $\text{cm}^{-1}$  belongs to thiols. Like the DM substrates, these peaks represent  $-\text{C}-\text{N}$ ,  $-\text{CH}_3$  and  $-\text{CH}_2$  groups. The weak S-H bond wasn't observed. As it is examined in detail, there are some other peaks on the surface. These can be impurities occurred into organic solution during the experiments. Stem from the surrounding area. Also these peaks can stem from the titanium defects. Since from these defects area organics could bond to silicon surface and this bond can seem as a new peak. So, it can be said that the organic bond to surface.

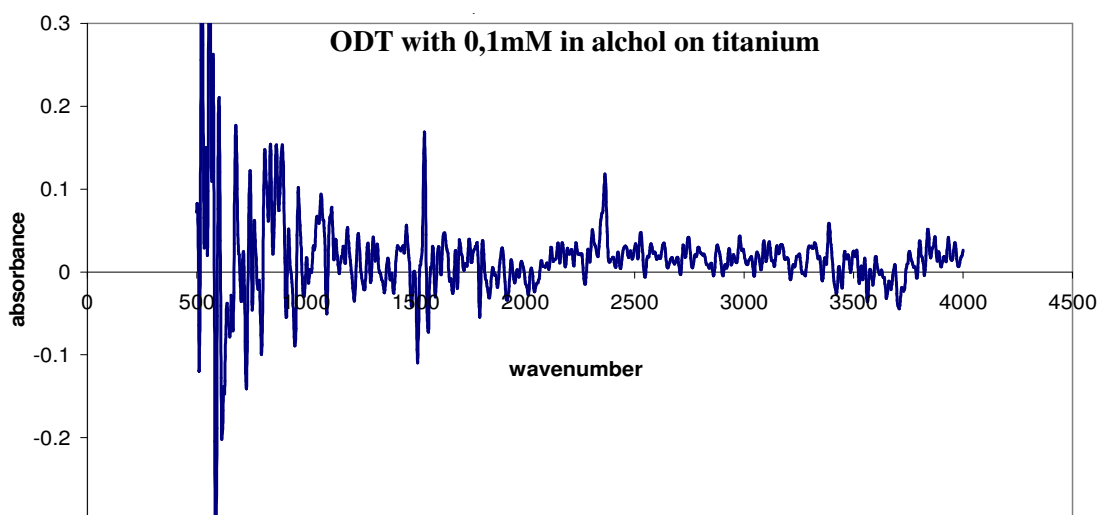


Figure 3.42. FTIR results of titanium with the SAM solution of ODT with 0,1 mM in ethanol

### 3.4. XRD Results

X-Ray Diffraction (XRD) characterization was done with Phillips X'pert Pro system. It was used for examining any crystal structure whether form or not on the surfaces. It is expected that if any crystal structure forms, it can be observe as a peak.

XRD analysis applied on substrates prepared with organics. But there isn't any clear information observed about SAM for either amines or thiols due to thicknesses of the films. Nothing was observed from the XRD because of the higher penetration capacity of the x-rays and even titanium surface couldn't be observed.

XRD analysis of mica with SAM consist of ODA-HCl at 0,1 mM concentration with water solvent is illustrated at Figure 3.14. It just gives mica's peak with higher intensities than bare mica. Higher intensity means more x-ray diffraction detected from the same direction (contractive). The more diffraction could stem from the mica's layered structure. Different diffractions can come from distinct planes with the same directions and this can cause contractive diffractions. The observed peaks from the figure 3.14 belong to mica having characteristic peaks about 26 degree of 2 theta. On the other hand, because of the thickness of the monolayers (about approximately 3 nm), it is impossible to observed these layers. This could be because of the higher penetration capacity of the x-rays.

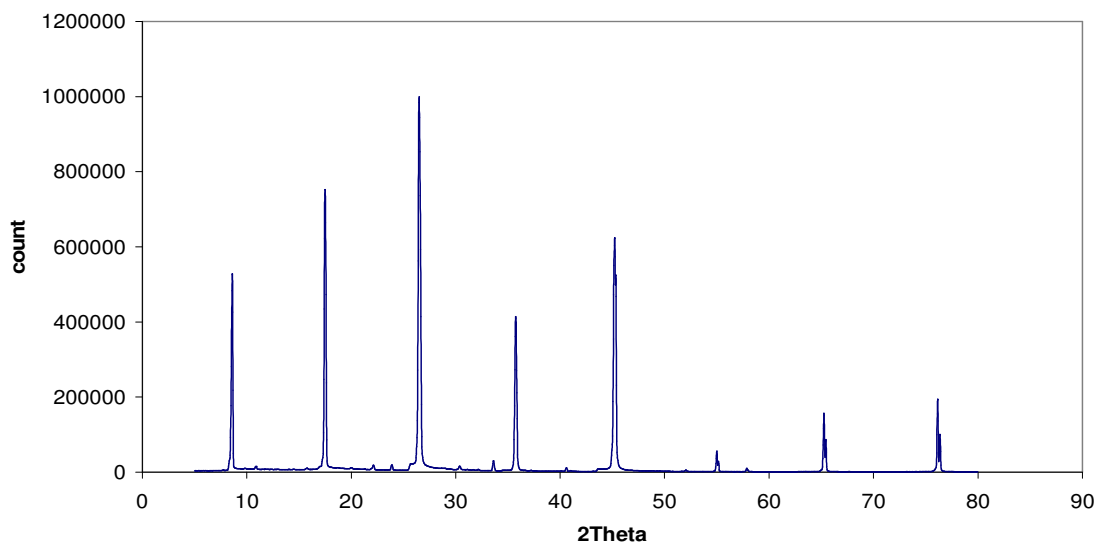


Figure 3.14. XRD results of SAM consist of ODA-HCl with 0,1mM in water on mica

## CHAPTER 4

### SUMMARY AND CONCLUSION

We investigated nanolithography on self assembled monolayers. Octadecylamine-HCl, Octadecanetriol (ODT) and Decylmercaptan SAM organic films were fabricated on various substrates; i.e., mica, silica, titanium surface deposited on silicon, n and p silicon, using self assembly film preparation techniques. The film thicknesses were measured with Atomic Force Microscope (AFM). Nanopatterns were fabricated on SAMs by the AFM tip exerting a high local pressure at the contact that causes the displacement of SAM molecules by a high shear force. It was observed that there was no formation of SAMs on n type Si and silica substrates whereas there were organic assemblies on the other substrates mentioned above. Fabricated nanopatterns were examined and thickness measurement was done. Molecular lengths of the organics were calculated by SPARTAM 02 LINUX-UNIX with the method of PM3 and the measured values were compared with the calculated ones and it was concluded that monolayers were formed on the surfaces.

Scanning probe microscopy (SPM) lithography that uses a sharpened tip of an atomic force microscope was preferred because of not only demonstrates outstanding capabilities for nanometer level patterning on surfaces but also offering molecular precision and visualizing surfaces with the highest spatial resolution. The nanolithography on substrates surfaces by atomic force microscopy operated in both contact and noncontact mode was performed.

Scanning probe microscope (SPM) nanolithography was successfully performed by scratching and oxidation lithography on metallic surfaces as an example. Nanoscratching and nanoindentation techniques were investigated as a physical surface modification. Nanoscratches on gold thin films deposited on mica using RF magnetron sputtering method were made with a silicon AFM tip. The depth profile of nanoscratches made by the tip on the metallic surface was performed as a function of applied normal force. Oxidation lithography was performed as a chemical surface modification technique. Titanium surface deposited on p type silicon was used as a substrate. Titanium oxide patterns were obtained using SPM oxidation nanolithography

technique by applying voltage between the conductive tip and titanium thin films. Parameters such as the spring constant of the cantilever, scratch resistance and hardness of the surface are critical on the formation of patterns. The spring constant of the cantilever should be high enough to be able to scratch metallic films.

Monolayers were investigated in details after making lithographic experiments on metallic thin films. Each type of surface modification technique was successfully performed on metallic surfaces. Then SAM thin films were utilized with lithographic experiment. Before preparing monolayers, bare substrates surfaces were investigated for the aim of minimizing the substrates affect. These studies show that nanolithography must be done under 50.000 nN, since, under this value, deformation couldn't be observed on any of the bare substrates. In fact above this value, only mica deformed by locally. After defining the force limit, surface deformations on organics were studied. By applying high contact forces on surfaces, nanolithography was tried. It was seen that; increasing forces to surface causes increasing in depth until the certain thickness value which gives the molecules thicknesses. This application was also used substrates eliminations. Since, it is the way to determine that monolayer form or not according to done deformation or not. If the deformation is observed, it must come from organic film on the surface since the bare substrates couldn't be deformed. On the other hand, lack of deformation means that SAM film wasn't formed on the surface. So, substrates have nonexistence formation can be eliminated and the substrates thought to be monolayers formed was left. Among the substrates that were used, n type silicon and silica were eliminated because of the lack of SAM formation. The other substrates were investigated for nanolithography. Development patterning and thickness measurements were done on these substrates. Comparing the thicknesses of calculated and measured showed that the values match each other approximately.

FTIR analyses were utilized after AFM experiment. Obtained data showed that both amines and thiols peak were observed on the mentioned substrates. Because of the thin formation, obtained peaks mostly had low absorbance intensity. Besides FTIR analyses, SEM with EDX and XRD analysis were also done. XRD didn't give any clear information about surface. Because of, the higher penetration capability of the x-rays it is impossible to detect thin layers. The results of the XRD just gave bare substrates peaks. When it comes to SEM especially amines of ODA-HCl prepared in water, gave information that the formation formed on the surface. Because of SEM pictures show some formation observed from the surfaces. It was observed from SEM images that

some pinhole defects were occurred on the surfaces. These defects point out the SAM formations on the surface. EDX data showed that the organic molecules were at the surfaces with different rates. Rates of the organics related with the formation. Higher ratio means more formation.

It is observed that, substrates prepared with amines especially prepared in water solvent give the better results than the thiols. Especially ODA-HCl with 0,1 mM concentration in water and in ethanol prepared on mica substrates are the best ones of the amines. They gave better result from all experimental analysis. For thiols groups; the substrates of DM and ODT prepared with 0,1 mM concentration in ethanol on mica were the better result. The mica substrate is convenient for the all type of organics. Since, nearly all condition for almost all type of organics formation observed on mica surface. The concentration of "0,1 mM" is also the better molar condition for both amines and the thiols.

The next step of this study can be a development devises using SAM as a resist. By doing some nanopatterns on the organics films electronic systems could be done. Working with organics thin films lower concentrations can be preferred.

## REFERENCES

- Amrein, M., Müller, D. J., 1999. "Sample preparation techniques in scanning probe microscopy." *Nanobiology*, pp. 229-256.
- Bigelow, W. C., Pickett, D. L., Zisman, W. A. J., 1946. "Colloid Interface", *Sci*, pp. 1-513.
- Bates, K. A., Rothschild, T. M., Bloomstein, T. H., Fedynyshyn, R., Kunz, R., Liberman, V., Switkes, M., 2001. "Advanced Semiconductor Lithography." *IBM J. Res. Dev.*, pp. 605 – 614.
- Carpick, R. W., Salmeron, M., 1997. "Scratching the Surface: Fundamental Investigations of Tribology with Atomic Force Microscopy", *Chem. Rev.* Vol. 97, pp. 1163-1194.
- Colthup, N. B., Daly, L. H., Wiberley, S. E., 1990. "Introduction to Infrared and Raman Spectroscopy" (Academic Press San Diego).
- Diao, P., Jiang, D., Cui, X., Gu, D., Tong, R., Zhong, B., 1999. "Studies of structural disorder of self-assembled thiol monolayers on gold by cyclic voltammetry and ac impedance." *Journal of Electroanalytical Chemistry*, pp. 61-67.
- Diao, P., Guo, M., Jiang, D., Jia, Z., Cui, X., Gu, D., Tong, R., Zhong, B., 2000. "Fractional Coverage of Defects in Self-assembled Thiol Monolayers on Gold." *Journal of Electroanalytical Chemistry*, pp. 59-63.
- Diao, P., Guo, M., Ruting T., 2001. "Characterization of defects in the formation process of self-assembled thiol monolayers by electrochemical impedance spectroscopy." *Journal of Electroanalytical Chemistry*, pp. 98-105.
- Gang, Y. L., Song, X., Yile, Q., 2000. "Nanofabrication of Self-Assembled Monolayers Using Scanning Probe Lithography" *Acc. Chem. Res.*, pp. 457-466.
- Hamelmann, F., Heinzmann, U., Siemeling, U., Bretthauerb, F., Vor der Brüggén, J., 2003. "Light-Stimulated Switching of Azobenzene-Containing Self-Assembled Monolayers", *Science Direct*, pp. 1-5.
- Hagenström, H., Schneeweiss M.A., Kolb D.M., 1999. "Copper Underpotential Deposition on Ethanethiol-Modified Au (111) Electrodes: Kinetic Effects", *Elsevier Science*, pp. 1141-1145.
- Hong, S., Zhu, J., Mirkin, C. A., 1999. "A New Tool for Studying the in Situ Growth Processes for Self-Assembled Monolayers under Ambient Conditions", *Langmuir*, Vol. 15, pp. 7897-7900.
- Ichii, T., Fukuma, T., Kobayashi, K., Yamada, H., Matsushige, K., 2003. "Phase separated alkanethiol self-assembled monolayers investigated by non-contact AFM." *Elsevier Science*, pp. 99-104.

- Ivanisevic, A., Mirkin, C. A., 2001. "Dip-Pen Nanolithography on Semiconductor Surfaces" *J. Am. Chem. Soc.*, Vol. 123, pp. 7887-7889.
- Kindt, J. H., 2002. "Biological probe microscopy in aqueous fluids." *Academic press*.
- Kondrashkina, E. A., Hagedorn, K., Vollhardt, D., Schmidbauer, M., Köhler, R., 1996. "Structure of Relaxed Monolayers of Arachidic Acid Studied by X-ray Reflectometry and Atomic Force Microscopy", *Langmuir*. Vol. 12, pp. 5148-5155.
- Kluth, G. J., Carraro, C., Maboudian, R., 1999. "Direct observation of sulfur dimers in alkanethiol self-assembled monolayers on Au.111. (Physical ReviewB)" *Rapid Communications*, Vol. 59., pp. 16.
- Lee, H., Jang, Y. K., Bae, E. J., Lee, W., 2002. "Organized Molecular Assemblies for Scanning Probe Microscope Lithography." *Current Applied Physics*, pp. 85-90.
- Lee, H., Bae, E., Lee, W., 2001. "Fabrication of Nanometer Scale Patterns with Organized Molecular Films", *Thin Solid Films*, pp. 237-242.
- Lee, W. B., Oh, Y., Kim, E. R., Lee, H., 2001. "Nanopatterning of Self-assembled Monolayers on Si-surfaces with AFM Lithography." *Synthetic Metals*, pp. 305-306.
- Lemeshko, S., Gavrilov, V., Shevyakov, V., Solomatenko, R., 2001. "Investigation of tip-induced ultrathin Ti film oxidation kinetics." *Nanotechnology*, pp. 273-276.
- Liu, G. Y., Xu, S., Qian, Y., 2000. "Nanofabrication of Self-Assembled Monolayers Using Scanning Probe Lithography." *Acc. Chem. Res.* Vol. 33, pp. 457-466.
- Magonov, S. N., 1996. "Surface Analysis with STM and AFM. Experimental and Theoretical Aspects of Image Analysis." *VCH*.
- Miller, S., Troian, M., Wagner, S., Vac. J., 2002. "Direct Printing of Polymer Microstructures on Flat and Spherical Surfaces Using a Letterpress Technique." *Sci. Technol.* Vol. 20, pp. 2320 - 2327.
- Nuzzo, R. G., Dubois, L. H., Allara, D. L., 1990. "Fundamental Studies of Microscopic Wetting on Organic Surfaces. 1. Formation and Structural Characterization of Self-Consistent Series of Polyfunctional Organic Monolayers." *J. Am. Chem. Soc.* Vol. 112, pp. 558-569.
- Nuzzo, R. G., Allara, D. L., 1983. "Adsorption of Bifunctional Organic Disulfid on Gold Surfaces." *J. Am. Chem. Soc.* Vol. 105, pp. 4481-4483.
- Piner, R. D., Hong, S., Mirkin, C. A., 1999. "Improved Imaging of Soft Materials with Modified AFM Tips", *Langmuir*, Vol. 15, pp. 5457-5460.

- Rachel K. S., Penelope A. L., Paul S. W., 2004. "Patterning self-assembled monolayers", *Progress in Surface Science*, pp. 1–68.
- Ras, R. H., Johnston, C. T., Schoonheydt, R. A., 2005. "Chemical Instability of Octadecylammonium Monolayers" *The Royal Society of Chemistry (Chem. Commun.)*, pp. 4095-4097.
- Richard D., Mirkin, P., Chad, A., 1997. "Effect of Water on Lateral Force Microscopy in Air." *Langmuir*, pp. 6864-6868.
- Robert W. C., Miquel, S., 1997. "Scratching the Surface: Fundamental Investigations of Tribology with Atomic Force Microscopy." *Chem. Rev.* pp. 163-1194.
- Samuel H., Gyepi, G., Ilerova, R. S., 2001. "Probing Temperature-Dependent Behaviour in Self-Assembled Monolayers by ac-impedance Spectroscopy", *Science Place*, pp. 110.
- Shao, Z., Mou, J., Czajkowsky, D.M., Yang, J., Yuan, J. Y., 1996. "Biological atomic force microscopy: what is achieved and what is needed." *Advances in Physics*, pp. 1-86.
- Silva da, L.P., 2002. "Atomic force microscopy and proteins." *Protein and Peptide Letters*, pp. 117-125.
- Song X. and Gang-yu L., 1997. "Nanometer-Scale Fabrication by Simultaneous Nanoshaving and Molecular Self-Assembly." *Langmuir*, pp. 127-129.
- Socrates, G., 2001. "Infrared and Raman Characteristic Group Frequencies: Table and Charts." *John Wiley & Sons, Chichester, UK*, pp.347.
- Sorrell, T. N., 1988. "Interpreting Spectra of Organic Molecules." *University Science Books, Mill Valley, Calif.*, pp. 106.
- Tamada, K. J., Nagasawa, F., Nakanishi, K., Abe, M., Hara, W., Knoll, T., Ishida, H., Fukushima, S., Miyashita, T., Usui, T., Koini, T., Lee, R., 1998. "Structure of SAMs generated from functionalized thiols on gold." *Thin Solid Films*, Vol. 327–329, pp. 150–155.
- Ulman, A., 1991. "An Introduction to Ultrathin Organic Films from Langmuir-Blodgett to Self-Assembly", *Academic Press*, pp. 117-130.
- Ulman, A., 1996. "Formation and Structure of Self- Assembled Monolayers", *Chem. Rev.* Vol. 96, pp. 1533- 1554.
- Ulman, A., Evans, S. D., Shnidman, Y., Sharma, R., Eilers, J. E., Chang, J. C. J., 1991. "A Concentration-Driven Surface Transition in the Wetting of Mixed Alkanethiol Monolayers on Gold." *Am. Chem. Soc.*

Wataru, M., Takao, I., Hiroshi, T., 1998. "Nanoscale Reversible Molecular Extraction from a Self-Assembled Monolayer on Gold (111) by a Scanning Tunneling Microscope." *Langmuir*, pp. 7197-7202.

Wouters, D., Schubert, U. S., 2004. "Nanolithography and Nanochemistry: Probe-Related Patterning Techniques and Chemical Modification for Nanometer - Sized Devices" *Angew. Chem. Int. Ed.*, pp. 2480 – 2495.